Molecular Mechanisms Underlying Cytokinin-induced Ornamental Flower Morphology and Its Application in Breeding : Using Torenia as a Model Floricultural Plant

著者	仁木 智哉
year	2013
その他のタイトル	サイトカイニンによる装飾的な花形の誘導機構の解明と育種への応用に関する研究 : トレニアをモデル系として
学位授与大学	筑波大学 (University of Tsukuba)
学位授与年度	2013
報告番号	12102甲第6732号
URL	http://hdl.handle.net/2241/00122790

Molecular Mechanisms Underlying Cytokinin-induced Ornamental Flower Morphology and Its Application in Breeding – Using Torenia as a Model Floricultural Plant –

（サイトカイニンによる装飾的な花形の誘導機構の解明と育種への応用に関する研究
―トレニアをモデル系として―）

A Dissertation Submitted to
the Graduate School of Life and Environmental Sciences,
the University of Tsukuba
in Partial Fulfillment of the Requirements
for the Degree of Doctor of Philosophy in Agricultural Science
(Doctoral Program in Advanced Agricultural Technology and Sciences)

Tomoya NIKI

Contents

Chapter 1

General introduction

For floricultural plants, flower morphology, as well as color and fragrance, is one of the most important traits determining the commercial value. Most major floricultural plants such as chrysanthemum, carnation, and rose have larger and more ornamental flowers than the corresponding wild ancestors. Although *Dianthus caryophyllus* L., one of the original species of carnation, has a single flower that is 1–2 cm in diameter, modern carnation cultivars have double flowers with up to 8 cm diameter. Flowers of these modern cultivars are much more attractive to consumers than those of *D. caryophyllus* (Nishijima, 2007; Nishijima, 2012). Furthermore, 50 years ago, *Eustoma grandiflorum* was a minor floricultural plant, with single flowers of size like those of its wild ancestor; however, with the development of double and larger flowers with diverse colors and patterns, it has recently been converted into a major floricultural plant (Yashiro, 1994).

Breeding programs aimed at producing ornamental flower morphologies featuring double and large flowers have been based mainly on mutation breeding and cross pollination. However, the occurrence of desirable mutants is rare, and in general, mutant phenotypes are weak or unstable, with long breeding periods required to yield fixed and stable phenotypes (Nishijima, 2007). For example, more than a thousand years were required to obtain double and large flowers comparable with those of modern carnation cultivars (Nishijima, 2012; Takeda, 1996). In *E. grandiflorum*, in which breeding was initiated after the establishment of modern breeding techniques including chemical- and radiation-induced mutations and embryo culture, more than 40 years were required to produce double and large flowers comparable with those of modern cultivars (Yashiro, 1994). Thus, it is important to develop

an efficient breeding method that can shorten the breeding period required to improve flower morphology. Such a breeding method would be useful for creating novel and attractive flowers in minor floricultural plants in which the attractiveness of the flower is still weak. It would be helpful to employ molecular techniques such as DNA markers and genetic transformation. Recently, genetic analysis has made remarkable progress, and the analysis of genomic information for floricultural plants such as chrysanthemum and carnation is ongoing (Tanase et al., 2012; Wang et al., 2013). Furthermore, the production of transgenic floricultural plants and the development of promoters for transgene expression have also progressed (Chandler and Sanchez, 2012; Potenza et al., 2004; Shibata, 2008). To apply those molecular tools to improve flower morphology, it is necessary to elucidate the molecular mechanism responsible for ornamental flower morphologies.

Of the various ornamental flower morphologies, double flowers are produced by homeotic conversion of the stamens and pistils to petals, induced by mutation of floral homeotic genes. In general, dicot flowers consist of four organs: sepals, petals, stamens, and pistils. The identities of these floral organs are determined by the expression patterns of three classes of floral homeotic genes encoding transcription factors. The relationship between the expression pattern and floral organ identity is well illustrated by the ABC model (Fig. 1; Bowman et al., 1991; Coen and Meyerowitz, 1991; Rijpkema et al., 2007). In this model, the expression of class A genes alone in whorl 1 forms sepals, combined expression of class A and B genes in whorl 2 forms petals, expression of class B and C genes in whorl 3 forms stamens, and expression of class C genes alone in whorl 4 forms pistils. Class A and C genes repress the expression each other and accordingly are not simultaneously expressed in the same whorl (Drews et al., 1991; Gustafson-Brown et al., 1994). In an *Arabidopsis* mutant of the class C gene (*AGAMOUS*, *AG*), the stamens and pistils are converted to petals and new flowers, respectively (Yanofsky et al., 1990). This conversion is caused by the loss of class

C gene expression and the resulting extension of class A gene expression in whorls 3 and 4, leading to petal induction via the combined expression of class A and B genes (Drews et al., 1991). In *Antirrhinum majus*, two class C genes (*PLENA*, *PLE*; *FARINELLI*, *FAR*) have been cloned, and loss of *PLE* function shows a phenotype in which both stamens and pistils are converted to petaloid organs (Bradley et al., 1993). In the *ple*/*far* double mutant, the pistils are completely converted to petals (Davies et al., 1999). In transgenic *Arabidopsis*, overexpression of class B genes (*APETALA3*, *AP3*; *PISTILLATA*, *PI*) in all the whorls in the *ag* mutant converts the sepals, stamens, and pistils into petals, resulting in a flower that consists solely of petals (Krizek and Meyerowitz, 1996). The ABC model has been further extended with D and E genes (Ferrario et al., 2004). In this model, ovules are regarded as separate floral organs of whorl 5, and the expression of class D genes is responsible for ovule formation. Class E genes express in whorls 2 to 5 and function as cofactors that are responsible for the identity of these whorls (Fig. 1).

Cytokinins also play an important role in the regulation of flower morphology. In *Arabidopsis*, the number of floral organs, such as petals, stamens, and pistils, is increased by BA treatment of flower buds (Lindsay et al., 2006; Venglat and Sawhney, 1996). Such an increase in the number of floral organs is promoted by cytokinin-mediated induction of gene expression involved in meristematic activity and organ differentiation (Lindsay et al., 2006; Rupp et al., 1999). In *Petunia hybrida*, cytokinin induces corolla enlargement via an increase in cell number (Nishijima, 2012; Nishijima et al., 2006). Furthermore, some genes involved in cytokinin biosynthesis and early signaling pathways are regulated by a *Grandiflora* gene, which is responsible for the large-flowered phenotype in petunia (Ewart, 1984; Nishijima, 2012; Nishijima et al., 2011a, b).

The biosynthetic pathways of cytokinins and their related genes in higher plants have been well documented (Summarized in Fig. 2; Frébort et al., 2011; Werner and Schmülling, 2009).

The first step of cytokinin biosynthesis is production of nucleotide cytokinin through isopentenylation of ATP and ADP, which is catalyzed by isopentenyltransferase (IPT) using dimethylallyl diphosphate as substrate (Kakimoto, 2001; Takei et al., 2001). Biologically active cytokinin nucleobases, N^6-(Δ^2-isopentenyl)adenine (iP) and tZ, are synthesized from nucleotide cytokinins in a single step, which is catalyzed by cytokinin nucleoside 5′-monophosphate phosphoribohydrolase (LOG; Kurakawa et al., 2007). In another suggested pathway, cytokinin nucleobases are synthesized from cytokinin nucleotides by a two-step reaction, i.e., comprising nucleotidation and nucleosidation (Auer, 2002; Chen and Kristopeit, 1981) However, the responsible genes remain to be identified. These biologically active cytokinins are degraded by cytokinin oxidase/dehydrogenase (CKX) through oxidative isoprenoid side chain cleavage (Schmüllung et al., 2003) or by conjugation to sugar moieties through glycosyltransferases (Hou et al., 2004). The early cytokinin signal transduction pathway which consists of a two-component signaling system has also been clarified in *Arabidopsis* (Summarized in Fig. 2; Mizuno, 2005; Müller, 2011). Binding of a biologically active cytokinin to the cytokinin receptor, i.e., receptor histidine protein kinase, induces His-Asp phosphorelay to histidine phosphotransfer proteins (HPt). The phosphorylated HPt phosphorylates and activates type-B response regulators (RRs), which act as transcription factors and induce target gene expression including type-A *RR*s. Type-A RRs act as a repressor of cytokinin signaling by competing with phosphorylation of type-B RR which causes a negative feedback loop to cytokinin signaling (Müller, 2011; Rashotte et al., 2003).

In torenia (*Torenia fournieri* L.), treatment with forchlorfenuron (CPPU), which inhibits cytokinin degradation by inhibiting CKX activity (Bilyeu et al., 2001), induces several different flower morphologies including increase in the number of petals and the development of a paracorolla and serrated petal margins (Nishijima and Shima, 2006). These changes in flower morphology are dependent on the floral stage at which CPPU is applied.

When CPPU is applied at or before the sepal initiation stage (Stage 2), the number of the petals increases. When CPPU is applied at the sepal development stage (Stage 3) and at the petal, stamen, and pistil initiation stage (Stage 4), petal-like wide paracorollas are induced. When CPPU is applied at the early corolla development stage (Stage 5), narrow paracorollas are induced. When CPPU is applied at the middle corolla development stage (Stage 6) and at the late corolla development stage (Stage 7), serrated petals are induced (Nishijima and Shima, 2006). Because CPPU inhibits CKX activity as mentioned above, CPPU may induce a specific spatial pattern of cytokinin accumulation in flower buds depending on the balance of cytokinin biosynthesis and degradation. This spatial pattern of cytokinin accumulation may be the cause of morphological changes in the flower. Of the floral morphologies induced by CPPU treatment in torenia, the paracorolla is formed in only a few species including *Narcissus* and *Passiflora* (Troll, 1957). Its unique and conspicuous appearance contributes to the high ornamental value of these species.

Torenia, a Linderniaceae plant (Huxley et al., 1992; Rahmanzadeh et al., 2005), is a summer annual widely used as a bedding and pot plant in Japan. Torenia is also an excellent model floricultural plant according to the following reasons. Genome size is small as approximately 171 Mbp (Kikuchi et al., 2006), which is comparable to that of *Arabidopsis* (approximately 157 Mbp: Bennett et al., 2003). Whole genome analysis is currently ongoing (Higashiyama, personal communication). Observation of flower morphology is easy because of the moderate flower size, i.e., with 2–3 cm in diameter. In addition, torenia is easily propagated by cutting and pollination. Life cycle is short, i.e., about 3 months from sowing to production of mature seeds. Because of high transgenic efficiency (Aida, 2008), transgenic torenia with extended flower longevity (Aida et al., 1998; Tanase et al., 2011), modified flower color (Aida et al., 2000; Ono et al., 2006), and plant height (Niki et al., 2006a) have already been produced. Furthermore, since torenia has little variation in flower

morphology, improvement of flower morphology may have an impact on commercial value of this species.

We conducted the following studies to elucidate the molecular mechanism responsible for the ornamental flower morphologies induced by cytokinin. In Chapter 2, we describe an investigation of the spatial and temporal distribution patterns of cytokinin signals in CPPU-treated flower buds in terms of the particular flower morphologies induced. In Chapter 3, we investigate the role of the expression patterns of floral homeotic genes in the morphologies of CPPU-induced paracorolla. In Chapter 4, we describe the production of transgenic torenia, based on the results in Chapters 2 and 3, to characterize the effects of floral organ-specific promotion of cytokinin biosynthesis on flower morphology. Finally, we discuss the applicability of this strategy to the production of ornamental flower morphologies.

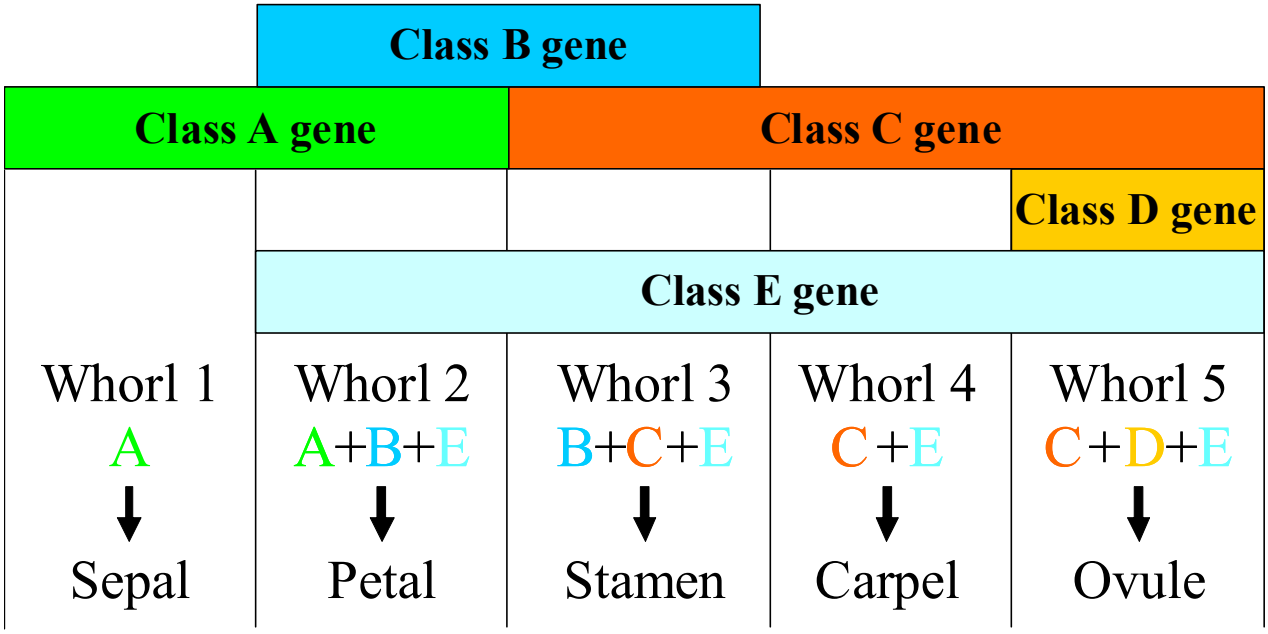

Fig. 1. The ABCDE model determining floral organ identity. Former model, i.e., ABC model, did not include class D and E genes, and both of carpel and ovule belong to whorl 4.

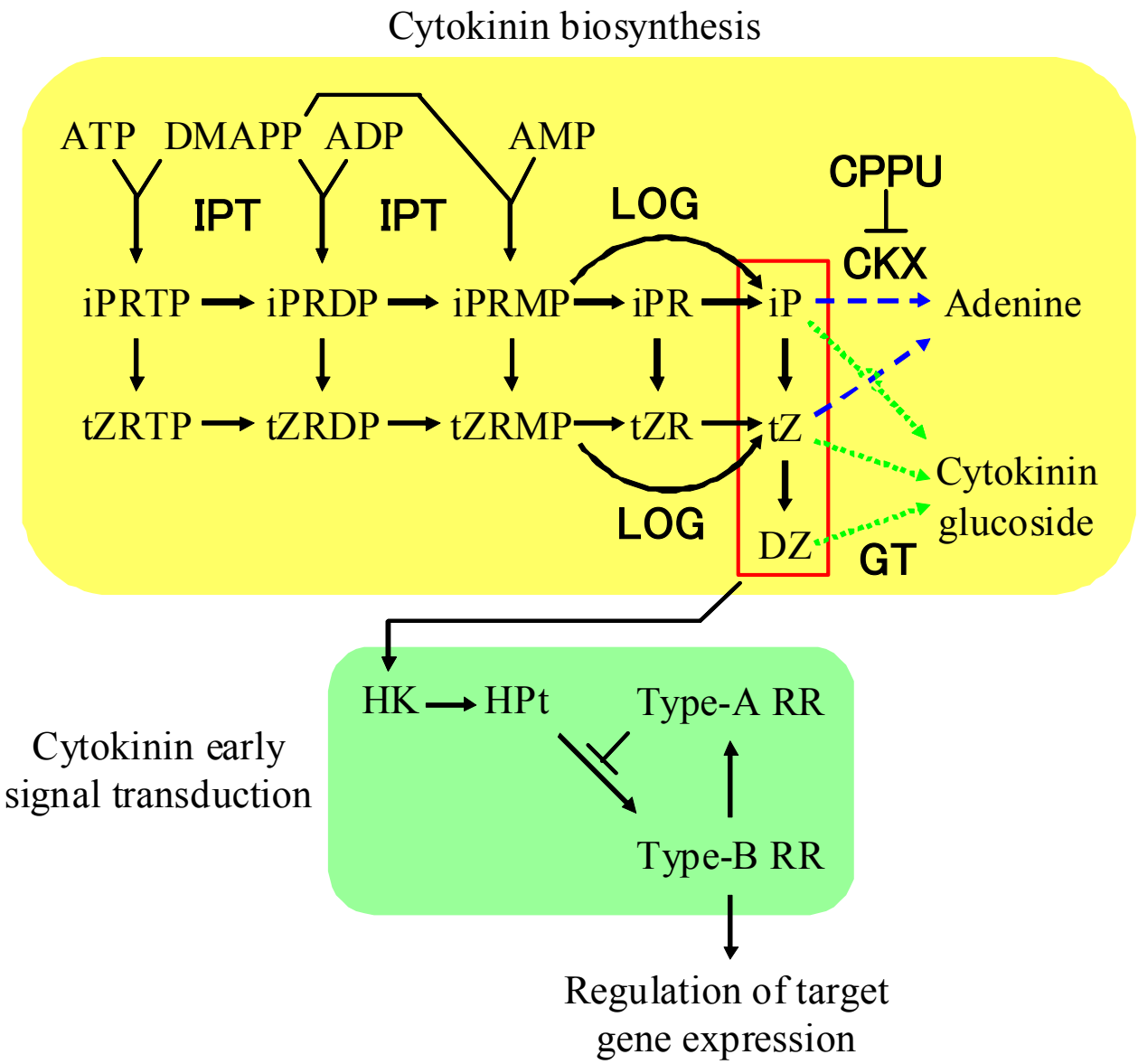

Fig. 2. Cytokinin biosynthesis and early signal transduction pathways. Bold letters indicate catalytic enzymes. Biologically active cytokinins are boxed by red line. Broken lines indicate inactivation of biologically active cytokinins by CKX (blue line) or GT (green line). CPPU inhibits CKX activity. ADP, adenosine 5′-diphosphate; AMP, adenosine 5′-monophosphate; ATP, adenosine 5′-triphosphate; DMAPP, dimethylallyl diphosphate; CKX, cytokinin oxidase/dehydrogenase; CPPU, forchlorfenuron; DZ, dihydrozeatin; GT, glycosyltransferase; HK, receptor histidine protein kinase; HPt, histidine phosphotransfer protein; iP, N^6-(Δ^2-isopentenyl)adenine; iPR, iP riboside; iPRDP, iPR 5′-diphosphate; iPRMP, iPR 5′-monophosphate; iPRTP, iPR 5′-triphosphate; IPT, isopentenyltransferase;

Be continued

phosphoribohydrolase; RR, response regulator; tZ, *trans*-zeatin; tZR, tZ riboside; tZRDP, tZR 5′-diphosphate; tZRMP, tZR 5′-monophosphate; tZRTP, tZR 5′-triphosphate.

Chapter 2

Role of localized cytokinin signal in flower bud in CPPU-induced ornamental flower morphology

1. Introduction

CPPU is a synthetic cytokinin categorized in diphenylurea type (Mok and Mok, 2001). CPPU is used as a plant growth regulator for the improvement of the growth and quality of melon fruit (Ikeda et al., 1990; Hayata et al., 1990), induction of parthenocarpy in watermelon (Hayata et al. 1991), reduction of puffiness in tomato (Kataoka et al., 1994), and induction of parthenocarpy in Japanese wild grape (Koiwai et al., 2012). In torenia, CPPU induces changes in flower morphologies depending on the floral stage at which CPPU is applied. When CPPU is applied at Stage 3 and Stage 4, primordia of wide paracorollas are initiated on basal part of young petal at late stage 4. When CPPU is applied at Stage 5, primordia of narrow paracorollas are initiated on middle part of developing petal at late Stage 6. When CPPU is applied at Stage 6 and Stage 7, serrated petals are induced at late Stage 7 (Nishijima and Shima, 2006). CPPU inhibits CKX activity (Bilyeu et al., 2001), which degrades endogenous cytokinins. Therefore, CPPU may induce localized high cytokinin concentrations in flower buds, depending on the uneven distribution of cytokinin biosynthetic activity, leading to morphological changes in flowers. Although it is difficult to investigate distribution of cytokinin in small young flower buds, distribution of the cytokinin signals can be determined by monitoring the expression of the cytokinin responsive genes.

Type-A *RR*s is a candidate gene used for such purpose. The expression of type-A *RR*s is rapidly and strongly induced in response to cytokinin, and thus, the expression level reflects

the extent of the cytokinin signals (Brandstatter and Kieber, 1998; D′Agostino et al., 2000; Nishijima et al., 2011b; Taniguchi et al., 1998). In addition, *CKX* expression is induced by cytokinin, which functions as negative feedback regulation of cytokinin biosynthesis through cytokinin degradation (Brugière et al., 2003; Kiba et al., 2005; Nishijima et al., 2011a). Thus, the expression of type-A *RR*s and *CKX*s may be used as indices of cytokinin signals.

In contrast to CPPU treatment, BA treatment induces no morphological change in torenia flower (Nishijima and Shima, 2006). CPPU activity is 10 times higher than BA in growth of tobacco callus (Takahashi et al., 1978). Almost similar result has been shown in promotion of corolla enlargement in petunia, in which CPPU activity is 30 times higher than BA (Nishijima et al., 2006). However, in induction of morphological changes in torenia flower, 0.3μM CPPU is highly effective, while BA has no effect even at 1mM, the highest concentration tested (Nishijima and Shima, 2006). Therefore, CPPU activity is more than 3000 times higher than BA. This great difference in the activity indicates that CPPU and BA has rather qualitatively-different mode of action to torenia flower.

In this chapter, we isolated type-A *RR* and *CKX* genes from torenia and selected ones highly responsive to cytokinin. This is because the extent of the response to cytokinin differs greatly among the members of the gene family (D′Agostino et al., 2000; Kiba et al., 2005). We investigated the spatial and temporal expression patterns of type-A *RR*s and *CKX*s in CPPU-treated flower buds, and the relationship between the localization of cytokinin signals and the induction of paracorollas and serrated petals are discussed.

2. Materials and Methods

2.1. Plant materials

Seeds of *Torenia fournieri*, ‘Dwarf White’ (Sakata Seed Co., Kanagawa, Japan), were

germinated in horticultural soil (Metro-Mix 350; Sun Gro Horticulture Canada Ltd, British Columbia, Canada), and the seedlings were transplanted to another horticultural soil (Kureha-Engei-Baido; Kureha Chemical Industry Co., Ltd., Tokyo, Japan) in plastic pots and then grown in an incubator kept at 25°C/20°C (day/night) under illumination from fluorescent lamps of 180 μmol·m^{-2}·s^{-1} PPFD (12 h light/12 h dark).

2.2. CPPU and BA treatment

The CPPU (Sigma-Aldrich Japan Co., Ltd., Tokyo, Japan) and BA (Wako Pure Chemical Industries Ltd., Osaka, Japan) solution was prepared in 20% (v/v) acetone (Nishijima and Shima, 2006). We applied 8 μL of 3 μM CPPU or 8 μL of 100 μM BA solutions to the apex of an inflorescence using micropipette. This concentration of CPPU is medial one within the range of concentrations which effectively induce morphological changes in torenia flower (Nishijima and Shima, 2006). BA concentration was set 30 times higher than CPPU referring to the difference of their activities to enlargement of petunia flower (Nishijima et al., 2006). To ensure the induction of the morphological changes, flower buds longer than 10 mm were removed before the treatment.

2.3. cDNA cloning of type-A RR and CKX genes and phylogenetic analyses

Young flower buds of torenia were frozen in liquid nitrogen. After homogenizing the sample with zirconia beads, total RNA was isolated using an RNeasy Plant Mini Kit (Qiagen Sciences, Germantown, USA) and treated with RNase-Free DNase Set (Qiagen). cDNA was synthesized using a CapFishing Full-length cDNA Premix Kit (Seegene, Seoul, Korea). Degenerate primers of type-A *RR* and *CKX* genes were designed using highly conserved regions of each gene, and partial cDNAs were amplified using the degenerate primers. Degenerate primer sequences were listed in Table 1. Each PCR fragment was cloned into a

pGEM-T Easy vector (Promega, Madison, WI, USA) and the nucleotide sequence was analyzed with a BigDye Terminator v3.1 Cycle Sequencing Kit and an ABI PRISM 3100 Genetic Analyzer (Applied Biosystems, Foster City, WI, USA). Based on the sequences of the PCR fragments, gene-specific primers were designed, and 5′ and 3′ RACE were performed using the CapFishing Full-length cDNA Premix Kit (Seegene). To isolate full-length cDNAs for each gene, PCRs were performed with KOD Plus DNA polymerase (TOYOBO, Osaka, Japan). Primer sequences used for isolation of full-length cDNAs were listed in Table 2. The nucleotide sequence of each PCR fragment was analyzed as the same procedure as described above and registered in the DNA Data Bank of Japan (DDBJ; http://www.ddbj.nig.ac.jp). Accession numbers of the cloned cDNAs are listed in the legend for Figs. 3 and 4.

For phylogenetic analyses, the full length of each amino acid sequence of type-A RR or CKX was used, respectively. Predicted amino acid sequences of the cloned type-A *RR* or *CKX* genes from torenia were compared with those of *Arabidopsis* by using CLUSTAL W (http://clustalw.ddbj.nig.ac.jp/top-j.html). The phylogenetic trees were constructed using the neighbor-joining method and were drawn with NJplot (http://pbil.univ-lyon1.fr/software/njplot.html).

2.4. Quantitative real-time PCR analysis

Total RNA was isolated separately from the sepals, petals, stamens, and pistils of flower buds after CPPU or BA treatment and those of non-treated controls using the same procedure used for cDNA cloning. cDNA was synthesized using a Transcriptor First Strand cDNA Synthesis Kit (Roche, Mannheim, Germany). Gene-specific primers for *TfRR* and *TfCKX* genes and the actin gene (*TfACT3*; AB330989), which was used as an internal standard, were designed for the 3′-terminal regions of the open reading frame and the 3′-untranslated

regions of each gene. Primer sequences and the lengths of PCR products used for quantitative real-time PCR (qPCR) reactions were listed in Table 3. Expression of the genes was quantified using SYBR Premix Ex Taq (Takara Bio, Shiga, Japan) and qPCR (LightCycler; Roche). PCR reactions were performed with an initial denaturation step of 10 s at 95°C, followed by 50 cycles of 5 s at 95°C, 10 s at 60°C, and 5–7 s at 72°C. Fluorescence was measured at the end of the extension phase at 73°C for *TfCKX1* and *TfCKX2*, at 74°C for *TfCKX3*, at 75°C for *TfRR2*, at 76°C for *TfRR1*, at 77°C for *TfACT3*, and at 78°C for *TfCKX4* and *TfCKX5*, to avoid detecting non-specific PCR products. The raw data were analyzed with LightCycler software version 3.5 (Roche). The plasmids harboring full-length cDNA of *TfRR* or *TfCKX* genes or a partial cDNA fragment of *TfACT3* were used to obtain the standard curves. The ratio of the expression of each gene to that of *TfACT3* was calculated. Expression analyses were conducted independently in triplicate.

2.5. *In situ* hybridization

Flower buds at 3 or 7 days after CPPU treatment and those of non-treated controls were used for *in situ* hybridization. The flower buds were fixed in FAA (50% (v/v) ethanol, 10% (v/v) formaldehyde, 5% (v/v) acetic acid) at 4°C, then dehydrated through a graded 2-methyl-2-propanol (2M2P) and ethanol series [0:30%, 0:50%, 10:50%, 20:50%, 35:50%, 50:40%, 75:25% (v/v)]. After replacement of ethanol with 2M2P, the tissues were embedded in paraffin. The tissues were sectioned (8 μm thick) with a rotary microtome (RM2145; Leica, Nussloch, Germany). *In situ* hybridization was performed as described by Hirai et al. (2007). The sections were dewaxed with xylene, and rehydrated through a graded ethanol series [100%, 90%, 80%, 70%, 50% (v/v)]. After washing with PBS (0.1 M NaCl, 10 mM NaH_2PO_4, 10 mM Na_2HPO_4, pH 7.4), the sections were treated with 1 $\mu g \cdot mL^{-1}$ proteinase K (Roche) in TE (20 mM EDTA, 0.1 M Tris-HCl, pH 7.5) at 37°C for 30 min and the reaction

was stopped by washing with PBS containing 0.2% glycine. After washing with PBS, the sections were acetylated in 0.1 M triethanolamine HCl (pH 8.0) and 0.25% acetic anhydride for 20 min. After incubation with 1% Triton X-100 in PBS and further washing with PBS, the sections were pre-hybridized at room temperature for 2 h in 150 μL hybridization buffer containing 50% formamide, 4× saline-sodium citrate (SSC), 1× Denhardt's solution, 1 $mg \cdot mL^{-1}$ *Escherichia coli* tRNA, and 0.5 $mg \cdot mL^{-1}$ salmon sperm DNA, and then hybridized with gene-specific digoxigenin (DIG)-labeled antisense or sense (control) RNA probes for *TfRR1* or *TfCKX5*. The RNA probes were prepared from PCR fragments with the T7 and SP6 promoter sequence of each gene with a DIG RNA Labeling Kit (Roche). The PCR fragments were generated with the primers listed in Table 4. DIG-labeled RNAs were synthesized by T7 (for sense probe) or SP6 (for anti-sense probe) RNA polymerases with a DIG RNA Labeling Kit (Roche). After purification by ethanol precipitation, the RNAs were used as probes. Hybridization was performed with each probe at a concentration of 800 $ng \cdot mL^{-1}$ in hybridization buffer at 62°C overnight. After hybridization, the sections were washed in 0.2× SSC at 65°C for 2 h, and then in NT buffer (0.15 M NaCl, 0.1 M Tris-HCl, pH 7.5) at room temperature. After treatment with 1% blocking reagent (Roche) for 1 h, the sections were incubated with diluted (1:500) anti-DIG-AP (Roche) for 1 h. Chemical staining was performed with NBT/BCIP solution (Roche). Hybridization analyses were conducted independently in triplicate using independent CPPU-treated flower buds.

3. Results

3.1. cDNA cloning and phylogenetic analyses of torenia type-A *RR* and *CKX* genes

Two type-A *RR* (*TfRR1* and *2*) and five *CKX* (*TfCKX1*, *2*, *3*, *4*, and *5*) genes were isolated from torenia cDNA. The deduced amino acid sequences of the isolated genes were highly

homologous to *Arabidopsis* type-A RRs (ARRs) and CKXs, respectively. In addition to the conserved amino acid sequence of Asp and Lys that needs His-Asp phosphorelay (Fig. 3), the short C-terminal sequence without a GARP domain suggested that TfRR1 and 2 are type-A RRs (D′Agostino et al., 2000; Mizuno, 2005). In amino acid sequences of C-terminal region, TfRR1 had a characteristic Asp, Ser, and Thr rich sequences as those of ARR7 and ARR15 (D′Agostino et al., 2000). All TfCKXs had a conserved FAD binding domain and cytokinin binding domain (Schmülling et al., 2003).

The phylogenetic analysis showed that *TfRR1* belonged to the same clade as *ARR5*, *6*, *7*, and *15* which are known to be induced by cytokinin and repressed specifically in the shoot apex by *WUSCHEL* (D′Agostino et al., 2000; Leibfried et al., 2005), and *TfRR2* belonged to the same clade as *ARR16* and *17* (Fig. 4A). Similarly, *TfCKX1*, *2*, *3*, *4*, and *5* were homologous to *AtCKX6*, *AtCKX5*, *AtCKX7*, *AtCKX1*, and *AtCKX3*, respectively (Fig. 4B).

3.2. Induction of *TfRR* and *TfCKX* genes in floral organs by CPPU treatment

The results of qPCR analyses showed low expression of *TfRR1* in all floral organs of non-treated flower buds; however, CPPU treatment increased the expression approximately 4-fold in the stamen and pistil, approximately 8-fold in the sepal, and approximately 10-fold in the petal, respectively (Fig. 5A). In contrast, *TfRR2* expression was very low and induction of the expression by CPPU was unclear (Fig. 5A). Of all *TfCKX*s, *TfCKX5* was more highly expressed than the other *TfCKX*s in all floral organs of non-treated flower buds, suggesting that *TfCKX5* mainly functions in the flower of torenia (Fig. 5B). Furthermore, the expression of *TfCKX5* was clearly induced by CPPU treatment in all floral organs, whereas no induction of *TfCKX1*, *TfCKX2*, or *TfCKX4* was observed in any floral organ. Although *TfCKX3* was induced by CPPU in the sepal and petal, the expression was much lower than that of *TfCKX5* (Fig. 5B).

3.3. Expression profiles of *TfRR1* and *TfCKX5* in CPPU or BA-treated flower buds

The expression of *TfRR1* was induced from 1 day after CPPU treatment in all floral organs (Fig. 6A). The expression was maintained at a high level until 5 days after the treatment, and decreased 7 days after the treatment (Fig. 6A). Approximately the same expression pattern was observed in *TfCKX5*; expression was induced from 12 h after the treatment in the petal, 1 day in the stamen and pistil, and 2 days in the sepal and was maintained at a high level until 5 days and decreased 7 days after the treatment (Fig. 6B). In contrast, BA treatment increased the expression of both *TfRR1* and *TfCKX5* 1–3 h after the treatment only in the sepal, and the level decreased to the same level observed in the control 6 h after the treatment (Fig. 6A, B). The expression level of those genes in the petal, stamen, and pistil was not changed by BA treatment (Fig. 6A, B).

3.4. Spatial pattern of *TfRR1* and *TfCKX5* expression in CPPU-treated flower buds

To clarify the distribution pattern of cytokinin signals when wide (Fig. 7A-k) and narrow paracorollas (Fig. 7B-k) or serrated petal (Fig. 7C-k) are induced, expression of *TfRR1* and *TfCKX5* in flower buds after CPPU treatment at the sepal development stage (Stage 3), the early corolla development stage (Stage 5), and the middle corolla development stage (Stage 6) was analyzed.

The results of *in situ* hybridization showed that, in non-treated flower buds of Stage 3 and 4, weak signals of both *TfRR1* and *TfCKX5* were detected in the stamen and pistil primordia (Fig. 7A-a, b, d, f, g, i). When CPPU was applied to flower buds at Stage 3, strong expression of both *TfRR1* and *TfCKX5* was detected in the stamen and pistil primordia 3 days after the treatment and the area of expression extended to the adaxial side of the sepals (Fig. 7A-c, h). In particular, *TfCKX5* was strongly expressed in the abaxial side of the stamen

primordia, which is the site of initiation of the wide paracorolla (Fig. 7A-h). At 7 days after CPPU treatment, when the primordia of the wide paracorollas were initiated, strong expression of both *TfRR1* and *TfCKX5* was observed not only in the stamen and pistil primordia, but also in the primordia of the wide paracorollas (Fig. 7A-e, j).

Low expression of both *TfRR1* and *TfCKX5* was detected in the stamen and pistil primordia at Stage 5 of non-treated flower buds, and the expression was limited to the anther and ovule at Stage 7 (Fig. 7B-a, b, d, f, g, i). When CPPU was applied to flower buds at Stage 5, both genes were strongly expressed in the stamen and pistil 3 days after the treatment. *TfRR1* was expressed in the entire petal, whereas *TfCKX5* was strongly expressed in the middle and basal parts of the petal; the middle part of the petal is the site of initiation of the narrow paracorolla (Fig. 7B-c, h). In the flower buds 7 days after CPPU treatment, strong expression of both *TfRR1* and *TfCKX5* was observed in the stamen and pistil; however, expression was limited to the anthers and ovule, as observed in non-treated flower buds (Fig. 7B-d, e, i, j). Furthermore, strong expression of both genes was observed in the middle to the apical part of the petal, whereas the expression level was low in the basal part of the petal (Fig. 7B-e, j).

When CPPU was applied to flower buds at Stage 6, both *TfRR1* and *TfCKX5* were strongly expressed in the anther, pistil, and middle to apical part of the petal 3 days after the treatment, whereas weak expression of both genes was detected in the anther and ovule of non-treated flower buds (Fig. 7C-a, b, c, f, g, h). However, the expression of both genes in CPPU-treated flower buds was very low at the basal part of both the petal and stamen (Fig. 7C-c, h). The site of high expression of both genes 7 days after CPPU treatment was limited to the apical part of the petal, which corresponds to the limb of the opened flower (Fig. 7C-e, j).

4. Discussion

The expression of *TfRR1* and *TfCKX5* is markedly increased in all floral organs by CPPU treatment, suggesting these genes function as indicators of cytokinin signals. Furthermore, the expression profiles of *TfRR1* and *TfCKX5* in CPPU and BA-treated floral organs clearly show that cytokinin signals are greatly increased by CPPU treatment and the high level continues until 5 days after the treatment when the earliest CPPU-induced morphological changes in flower buds were observed (Nishijima and Shima, 2006). It has been shown that BA treatment caused no morphological change in torenia (Nishijima and Shima, 2006). Those observations coincide with the results that cytokinin signals were not elevated by BA treatment except in the sepal (Fig. 6A, B). Flower buds of torenia are completely enclosed with the sepals after initiation of the stamen and pistil (Stage 4). The chemical solution was not seemingly translocated into the other floral organs after being absorbed by the sepals; thus, elevation of cytokinin signals by BA treatment may have been limited to the sepals (Fig. 6A, B). In contrast, CPPU might have been translocated to other floral organs, and its effects were long-lasting in flower buds (Fig. 6A, B). Different chemical structures between BA and CPPU might cause the different extent of translocation and lasting (Mok and Mok, 2001). BA, which has an isoprenoid side chain, may markedly be degraded by CKX activity elevated by BA treatment. In contrast, CPPU, a diphenylurea compound, is not degraded by CKX (Bilyeu et al., 2001).

These results also indicate that cytokinin signals are elevated by CPPU treatment at the paracorolla initiation site. When CPPU was applied to flower buds at Stage 3, cytokinin signals were elevated on the abaxial side of the stamen primordia, which is the site of initiation of the wide paracorolla, although high levels of cytokinin signals were also observed in the petals (Figs. 7A-c, e, h, j and 8). When CPPU was applied to flower buds at

Stage 5, cytokinin signals were elevated in the petal and stamen at first, and later the elevated cytokinin signals were occurred in the middle part of the petal, which is the site of initiation of the narrow paracorolla (Figs. 7B-c, e, h, j and 8). The wide paracorollas of torenia are formed at the abaxial and lateral side of the stamen primordia (Nishijima and Shima, 2006). The narrow paracorollas are also formed on the lateral side of the stamen; however, the primordia of the narrow paracorollas are relatively separate from the stamen, because they are formed on the border between the limb and tube of a rather developed petal. Since the basal part of the stamen is fused with the tube in torenia, the basal part of the narrow paracorolla may be fused with the petal tube. Thus, the narrow paracorolla is seemingly formed just at the lateral side of the stamen, similar to the wide paracorolla, concerning its fusion to the tube. CPPU elevated cytokinin signals at the abaxial side of the basal part of the stamen when the wide paracorollas were induced, and at the middle and basal part of the petal and basal part of the stamen when the narrow paracorollas were induced (Figs. 7A, B and 8). These results suggest that the high level of cytokinin signals in CPPU-treated flower buds is localized to the site where the stipule of the stamen, i.e., the paracorolla, originates.

Localized auxin accumulation called ‘localized auxin maxima’ at the site of organ formation acts as a trigger of the organogenic process (Benková et al., 2003; Reinhardt et al., 2000). Cytokinins modulate the spatial distribution of auxin via regulation of auxin efflux, and it is evident that spatial distribution of distinct endogenous cytokinin levels is necessary to form localized auxin maxima (Pernisová et al., 2009), although the detailed relationship between the distribution pattern of endogenous cytokinin and that of auxin maxima is still unknown. In this experiment, CPPU caused localized strong cytokinin signals in flower buds of torenia, which was not observed in untreated flower buds (Fig. 7). Thus, it is probable that ectopic auxin maxima were formed by CPPU treatment, which triggered extra organ

formation, i.e., the paracorolla formation.

In contrast to the spatial distribution of the high levels of cytokinin signals observed when paracorolla was induced (Figs. 7A-c, h, 7B-c, h and 8), high levels of cytokinin signals were limited to the middle to apical part of the petal when the serrated petal was induced by CPPU (Figs. 7C-c, h, and 8). CPPU changes the arrangement of vascular bundles from an intensively branched arrangement to a non-branched parallel one in the whole limb, which causes the serrated petals (Nishijima and Shima, 2006). Therefore, the site of CPPU-induced high levels of cytokinin signals, i.e., the whole limb, corresponds to the site of the morphological changes causing the serrated petal, i.e., changes in the spatial arrangement of vascular bundles (Figs. 7C and 8).

In summary, CPPU induces marked long-term elevation of cytokinin signals in flower buds, inducing changes in flower morphology. Furthermore, localization of high levels of cytokinin signals to the sites of morphological changes at specific floral stages induces formation of the paracorolla and serrated petals. It may accordingly be possible to induce a desired flower morphology by localizing cytokinins to a particular site in flower buds at an appropriate floral stage. For example, a wide paracorolla is induced when cytokinin accumulates at the abaxial side of stamen primordia at the sepal development stage, a narrow paracorolla is induced when cytokinin accumulates in the region from the basal part of the stamen to the middle of the petal during the early corolla development stage, and serrated petals are induced when cytokinin accumulates in the limb at the middle corolla development stage.

Table 1. Primers used for isolation of cDNAs of *TfRR* and *TfCKX* genes.

Target gene	Direction	Primer sequence
TfRRs	forward	5'-CAYGTIYTIGCIGTIGAYGA-3'
	reverse	5'-YTSIGCICCYTCYTCIARRCA-3'
TfCKXs	forward	5'-GTIKCIGCIMGIGGICAIGGICA-3'
	forward	5'-TGGACIGAYTAYYTIYAYYTIACIGTIGG-3'
	forward	5'-GGIGGIYTIGGICARTTYGGIRTIATHAC-3'
	forward	5'-TGGGAIGTICCICAYCCITGGYTIAA-3'
	forward	5'-CCIGTITCITGGACIGAYTAYTTRTA-3'
	reverse	5'-TGICCIGGIGMIARIAKIGYYHKIGGRTC-3'
	reverse	5'-TTIARCCAIGGRTGIGGIACITCCCA-3'
	reverse	5'-GTDATIAYICCRAAYTGICCIARICCICC-3'
	reverse	5'-TGICCIGGIGAYAAIAGIITYTTIGGRTCRAA-3'

Table 2. Primers used for isolation of full-length cDNAs of *TfRR* and *TfCKX* genes.

Target gene	Direction	Primer sequence
TfRR1	forward	5'-TTACCTCTCATCACTGTAACGCA-3'
	reverse	5'-AATGAAACAACTGACTTGGAAATTC-3'
TfRR2	forward	5'-TACTATGATTCTGTAGGTTGGCGT-3'
	reverse	5'-GCAGCGCACCTCAATTATAAG-3'
TfCKX1	forward	5'-TTCCCCTCCTCATCTTACACC-3'
	reverse	5'-TTGCCATAAAGCGTCGAAAT-3'
TfCKX2	forward	5'-CACAAAATCACGCACTGACACA-3'
	reverse	5'-CAGAATAATTAACAATTACCATTGCG-3'
TfCKX3	forward	5'-CTTTCCTTCCTACGGTCAAATC-3'
	reverse	5'-TGAAGCAAAGGCAGGACTAAC-3'
TfCKX4	forward	5'-ACTTTCAAGAATCTCGACAGCA-3'
	reverse	5'-AATTCGATAGTAAAAGCGCATA-3'
TfCKX5	forward	5'-ACCACACTAAAATCATACTCTCCTC-3'
	reverse	5'-CCACTAATATTAAAAATGTAAACTCCAC-3'

Table 3. Primers used for qPCR analysis of *TfRR* and *TfCKX* genes.

Target gene	Product length	Direction	Primer sequence
TfRR1	155 bp	forward	5'-AGATTATTAGTTGTTCTCCTCTGT-3'
		reverse	5'-CTTGGAAATTCAACCACATCA-3'
TfRR2	155 bp	forward	5'-GCTGCAATGTTGAAGAACATG-3'
		reverse	5'-CAGCGCACCTCAATTATAAG-3'
TfCKX1	124 bp	forward	5'-CCCATATCAGTTTTGTGACACA-3'
		reverse	5'-CATACTTACAGTTGTTGAGGAGGA-3'
TfCKX2	158 bp	forward	5'-CCGTTGATTAATCCTAGTG-3'
		reverse	5'-AGAGAGACAATCACGATACATC-3'
TfCKX3	169 bp	forward	5'-TCAAGAAATTGGAAGAAGGCC-3'
		reverse	5'-CCAATATATAATTCATTTCCCCACT-3'
TfCKX4	146 bp	forward	5'-CCAAAGACTTGGAACAACAGTG-3'
		reverse	5'-GATTGCTCTACATCTGAGAGACC-3'
TfCKX5	117 bp	forward	5'-AGAAAGTTGAAGTTCGATCCCG-3'
		reverse	5'-TTACATTCCACAGACCACAACTG-3'
TfACT3	145 bp	forward	5'-TGCAGTAAAGTGTATTGTGGAAG-3'
		reverse	5'-GGAACTATCTGGGTAGGATC-3'

Table 4. Primers used to synthesize probes for *in situ* hybridization analysis of *TfRR1* and *TfCKX5* genes.

Target gene	Product length	Direction	Primer sequence
TfRR1	180 bp	forward	5'-GAATAATACGACTCACTATAGGGTCAGAGATTTCGTTATCAAAGGC-3'
		reverse	5'-TGCATTTAGGTGACACTATAGAAATGAAACAACTGACTTGGAAATTC-3'
TfCKX5	154 bp	forward	5'-GAATAATACGACTCACTATAGGGCTGCTGTTGTACCAGATGAAGAC-3'
		reverse	5'-TGCATTTAGGTGACACTATAGAACCACTAATATTAAAAATGTAAACTCCAC-3'

T7 and SP6 promoter sequences were underlined.

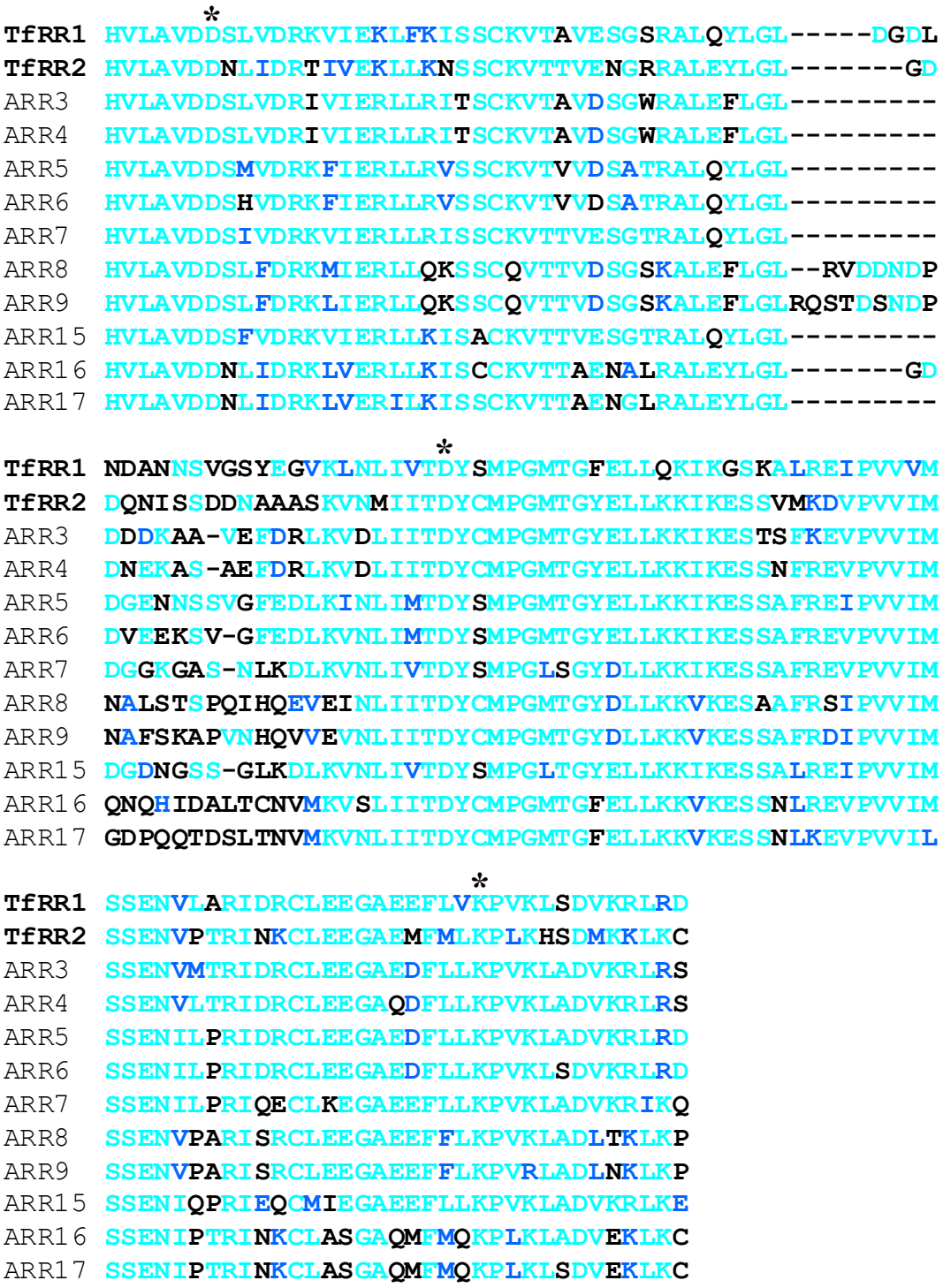

Fig. 3. Amino acid sequence of receiver domain of torenia type-A response regulator (RR) and the sequence homology with *Arabidopsis* type-A RR. Asterisks represent conserved amino acid sequences in RRs for phosphorelay. Accession numbers were as follows: torenia type-A RR genes, TfRR1, AB740033; TfRR2, AB740034; *Arabidopsis* type-A RR genes, ARR3, At1g59940; ARR4, At1g10470; ARR5, At3g48100; ARR6, At5g62920;

Be continued

ARR7, At1g19050; ARR8, At2g41310; ARR9, At3g57040; ARR15, At1g74890; ARR16, At2g40670; ARR17, At3g56380. Identical and homologous amino acid was indicated by light blue and blue letters, respectively.

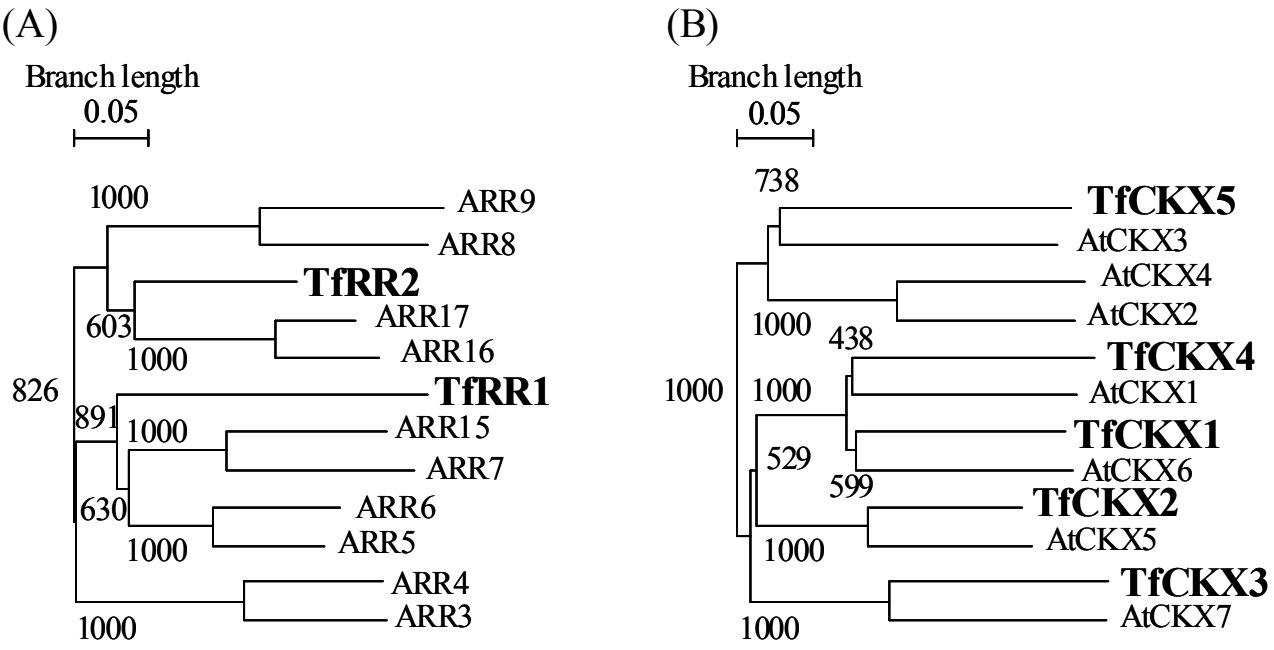

Fig. 4. Phylogenetic tree of type-A RR and CKX in torenia and *Arabidopsis*. Bootstrap values from 1000 replicates are indicated near the branching points. Accession numbers of CKX genes were as follows: torenia CKX genes, TfCKX1, AB740035; TfCKX2, AB740036; TfCKX3, AB740037; TfCKX4, AB740038; TfCKX5, AB740039; *Arabidopsis* CKX genes, AtCKX1, At2g41510; AtCKX2, At2g19500; AtCKX3, At5g56970; AtCKX4, At4g29740; AtCKX5, At1g75450; AtCKX6, At3g63440; AtCKX7, At5g21482. Accession numbers of type-A RR genes were the same as described in legend of Fig. 3.

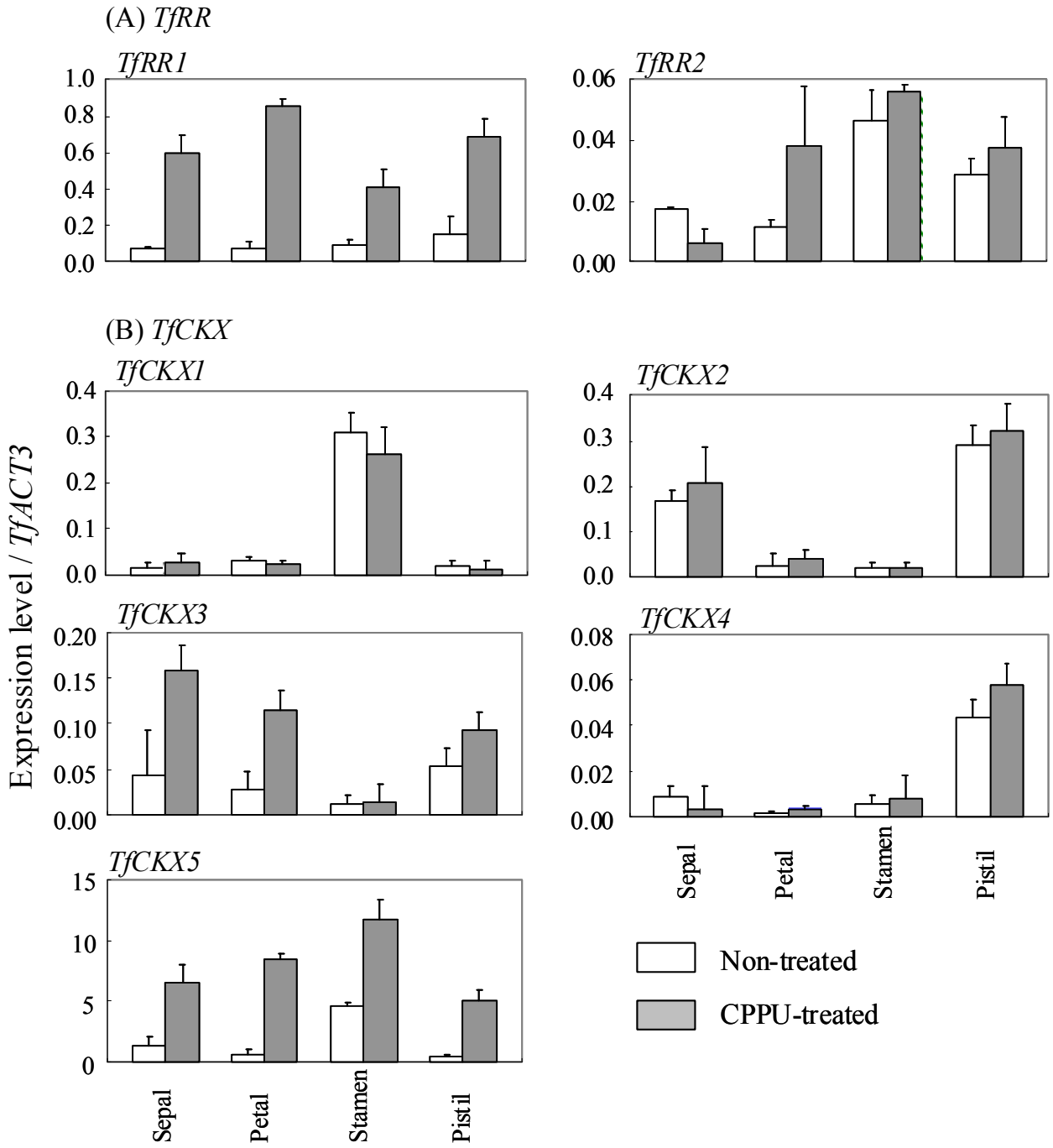

Fig. 5. Quantitative real-time PCR analyses of *TfRR* and *TfCKX* in floral organs 2 days after CPPU treatment. The expression levels of *TfRRs* (A) and *TfCKXs* (B) are shown as values relative to that of *TfACT3*, which was used as an internal standard. Open and gray columns indicate non-treated and CPPU-treated floral organs, respectively. Vertical bars indicate SE (n = 3).

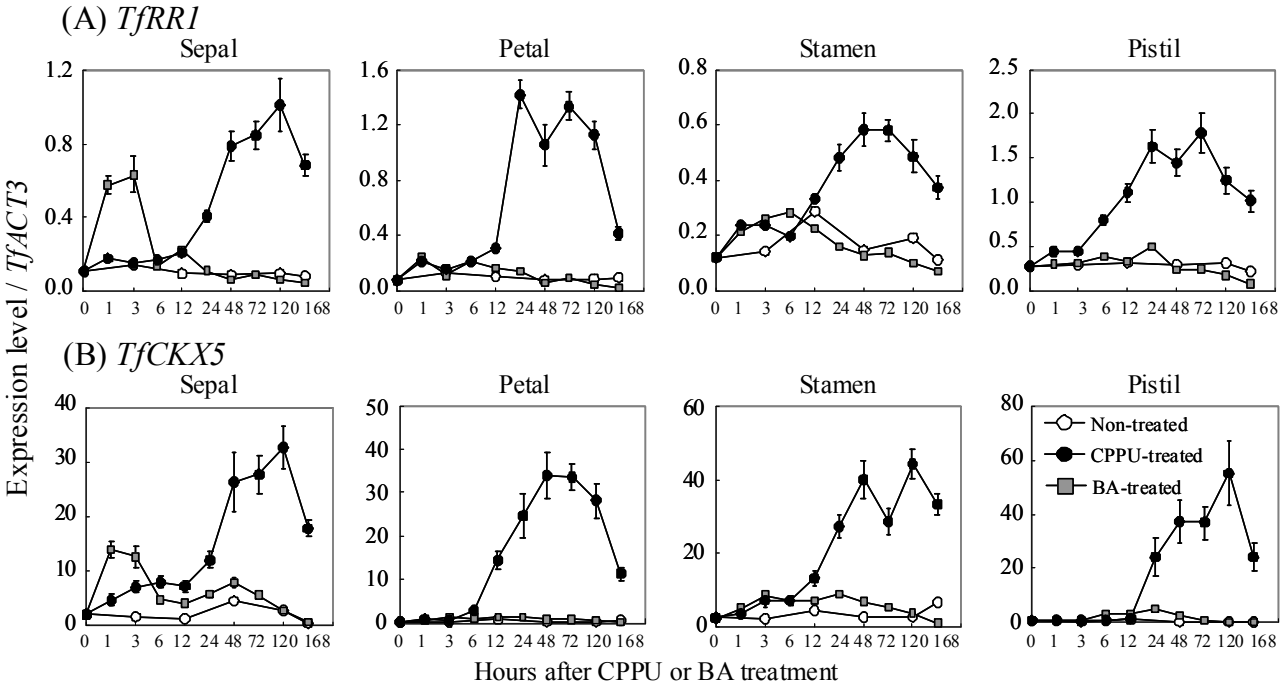

Fig. 6. Quantitative real-time PCR analyses of *TfRR1* and *TfCKX5* in CPPU or BA-treated floral organs. The expression levels of *TfRR1* (A) and *TfCKX5* (B) are shown as values relative to that of *TfACT3*, which was used as an internal standard. Open circles, closed circles, and gray squares indicate non-treated control, CPPU or BA-treated flower buds, respectively. Vertical bars indicate SE (n = 3).

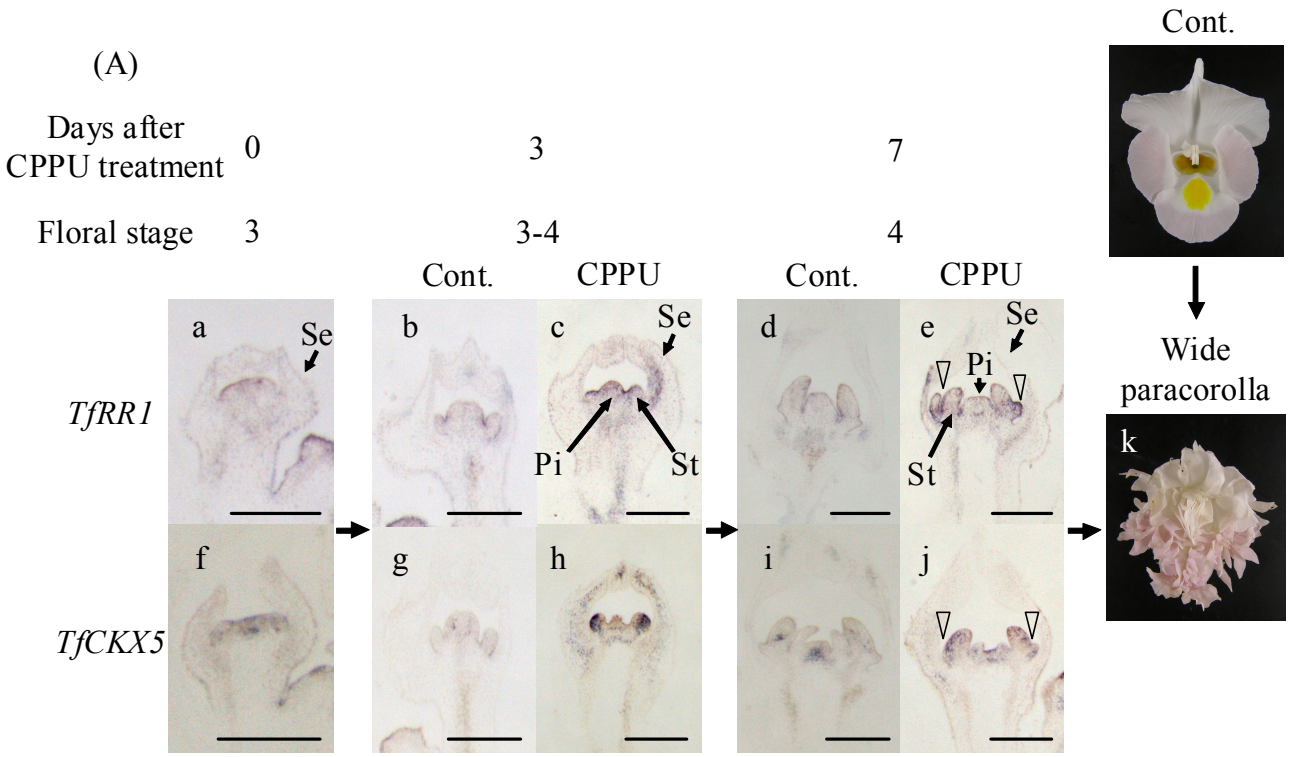
(A)
Days after CPPU treatment
0
3
7
Floral stage
3
3-4
4
Cont.
CPPU
Cont.
CPPU
Cont.
Wide paracorolla
TfRR1
TfCKX5
a
b
c
d
e
f
g
h
i
j
k
Se
Pi
St

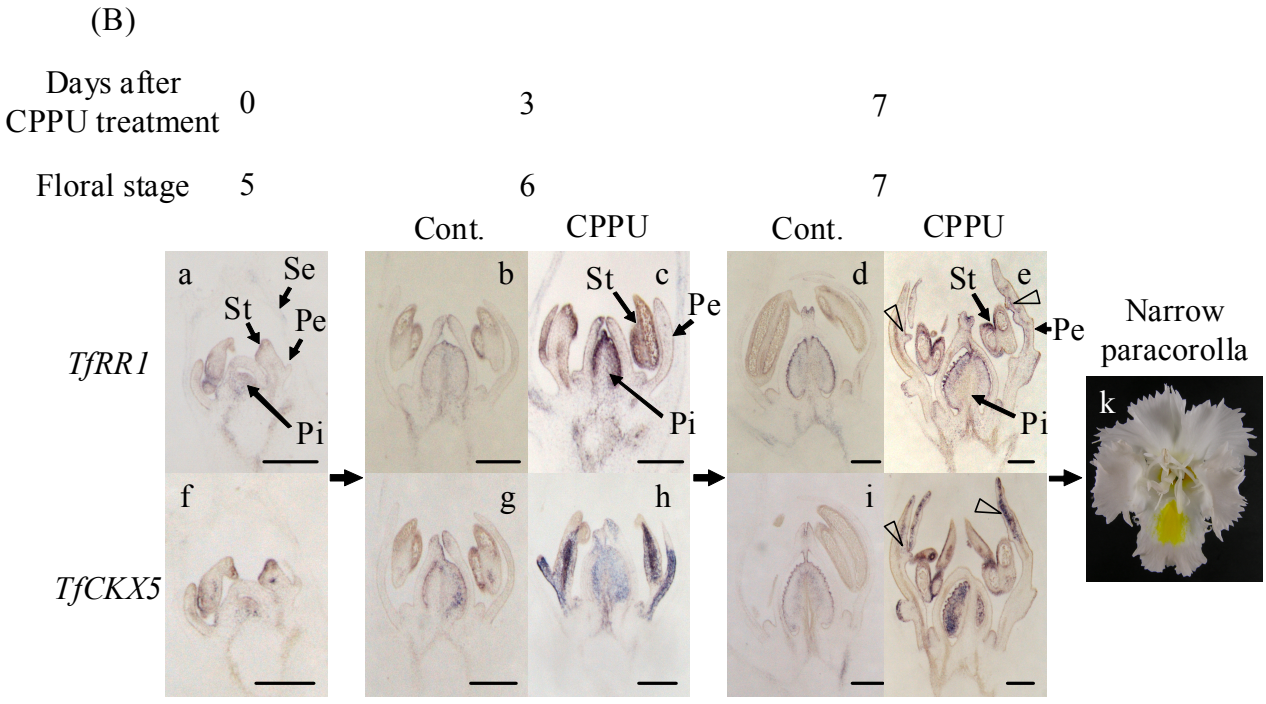
(B)
Days after CPPU treatment
0
3
7
Floral stage
5
6
7
Cont.
CPPU
Cont.
CPPU
Narrow paracorolla
TfRR1
TfCKX5
a
b
c
d
e
f
g
h
i
k
Se
St
Pe
Pi

Be continued

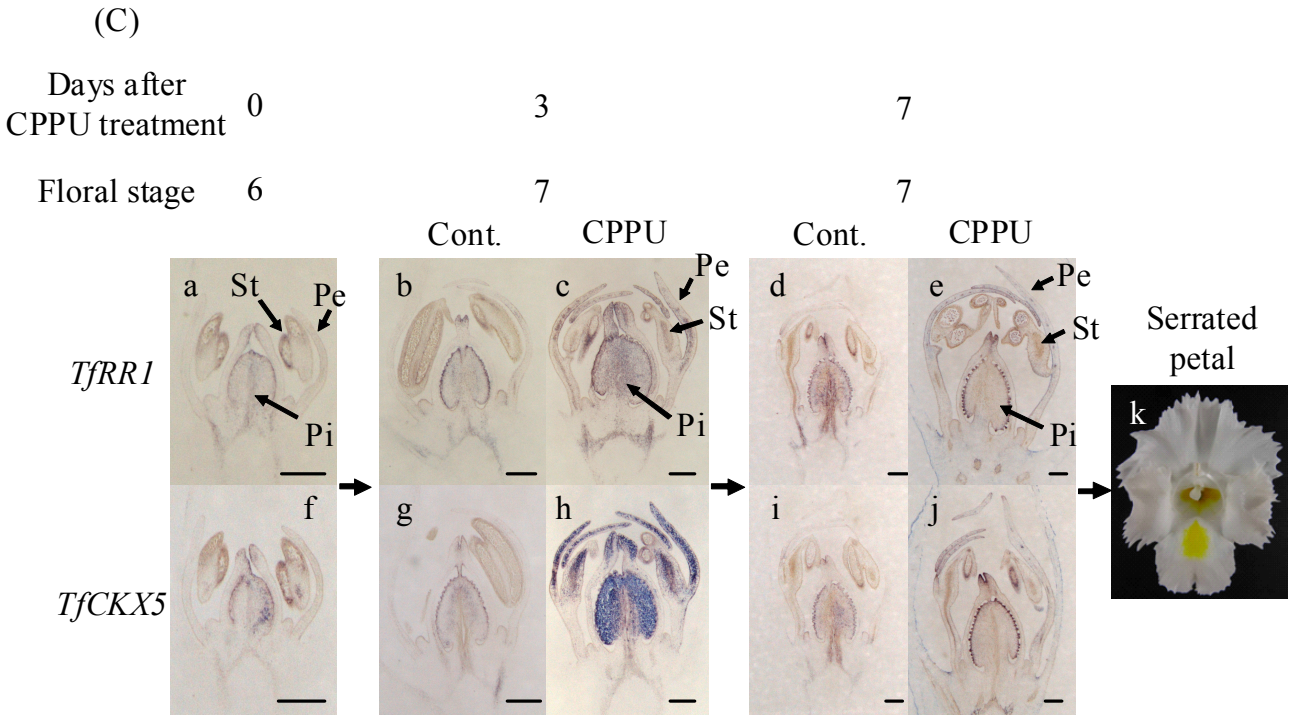

Fig. 7. *In situ* hybridization of *TfRR1* and *TfCKX5* in flower buds treated with CPPU. CPPU treatment induces formation of a wide paracorolla in (A), a narrow paracorolla in (B), and a serrated petal margin in (C). CPPU-treated flower buds were collected at 3 (c, h) or 7 days (e, j) after the treatment, whereas non-treated flower buds were collected at the corresponding stage (a, b, d, f, g, i). The representative data at each floral stage inducing each flower morphology are shown. Panel k shows flower morphology induced by CPPU treatment at each floral stage. Panel b, d, g, and i in (B) are the same as a, b, f, and g in (C), respectively, because each shows the same stage of non-treated flower buds. Floral stages were defined as described in Nishijima and Shima (2006): Stage 3, development of sepals; Stage 4, initiation of sex organs and petals; Stage 5, early corolla development; Stage 6, middle corolla development; Stage 7, late corolla development. Triangles represent the initiation site of paracorollas. Scale bars = 200 μm.

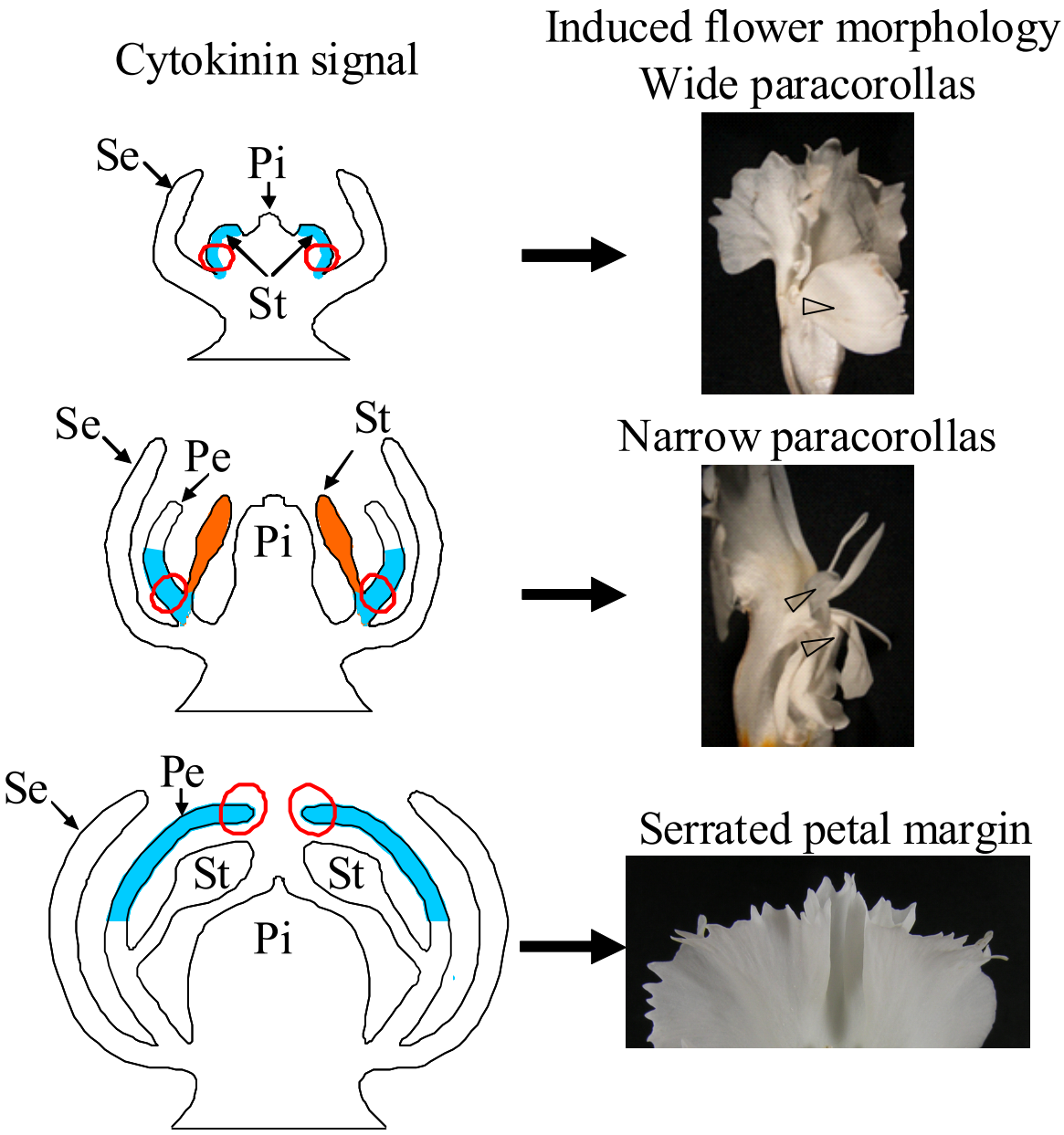

Fig. 8. Hypothetical model accounting for the effect of CPPU-induced localization of enhanced cytokinin signal in flower buds to flower morphology in torenia. Floral organ with enhanced cytokinin signal is colored with blue in the petal and orange in the stamen. Triangles and red circles indicate the site of paracorolla initiation and serrated petal margin. Pe, Petal; Pi, Pistil; Se, Sepal;

Chapter 3

Role of floral homeotic genes in the regulation of CPPU-induced paracorolla morphology

1. Introduction

The paracorolla is a floral organ observed only in several species. Morphology of the paracorolla has some variety, e.g., synpetalous infundibular one in *Narcissus*, acropetalous one in *A. majus*, or acerose one in *Passiflora*. The decorative appearance of the paracorollas contributes to the unique attractiveness of these species. Morphologically, the paracorolla resembles the petals; however, it originates from the stipule of the stamen in *Narcissus*, *Asclepias*, and *A. majus*, and from the receptacle in *Passiflora* (Troll, 1957; Yamaguchi et al., 2010). In *A. majus*, the paracorolla belongs to whorl 3 as in the stamen because of its origin from the stipule of the stamen. However, the anatomical characteristics of the paracorolla are petaloid, and the expression of floral homeotic genes shows petal-like pattern (Yamaguchi et al., 2010). Thus, paracorolla morphology is regulated by the expression patterns of floral homeotic genes as in the other floral organs.

In CPPU-treated torenia, the paracorollas are formed on lateral sides of the stamen. This arrangement is identical to that of leaf and leaf bases which develop into the stipules. Thus, CPPU-induced paracorollas apparently originate from the stipule of the stamen as in *A. majus* (Nishijima and Shima, 2006; Yamaguchi et al., 2010). The paracorollas have two different morphologies depending on the floral stage at CPPU treatment, i.e., wide and narrow paracorollas (Nishijima and Shima, 2006). The wide paracorollas are pigmented with anthocyanin and morphologically resembles the petals. In contrast, the narrow paracorollas

have a stamen-like, slender morphology. Some of the narrow paracorollas are unpigmented like the filament of the stamens, while the others are pigmented like the petals. Thus, it appears that floral homeotic genes are involved in the regulation of paracorolla morphology.

In this chapter, we anatomically analyzed the two types of torenia paracorolla in terms of the identity as floral organs. Furthermore, we isolated and analyzed the expression patterns of floral homeotic genes in CPPU-treated flower buds. Based on these results, the role of floral homeotic genes in the regulation of paracorolla morphology is discussed.

2. Materials and Methods

2.1. Plant materials

Plant materials and growth conditions were the same as described in Chapter 2.2.1.

2.2. CPPU treatment

Preparation and treatment of CPPU were the same as described in Chapter 2.2.2. Flower buds longer than 8 mm were removed before the treatment, because paracorolla formation is not induced in developed flower buds.

2.3. Morphological analyses

Flowers with and without paracorollas were used for morphological analyses. The raw flower was directly subjected to scanning electron microscopy (SEM; VE-7800, Keyence, Osaka, Japan) to observe the surface structure.

For the anatomical analyses, the floral organs were fixed, dehydrated, and embedded in paraffin as described in Chapter 2.2.5. Transverse sections (10 μm thick) of the paraffin-embedded tissues were prepared with a rotary microtome (Leica). The sections were

dewaxed and rehydrated as described in Chapter 2.2.5. After staining with 0.5% (w/v) toluidine blue, the tissues were observed by stereomicroscopy.

For observations of vascular bundles, fixed samples were immersed twice in 70% (v/v) ethanol for 1 h, then incubated for 1 h in a chloral hydrate solution (chloral hydrate, 8 g; glycerol, 1 mL; distilled water, 4 mL) to make the tissues transparent. The samples were then subjected to dark-field stereomicroscopy.

2.4. cDNA cloning of floral homeotic genes and phylogenetic analysis

The methods for total RNA isolation from young flower buds using an RNeasy Plant Mini Kit (Qiagen) and RNase-Free DNase Set (Qiagen), and cDNA synthesis using a CapFishing Full-length cDNA Premix Kit (Seegene) were the same as described in Chapter 2.2.3. Degenerate primers of the floral homeotic genes were designed using highly conserved regions of each class of floral homeotic genes, and partial cDNAs were isolated using the degenerate primers. Degenerate primer sequences were listed in Table 5. The nucleotide sequence of each cDNA fragment was analyzed as same procedure as in Chapter 2.2.3. Based on the sequences of the PCR fragments, gene-specific primers were designed and 5′ and 3′ RACE were performed, and full-length cDNAs for each gene were isolated as same procedure as in Chapter 2.2.3. using the primers listed in Table 6. The nucleotide sequence of each PCR fragment was analyzed and registered in DDBJ. Accession numbers are listed in the legend for Fig. 11.

Phylogenetic analysis was performed using predicted amino acid sequences of the cloned floral homeotic genes from torenia and those from other plants as the same procedure as described in Chapter 2.2.3.

2.5. *In situ* hybridization

Flower buds 7 days after CPPU treatment and those of controls not treated with CPPU were used for *in situ* hybridization. The samples were fixed and embedded in paraffin, and the tissues were sectioned (8 μm thick) as described in Chapter 2.2.5. *In situ* hybridization was performed as described in Chapter 2.2.5, except the hybridization temperature and the method of RNA probe preparation were modified.

Gene-specific DIG-labeled antisense or sense (control) RNA probes were prepared from vectors harboring PCR fragments of each floral homeotic gene with the DIG RNA Labeling Kit (Roche). The PCR fragments inserted into the pGEM-T Easy vector (Promega) were generated with the primers listed in Table 7. The vectors were cut by *Nae* I and *Spe* I restriction enzymes when used with T7 RNA polymerase or *Nco* I and *Pvu* II restriction enzymes for SP6 RNA polymerase. DIG-labeled RNAs were synthesized by either of the RNA polymerases with a DIG RNA Labeling Kit (Roche). After purification by ethanol precipitation, the RNAs were used as probes. Hybridization was performed with each probe at a concentration of 800 $ng \cdot mL^{-1}$ in hybridization buffer at 65°C overnight. Washing to detection procedures after hybridization were the same as described in Chapter 2.2.5. Hybridization analyses were conducted independently in triplicate using independent CPPU-treated flower buds.

2.6. Quantitative real-time PCR analysis

The methods for total RNA isolation from the sepals, petals, paracorollas, stamens, and pistils of flower buds with or without CPPU treatment using an RNeasy Plant Mini Kit (Qiagen) and RNase-Free DNase Set (Qiagen), and cDNA synthesis using a CapFishing Full-length cDNA Premix Kit (Seegene) were the same as described in Chapter 2.2.4. Gene-specific primers for torenia floral homeotic genes were designed for the 3′-terminal regions of the open reading frame and the 3′-untranslated regions of each gene. Primer

sequences and the lengths of PCR products used for qPCR reactions were listed in Table 8. As described in Chapter 2.2.4, *TfACT3* was used as an internal standard. qPCR and data analysis was performed as the same procedure as described in Chapter 2.2.4. Fluorescence was measured at the end of the extension phase at 75°C for *TfSQUA* and *TfFAR*, at 76°C for *TfDEF*, at 77°C for *TfGLO* and *TfACT3*, and at 79°C for *TfPLE1*, to avoid calculating non-specific PCR products. The ratio of the expression of each floral homeotic gene to that of *TfACT3* was calculated. Expression analyses were conducted independently in triplicate.

3. Results

3.1. Morphological analyses of the paracorollas

Wide paracorollas were colored with anthocyanin and morphologically resembled the petal (Fig. 9a, b). The narrow paracorollas had various morphologies, typically flat, a spoon-like top with a cylindrical base, or a rod with two lobes (Fig. 9c–e). The narrow paracorollas with two lobes at the tip morphologically resembled the two anthers developed at the tip of the filament (Fig. 9e, f). The narrow paracorollas were either colored like the petal or colorless like the stamen (Fig. 9a, c–e). Thus, the narrow paracorollas had either stamen-like or petal-like morphological characteristics.

Observing the surface structure by SEM showed that conical cells were arranged on the petal epidermis (Fig. 10a), whereas the epidermis of the filament of the stamen had slender cells and a smooth surface (Fig. 10e). Conical cells were arranged on the epidermis of the wide paracorollas as in the petal (Fig. 10b). In contrast, the epidermis of the narrow paracorollas had either conical or slender cells (Fig. 10c, d). Within the category of the narrow paracorollas, wider ones as shown in Fig. 9c tended to have conical epidermal cells, while narrower ones as shown in Fig. 9d and 9e tended to have slender epidermal cells. This

indicates that the epidermis of the narrow paracorollas is either petal- or filament-like.

Analyses of transverse sections of the floral organs showed that the parenchyma of the petals had sparsely distributed round cells (Fig. 10f). In contrast, densely distributed slender cells were observed in the parenchyma of the filament (Fig. 10i). In the wide paracorollas, parenchyma with sparsely distributed round cells resembled that of the petal (Fig. 10g). In the parenchyma of the narrow paracorollas, cells were distributed sparsely as in the petal; however, the cells were slender like those of the filament (Fig. 10h). Within the category of the narrow paracorollas, wider ones, as shown in Fig. 9c, tended to have parenchyma morphologically resembling that of the wide paracorollas, while narrower ones, as shown in Fig. 9d and 9e, tended to have parenchyma morphologically resembling that of the filament.

Furthermore, observation of vascular bundles showed that the petal had thin and extensively branched vascular bundles (Fig. 10j). In contrast, thick and unbranched bundles were observed in the filament (Fig. 10o). The wide paracorollas had extensively branched vascular bundles like the petal (Fig. 10k), while thick and scarcely branched bundles were observed in the narrow paracorollas (Fig. 10l). The narrow paracorollas with a stamen-like morphology, such as the cylindrical paracorolla and the paracorolla with two lobes, had thick and unbranched vascular bundles like the filament (Fig. 10m, n).

These results indicate that the wide paracorollas induced by CPPU treatment have the same morphological and anatomical characteristics as in the petal (Figs. 9b and 10b, g, k), whereas the narrow paracorollas have either petal-like or stamen-like characteristics (Figs. 9c–e and 10c, d, h, l–n).

3.2. cDNA cloning and phylogenetic analysis of floral homeotic genes from torenia

To investigate whether the petal- and stamen-like characteristics observed in the wide and narrow paracorollas are controlled by floral homeotic genes, we isolated the floral homeotic

genes from torenia. One class A gene, two class B genes, and two class C genes were isolated from torenia cDNA. The results of a database search using the deduced amino acid sequences suggested that all of the isolated genes had MADS and K domains, which are highly conserved in MADS-box genes (Fig. 11). These torenia genes were classified into predicted classes by phylogenetic analysis based on the deduced amino acid sequences of MADS-box floral homeotic genes in other plant species (Fig. 12). Furthermore, the euAP1 motif and farnesylation motif, which are conserved in euAP1 class A genes (Litt and Irish, 2003), were contained at the C-terminal of *TfSQUA* (Fig. 11A). AG motif I and II, which are conserved in class C genes (Kramer et al., 2004), were contained at the C-terminal of both *TfPLE1* and *TfFAR* (Fig. 11C). In class B genes, the PI motif in *TfGLO* and both the PI motif-derived sequence and euAP3 motif in *TfDEF*, which are conserved in class B genes, have been shown at the C-terminal of each gene (Sasaki et al., 2010; Fig. 11B); thus, these genes probably function as floral homeotic genes. Since these genes have a high similarity to those of *A. majus*, which like torenia belongs to the Lamiales, these genes were designated as *TfSQUA*, *TfDEF*, *TfGLO*, *TfPLE1*, and *TfFAR* (Fig. 12).

3.3. Expression analyses of floral homeotic genes in CPPU-induced paracorollas

The results of *in situ* hybridization of floral homeotic genes at the initiation of the wide paracorollas showed strong and clearly localized signals; however, at the initiation of the narrow paracorollas, the signals detected were relatively weak and their localizations were to some extent obvious (Fig. 13). In the primordia of the wide paracorollas, the class A gene, *TfSQUA*, was highly expressed in the basal position (Fig. 13A). Class B genes, *TfDEF* and *TfGLO*, were also highly expressed throughout the primordia (Fig. 13B). These expression patterns were the same as those observed for the petal (Fig. 13A, B). Low expression of class C genes *TfPLE1* and *TfFAR* was detected at the margin of the primordia (Fig. 13C).

However, in the primordia of the narrow paracorollas, *TfSQUA* and *TfPLE1* showed low expression only at the margin (Fig. 13A, C), while both *TfDEF* and *TfGLO* were expressed throughout the primordia (Fig. 13B). No substantial expression of *TfFAR* was detected (Fig. 13C). The organs used for *in situ* hybridization were selected based on SEM images of flower buds at the same developmental stages (Fig. 13D).

In the later stages of floral organ development, the results of qPCR analyses showed that, in the wide paracorollas, *TfSQUA*, *TfDEF*, and *TfGLO* were highly expressed, as in the petal (Fig. 14A, B), while *TfPLE1* and *TfFAR*, which were highly expressed in the stamen and pistil, had low expression, as in the sepal and petal (Fig. 14C). In the narrow paracorollas, *TfDEF* and *TfGLO* were also highly expressed, as in the petal and the wide paracorollas (Fig. 14B); however, *TfSQUA* expression was low, as in the stamen (Fig. 14A). Expression of *TfPLE1* and *TfFAR* was also low, as in the sepal and petal (Fig. 14C).

4. Discussion

Of the CPPU-induced paracorolla, class A and B genes were mainly expressed in the primordia of the wide paracorollas, suggesting petal-like expression patterns render wide paracorolla petaloid organs (Figs. 13A–C and 15). In contrast, class B genes were mainly expressed in the primordia of the narrow paracorollas (Fig. 13A–C). These expression patterns became more distinct during the later stages of paracorolla development (Fig. 14). That is, expression of both class A and C genes was low in the narrow paracorollas, as in the stamen and the petal, respectively, while class B genes were highly expressed, as in the petal and wide paracorolla (Fig. 14). This expression pattern may make the identity of the paracorolla unstable, because it is neither a petal nor stamen expression pattern (Fig. 15). Furthermore, this expression pattern may reflect the mixed petal and stamen morphological

characteristics of the narrow paracorollas (Figs. 9c–e and 13A–C). Thus, these results indicate that the expression patterns of floral homeotic genes at paracorolla primordia initiation determine paracorolla morphology (Fig. 15).

Because CPPU accumulates endogenous cytokinin in plant tissue, high concentrations of endogenous cytokinin induce paracorolla formation in torenia (Nishijima and Shima, 2006). It is known that the expression of floral homeotic genes is regulated by cytokinin (Estruch et al., 1993; Li et al., 2002). The effect of the elevated cytokinin level on the expression of floral homeotic genes could not be investigated because the CPPU-untreated flower buds had no paracorolla. However, it is unlikely that the elevated cytokinin level directly regulates the expression patterns of floral homeotic genes observed for the wide and narrow paracorollas, because CPPU treatment did not markedly change the expression of floral homeotic genes in the other floral organs, i.e., the sepals, petals, stamens, and pistils (Figs. 13 and 14).

As described above, paracorollas induced by CPPU treatment in torenia probably originate from the stipule of the stamen, like *A. majus* (Nishijima and Shima, 2006; Yamaguchi et al., 2010); therefore, the paracorollas belong to the same whorl as the stamen. In *A. majus*, class B and C genes are expressed in the anther, all of the class A, B, and C genes are expressed in the filament, and class A and B genes are expressed in the petaloid paracorolla. This gradient of expression pattern in the same whorl is critical for the paracorolla to develop into a petaloid organ (Yamaguchi et al., 2010). It has also been reported that the expression pattern of floral homeotic genes differs between the tube and limb of the petal in torenia (Niki et al., 2006b); therefore, the different expression patterns of floral homeotic genes in the wide and narrow paracorollas may have been caused by the site where they were formed. The wide paracorollas were initiated at the basal end of the petal during the early developmental stage (Fig. 13D). In this position, class A and B genes were expressed (Fig. 13A–C). The narrow paracorollas were formed in the middle sections of more developed petals (Fig. 13D). Class

B genes were mainly expressed at this site, while the expression of both class A and C genes was low, as in the stamen and the petal, respectively (Fig. 13A–C). These expression patterns persisted during subsequent flower development (Niki and Nishijima, 2008, Fig. 14). These data clearly suggest that the expression pattern of floral homeotic genes in paracorollas is determined by the site where the paracorolla is formed.

In summary, these results suggest that the expression pattern of floral homeotic genes determines paracorolla morphology, and the expression pattern in paracorollas is determined by the site where the paracorolla is formed. Paracorolla morphology may thus be artificially changed via changes in the expression of floral homeotic genes at the primordia initiation site using mutagenesis or transgenic technologies.

Table 5. Degenerate primers used for isolation of cDNAs of floral homeotic genes.

Target gene	Direction	Primer sequence
Class A genes	forward	5'-ATGGGIAGRGGIARRGTISARYTRA-3'
	reverse	5'-CATIAGRTTYTTYCTIGWICGDAT-3'
Class B genes	forward	5'-ATGGCIMGWGGIAARATYCARATYAA-3'
	reverse	5'-TCITCICCYTTYARRTGYCTIAG-3'
	reverse	5'-TTYTTYYTRDWIGTITCRRTYTGRKT-3'
Class C genes	forward	5'-ATGGGIMGIGGIAARATYGARATHAA-3'
	reverse	5'-ARBAIYTCRTTYTTYTTIGMYCKDA-3'
	reverse	5'-TCYCTYYTYTGCATRWRITCDAYYTC-3'

Table 6. Primers used for isolation of full-length cDNAs of floral homeotic genes.

Target gene	Direction	Primer sequence
TfSQUA	forward	5'-CCATTTTTAGGGATAACATCT-3'
	reverse	5'-CATAGGCATCTCATGTTCGAT-3'
TfDEF	forward	5'-TCTCTATACCTCACCTCGAGAGT-3'
	reverse	5'-AACAAAGCAACATTGCACC-3'
TfGLO	forward	5'-TTCCTTGGAGGGGTTTCTAGT-3'
	reverse	5'-GAAAACATGGGAACAAACTCGT-3'
TfPLE1	forward	5'-CTGCAACTCTCCTGTCCACAA-3'
	reverse	5'-GAACAAAAGCCATGCAATGA-3'
TfFAR	forward	5'-CTTTCTGCATCAACCATCCC-3'
	reverse	5'-GTAAATAATTGTCCCTTGACTTC-3'

Table 7. Primers used to synthesize probes for *in situ* hybridization analysis of floral homeotic genes.

Target gene	Product length	Direction	Primer sequence
TfSQUA	481 bp	forward	5'-AACCAGCTCATACAGGATTCA-3'
		reverse	5'-GCGTTGTTTTGTTGCATCT-3'
TfDEF	499 bp	forward	5'-ACAGGAATCTGAAGAGGGA-3'
		reverse	5'-GCCCTACGAAATTAGTAGTACC-3'
TfGLO	479 bp	forward	5'-GCAGATTGAGCTCAGGCA-3'
		reverse	5'-AAGGTTTTGGCTTAACGAGAG-3'
TfPLE1	498 bp	forward	5'-GGAACTCAAGAACATGGAGTCA-3'
		reverse	5'-ACAAGTACGAGGAGAAATTGAGG-3'
TfFAR	481 bp	forward	5'-CATAACAAGAACATGCTCGGTG-3'
		reverse	5'-GAACAAACATAATCAGCAGAGGATC-3'

Table 8. Primers used for qPCR analysis of floral homeotic genes.

Target gene	Product length	Direction	Primer sequence
TfSQUA	151 bp	forward	5'-GCTTTGCTGCATGATGATATA-3'
		reverse	5'-GCGTTGTTTTGTTGCATCT-3'
TfDEF	103 bp	forward	5'-GGTACTACTAATTTCGTAGGG-3'
		reverse	5'-TAATATGGATCGAAATCATC-3'
TfGLO	111 bp	forward	5'-CGAATCTTCAGGAACGTTTC-3'
		reverse	5'-AAGGTTTTGGCTTAACGAGAG-3'
TfPLE1	172 bp	forward	5'-CCTTTGGCTGTTAGGATG-3'
		reverse	5'-GACACAGCCCGAGTCGATGAG-3'
TfFAR	129 bp	forward	5'-ATGGGATCCTCTGCTGATTAT-3'
		reverse	5'-TTCAAATTGAACAACACATGG-3'

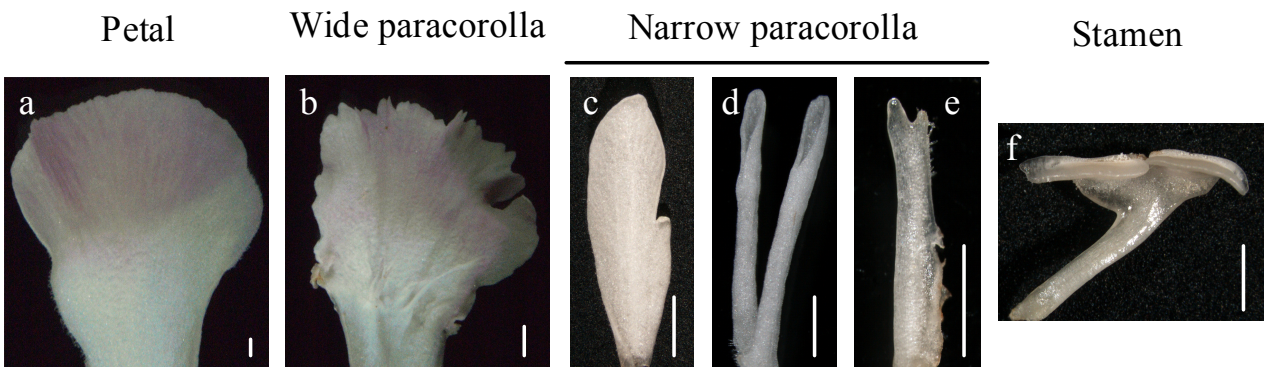

Fig. 9. Morphology of a CPPU-induced paracorolla compared with a petal and stamen. The wide and colored paracorollas resembling the petal were grouped as ‘wide paracorollas’, while the narrow paracorollas resembling the filament were grouped as ‘narrow paracorollas’. Samples are as follows: Petal (a); wide paracorolla (b); narrow paracorolla (c, d, e); stamen (f). Petals and stamens were collected from flowers not treated with CPPU. Scale bars = 1 mm.

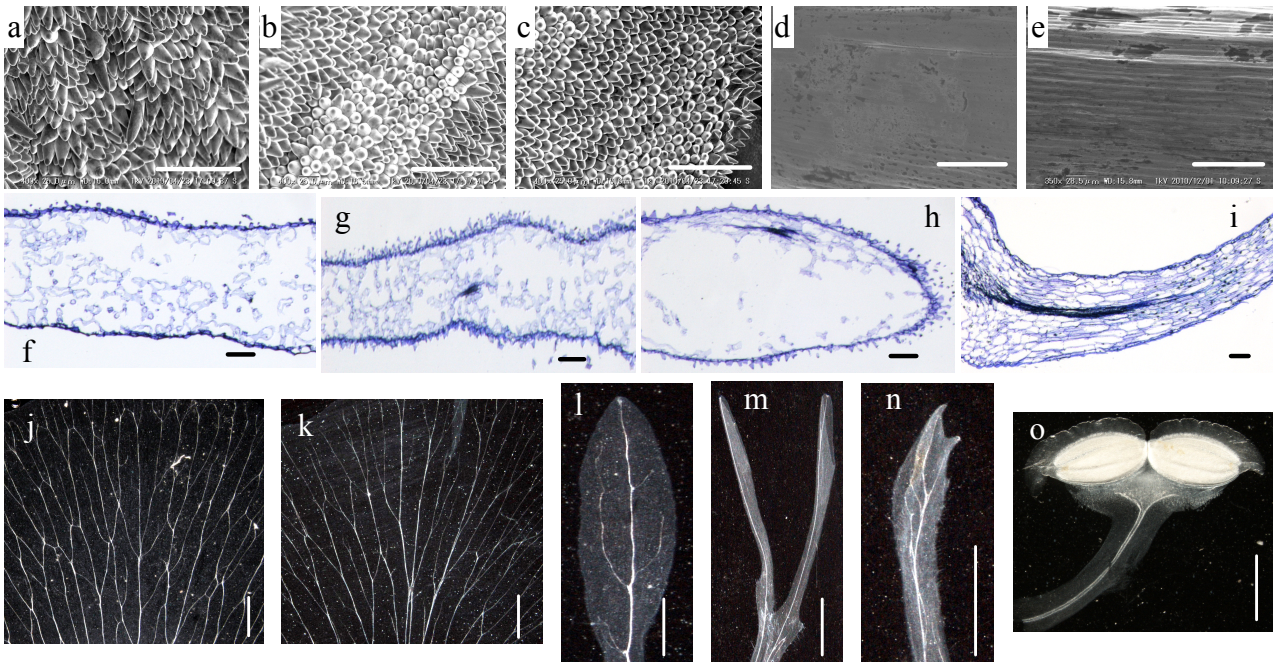

Fig. 10. Microscopic analyses of CPPU-induced paracorollas. (upper row) Scanning electron micrographs of the adaxial face; (middle row) Photomicrographs of transverse sections; (lower row) Photo of vascular bundles. Samples are as follows: Petal (a, f, j); the wide paracorolla (b, g, k); the narrow paracorolla (c, d, h, l, m, n); stamen (e, i, o). Photo of c and g represents the narrow paracorolla of Fig. 9c, and photo of d and h represents the narrow paracorolla of Fig. 9d and e. Petals and stamens were collected from flowers not treated with CPPU. Scale bars = 100 μm (a–i) and 1 mm (j–o).

(A) Class A genes

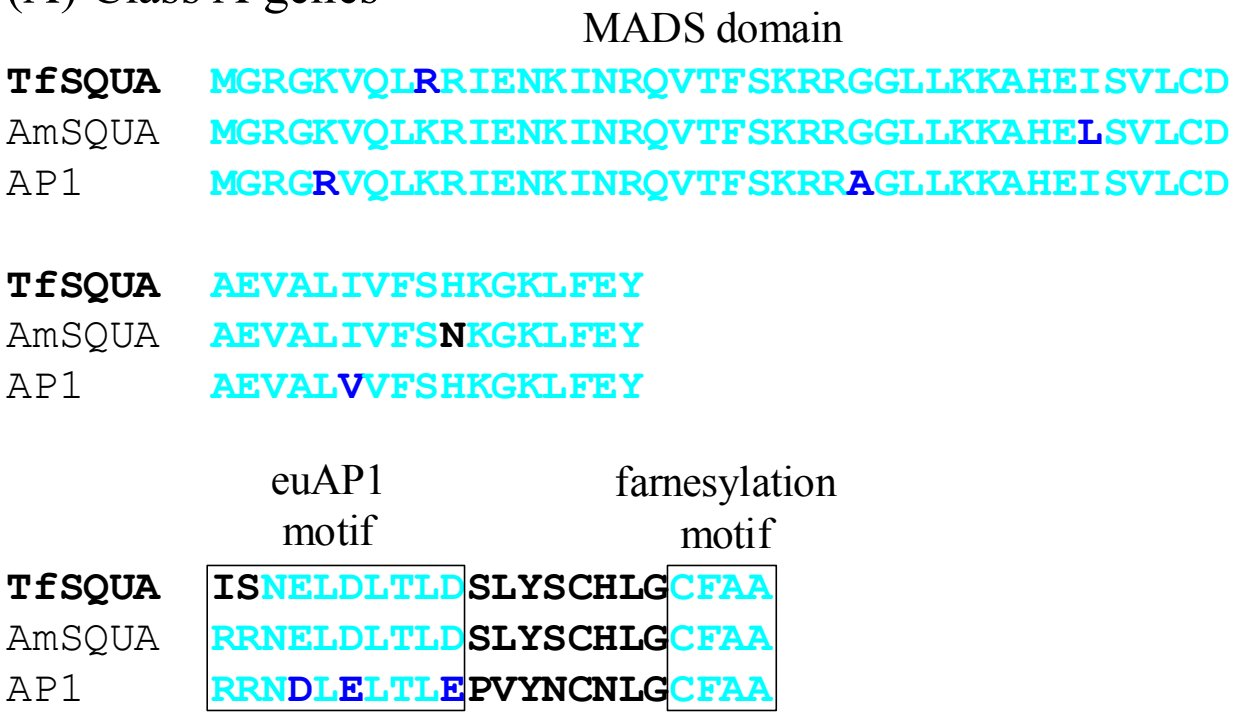

Be continued

(B) Class B genes

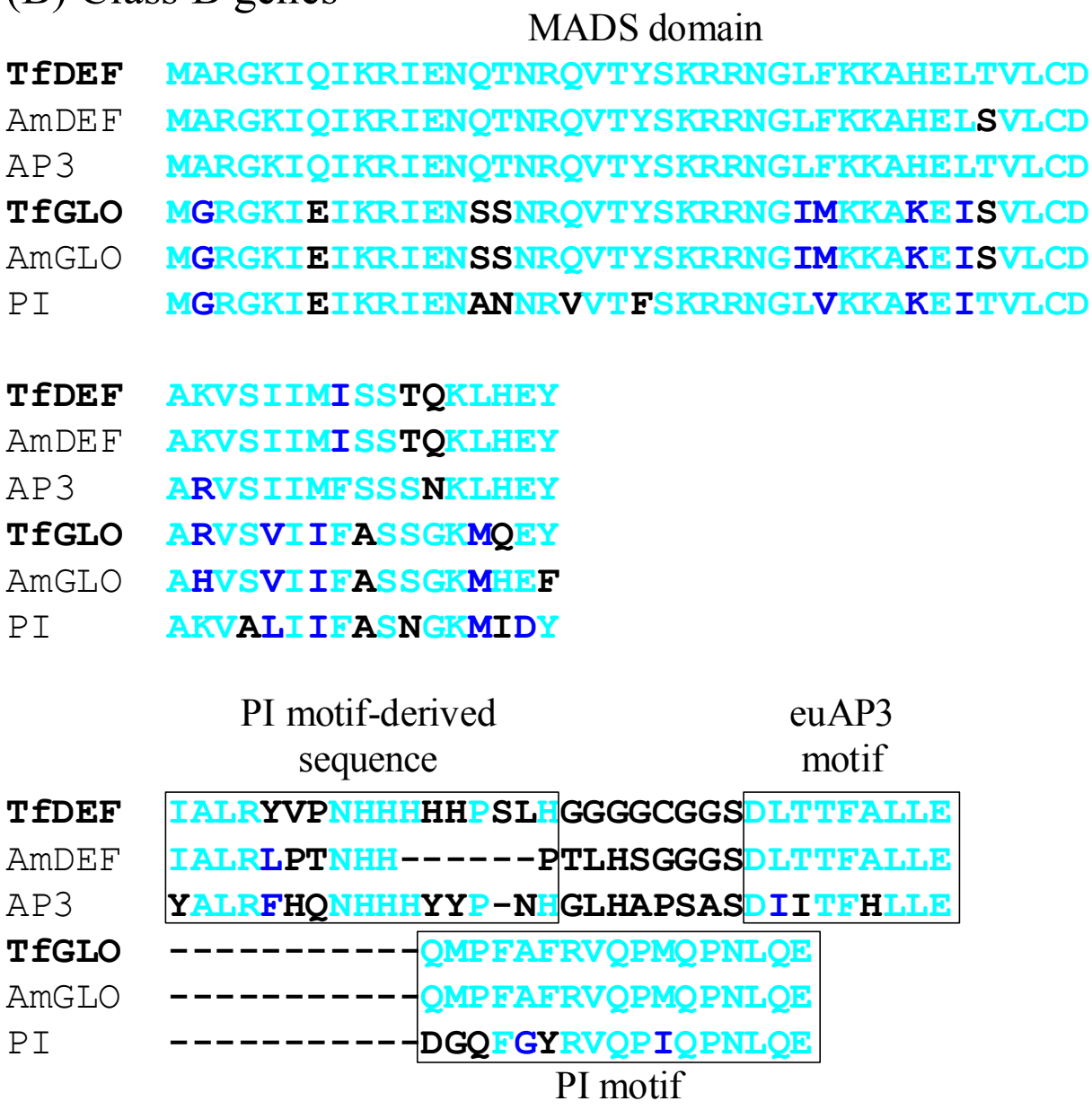

Be continued

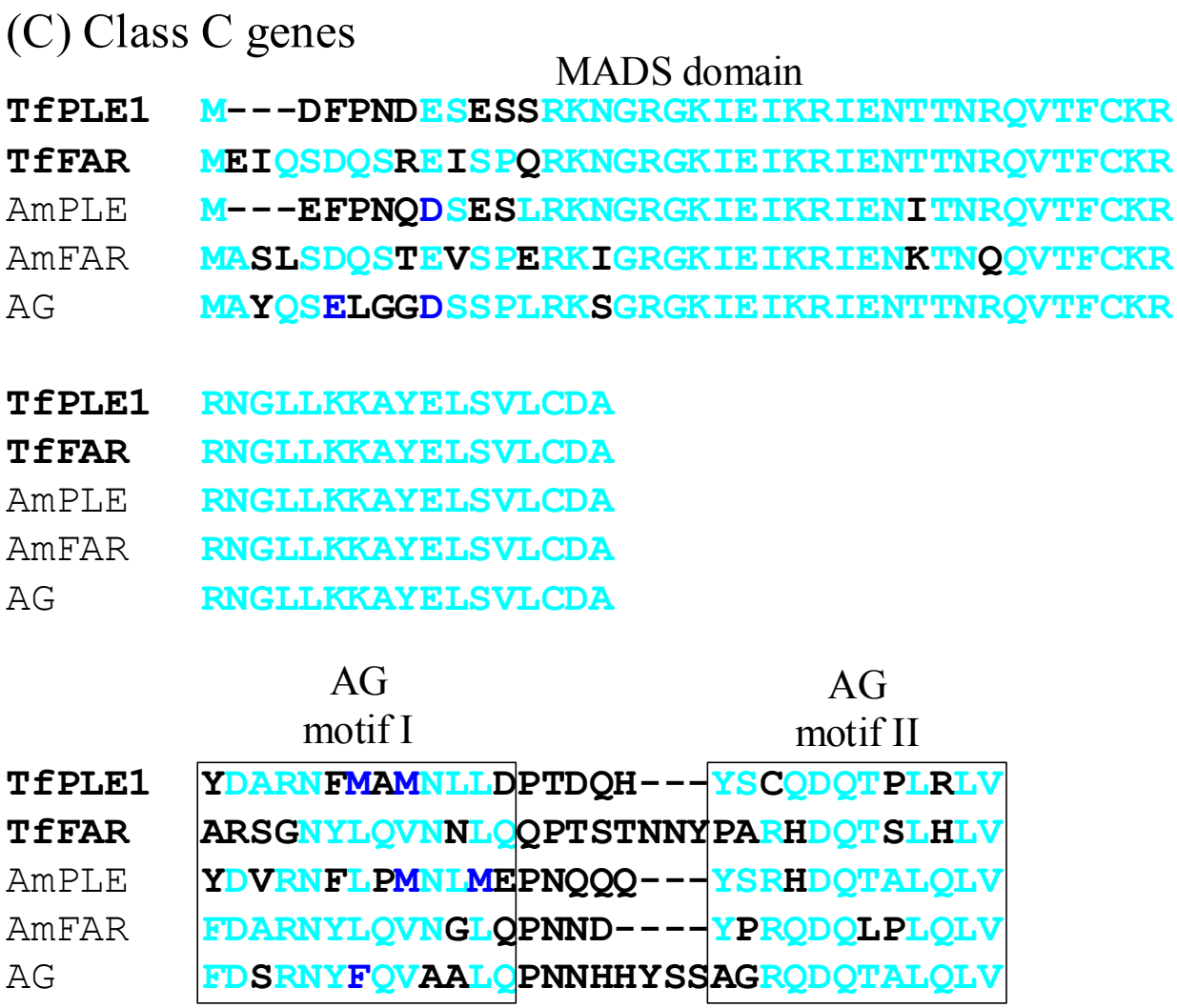

Fig. 11. Alignment of amino acid sequences of floral homeotic genes in torenia, *A. majus*, and *Arabidopsis*. (A) Class A, (B) class B, (C) class C genes. Accession numbers were as follows: Class A genes; AmSQUA (*Antirrhinum majus*), X63701; AP1 (*Arabidopsis thaliana*), Z16421; TfSQUA (*Torenia fournieri*), AB359949: Class B genes; AmDEF (*Antirrhinum majus*), X52023; AmGLO (*Antirrhinum majus*), X68831; AP3 (*Arabidopsis thaliana*), M86357; PI (*Arabidopsis thaliana*), D30807; TfDEF (*Torenia fournieri*), AB359951; TfGLO (*Torenia fournieri*), AB359952: Class C genes; AG (*Arabidopsis thaliana*), NM_118013; AmFAR (*Antirrhinum majus*), AJ239057; AmPLE (*Antirrhinum majus*), S53900; TfFAR (*Torenia fournieri*), AB359953; TfPLE1 (*Torenia fournieri*), AB359954.

Be continued

Motifs conserved in each class of floral homeotic genes were boxed. Identical and homologous amino acid was indicated by light blue and blue letters, respectively.

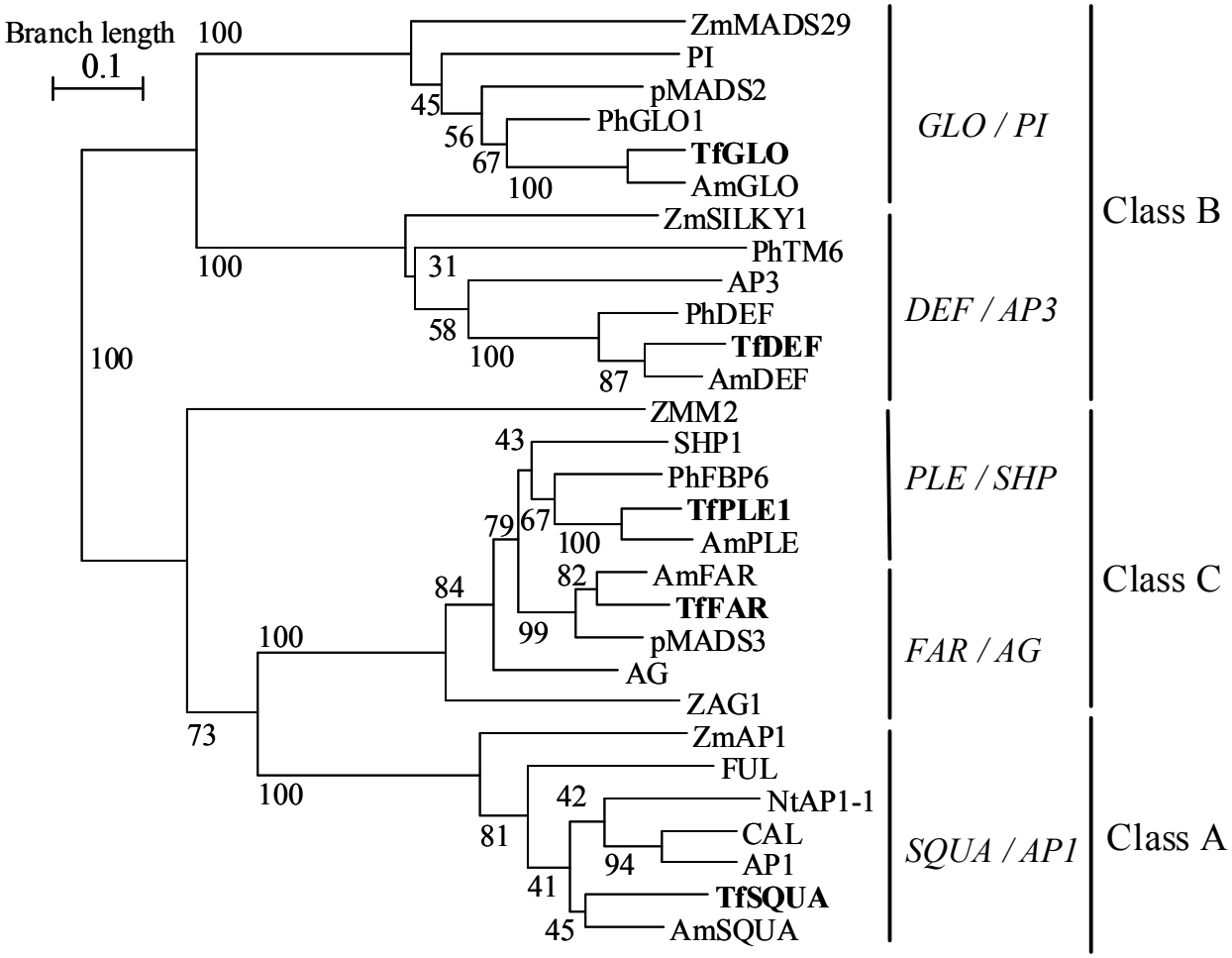

Fig. 12. Phylogenetic tree of homeotic genes in torenia and other plant species. The neighbor-joining tree was generated based on amino acid sequences using CLUSTAL W, and was drawn with NJplot. Bootstrap values from 100 replicates are indicated near the branching points. Accession numbers were the same as described in legend of Fig. 11 and follows: Class A genes; CAL (*Arabidopsis thaliana*), L36925; FUL (*Arabidopsis thaliana*), U33473; NtAP1-1 (*Nicotiana tabacum*), AF009126; ZmAP1 (*Zea mays*), L46400: Class B genes; PhDEF (*Petunia hybrida*), DQ539416; PhGLO1 (*Petunia hybrida*), M91190; PhTM6 (*Petunia hybrida*), DQ539417; pMADS2 (*Petunia hybrida*), X69947; ZmMADS29 (*Zea mays*), AJ292961; ZmSILKY1 (*Zea mays*), AF181479: Class C genes; PhFBP6 (*Petunia hybrida*), X68675; pMADS3 (*Petunia hybrida*), X72912; SHP1 (*Arabidopsis thaliana*), NM_001084842; ZAG1 (*Zea mays*), L18924; ZMM2 (*Zea mays*), AF112149.

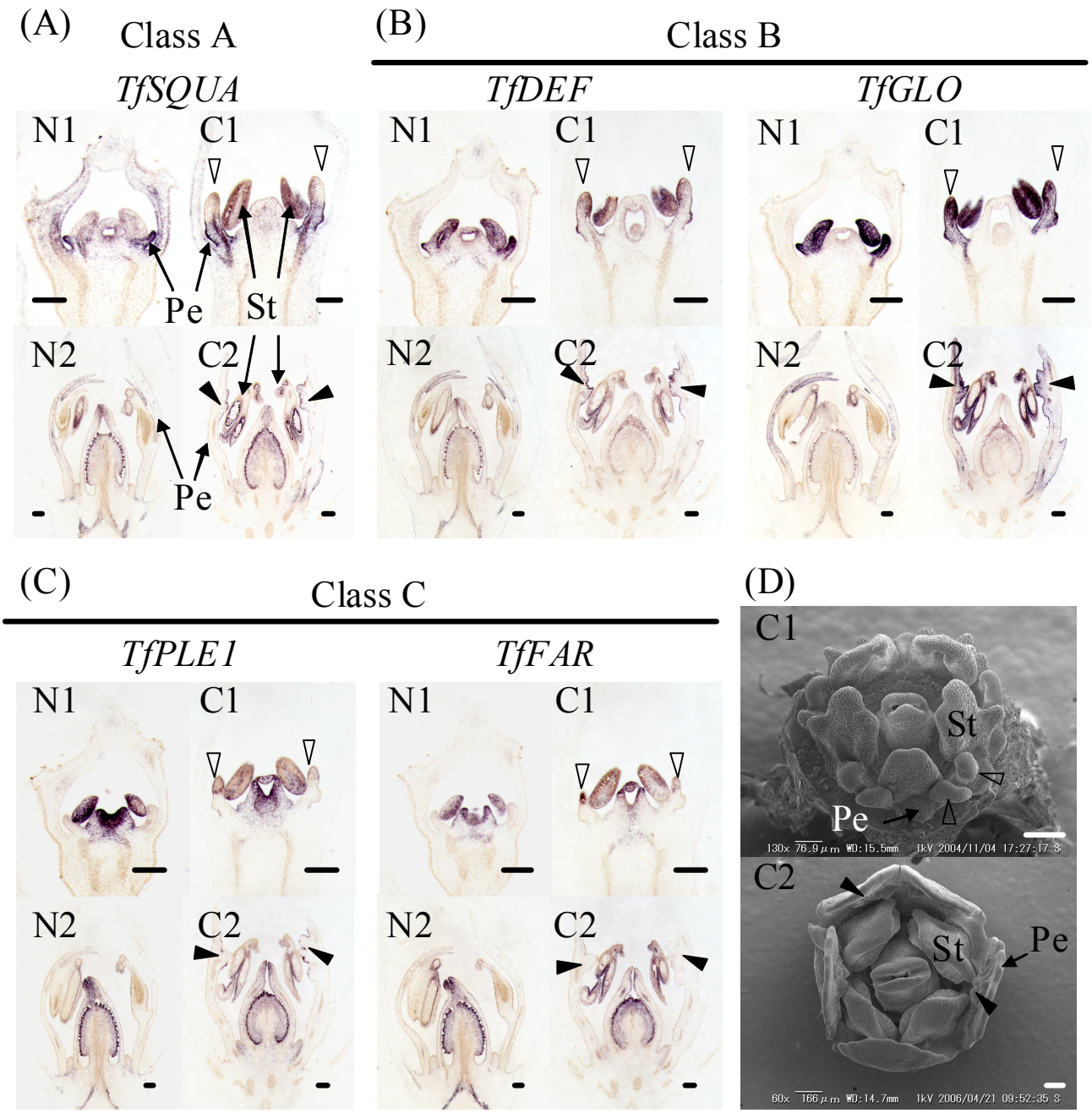

Fig. 13. *In situ* hybridization of homeotic genes in flower buds at paracorolla initiation. Gene-specific antisense RNA probes of a class A gene (A), class B genes (B), and class C genes (C) were used. Spatial distributions of floral organs at the paracorolla initiation stage are shown by scanning electron micrographs (D). CPPU-treated flower buds were collected at paracorolla initiation, while untreated buds were collected at the corresponding stage. N1, untreated flower buds at the same stage as C1; C1, CPPU-treated flower buds at wide paracorolla initiation; N2, untreated flower buds at

Be continued

the same stage as C2; C2, CPPU-treated flower buds at narrow paracorolla initiation. Triangles represent wide paracorollas (△) and narrow paracorollas (▲). Scale bars = 100 μm. Pe, Petal; St, Stamen.

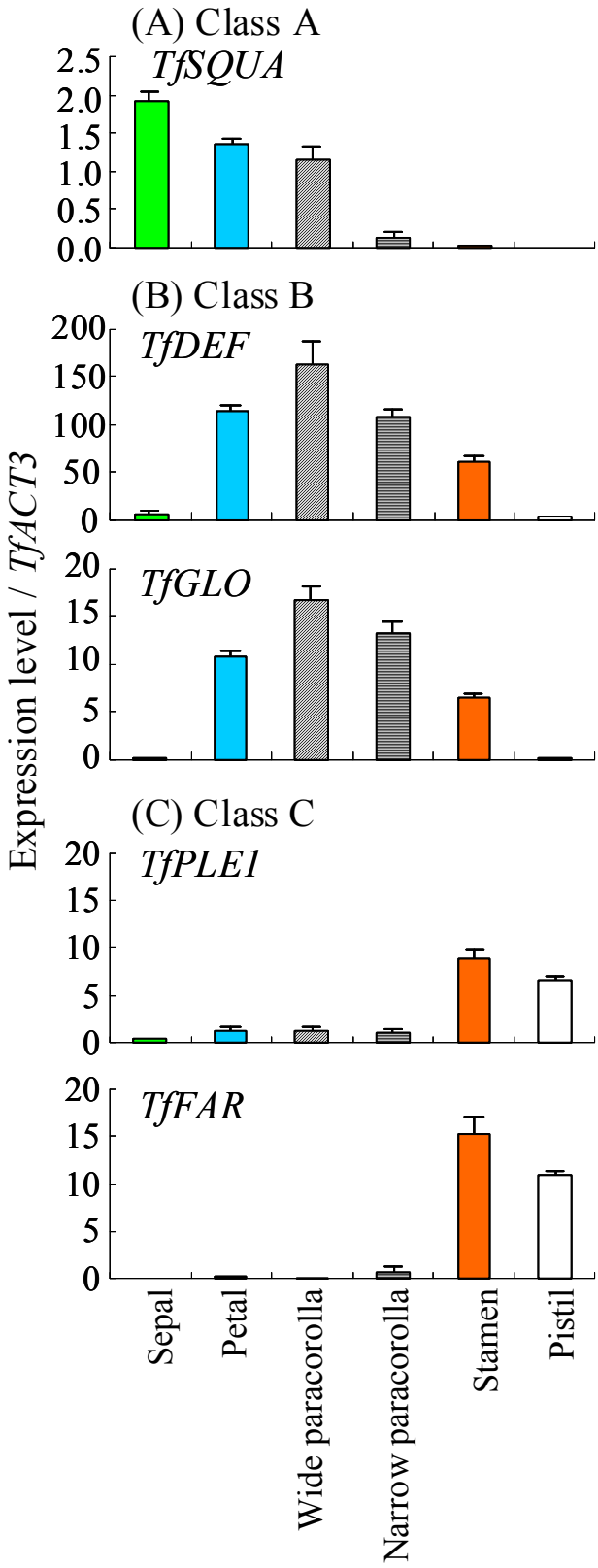

Fig. 14. Quantitative real-time PCR analyses of homeotic genes in CPPU-treated floral organs. The relative expression levels of class A (A), class B (B), and class C (C) genes are shown as values relative to that of *TfACT3*, which was used as an internal standard. Vertical bars indicate SE (n = 3).

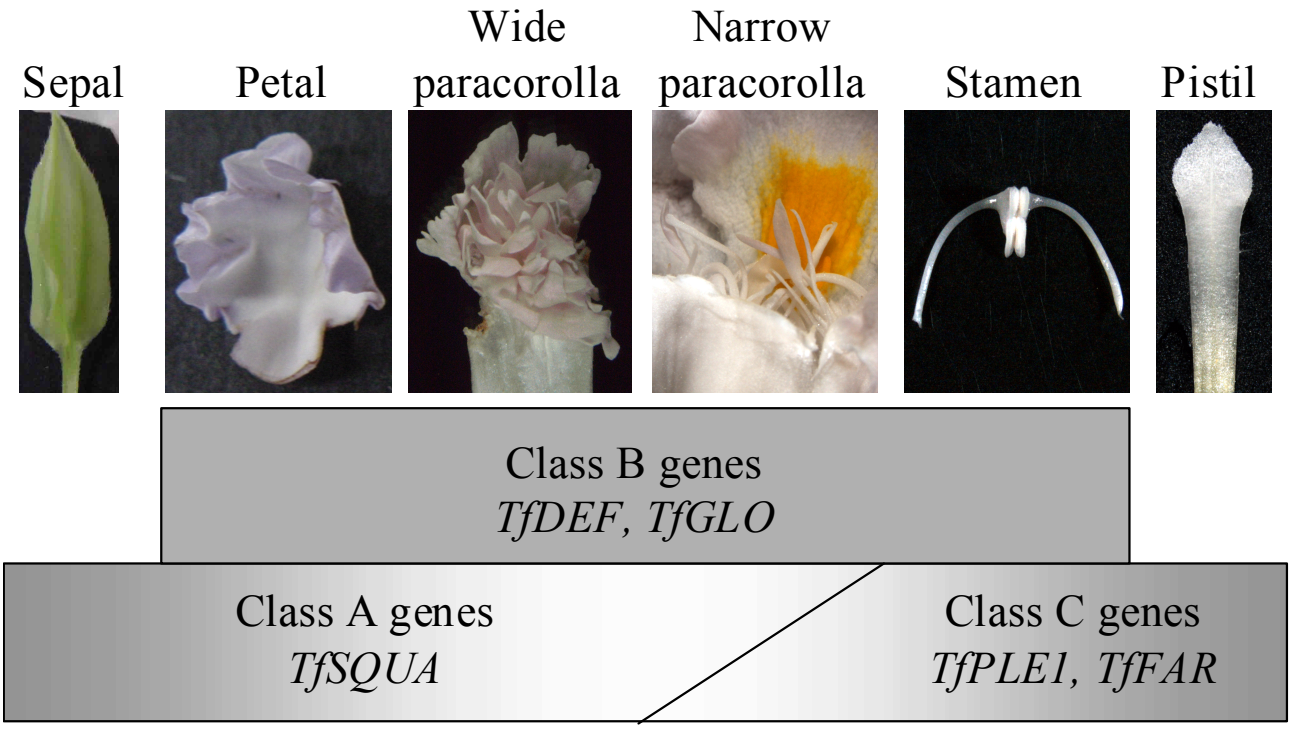

Fig. 15. Hypothetical role of floral homeotic genes in the identification of floral organs and the regulation of paracorolla morphology. The darkness of the belts indicates the extent of expression.

Chapter 4

Improvement of flower morphology through localized promotion of cytokinin biosynthesis in flower bud

1. Introduction

In Chapter 2, it was shown that the spatial distribution of elevated cytokinin signals changes depends on the floral stage at CPPU application, which causes induction of specific flower morphologies. In Chapter 3, it was further shown that the morphological differences observed in CPPU-induced torenia paracorollas are regulated by the expression patterns of floral homeotic genes at the site where the paracorolla is formed. It will thus be possible to induce a desired flower morphology by the localization of cytokinins to a particular site of flower buds at an appropriate floral stage. A wide paracorolla can be induced if cytokinin is accumulated, at the sepal development stage, at the abaxial side of stamen primordia in which class A and B floral homeotic genes are expressed. A narrow paracorolla can be induced if cytokinin is accumulated in the region from the basal part of the stamen to the middle of the petal, in which class B floral homeotic genes are expressed during the early corolla development stage. Serrated petals can be induced when cytokinin is accumulated in the limb of the petal at the middle corolla development stage.

For application of those hypothetical strategies to floricultural plants, it is difficult to obtain a breeding line accumulating cytokinin in specific floral organs by conventional breeding methods, including mutation breeding and cross pollination. CPPU treatment is also difficult for practical use because the chemical must be precisely applied at a specific floral stage to obtain the desired uniform flower morphology. The production of genetically

modified plants expressing a cytokinin biosynthesis gene under the control of a floral organ-specific promoter would accordingly be an effective tool.

The first step of cytokinin biosynthesis catalyzed by IPT is thought to be a rate-limiting step in higher plants (Kakimoto, 2001; Takei et al., 2001). In *Arabidopsis*, nine genes encoding IPT have been cloned, and transgenic plants overexpressing these genes show elevated concentrations of endogenous cytokinins (Sakakibara et al., 2005). Furthermore, the application of a promoter of floral homeotic genes would be useful for inducing transgenes in a floral organ-specific manner. The floral homeotic genes *APETALA1* (*AP1*) and *APETALA3* (*AP3*) are specifically expressed in whorls 1 and 2 and whorls 2 and 3, respectively (Jack et al., 1992; Mandel et al., 1992). Therefore, transgenic plants expressing *IPT* under the control of the promoters of these genes would specifically elevate cytokinin concentration and cytokinin signals in the sepals and petals and in the petals and stamens, respectively (Fig. 16).

In this chapter, we introduced *Arabidopsis IPT* (*AtIPT4*) into torenia under the control of *AP1* or *AP3* promoters to clarify the effects of floral organ-specific promotion of cytokinin biosynthesis on flower morphology. On the basis of the results, a strategy to produce ornamental flower morphologies with genetic engineering is discussed.

2. Materials and Methods

2.1. Plant materials

Torenia fournieri, 'Crown Violet' (Takii Seed Co., Kyoto, Japan), was used for transformation. Plant materials were aseptically maintained in a plant box supplemented with 1/2 Murashige and Skoog medium containing 3% sucrose (Aida et al., 2000).

For cloning of *Arabidopsis* genes, seeds of *Arabidopsis thaliana* were germinated and the

seedlings were grown as described in Chapter 2.2.1, and then grown an incubator kept at 20°C under illumination from fluorescent lamps of 70 μmol·m^{-2}·s^{-1} PPFD (16 h light/8 h dark).

2.2. Plasmid construction and transformation of torenia

For cloning *AtIPT4* in *Arabidopsis thaliana* (AB061402), the methods for total RNA isolation from flower buds and young flowers (Miyawaki et al., 2004) using an RNeasy Plant Mini Kit (Qiagen) and RNase-Free DNase Set (Qiagen), and cDNA synthesis using a CapFishing Full-length cDNA Premix Kit (Seegene) were the same as described in Chapter 2.2.3. For cloning *Arabidopsis AP1* (At1g69120) and *AP3* (At3g54340) promoters, genomic DNA was isolated from young *Arabidopsis* leaves using ISOPLANT II (Wako). The open reading frame of *AtIPT4* and the 5′-upstream region of *Arabidopsis AP1* and *AP3* were amplified using PCR with KOD Plus DNA polymerase (TOYOBO) with the primers including an *Eco* RI site listed in Table 9. All PCR fragments were digested using *Eco* RI, subsequently the *AtIPT4* fragment was ligated with the *AP1* or *AP3* fragment. The fragments produced were amplified by PCR using the primers listed in Table 9. These fragments were cloned into a pENTR/D-TOPO vector (Invitrogen, Carlsbad, CA, USA) and then transferred into a destination vector pGWB1 (Fig. 16; Nakagawa et al., 2007), which was derived from the plant transformation vector pBI101, using the Gateway LR clonase reaction (Invitrogen).

Transformation of torenia was performed as described by Aida and Shibata (1995, 2001). Plant materials were vegetatively reproduced by herbaceous cuttings and grown at 25°C with illumination from fluorescent lamps (85 μmol·m^{-2}·s^{-1} PPFD; 16 h light/8 h dark cycle). The vectors were introduced into torenia by *Agrobacterium*-mediated method. After selection with kanamycin and hygromycin, transformants were planted in horticultural soil (Kureha) in plastic pots and grown in a greenhouse under natural light at 25°C/20°C (day/night). Plants

showing any changes in flower morphology were selected, and their T_2 generations were obtained by selfing; the plants were used for subsequent investigations. Seeds of transgenic plants were germinated, planted and grown in the greenhouse as described in Chapter 2.2.1.

2.3. Morphological analysis of flower bud development

For observation of the morphological changes that occurred in the developing flower buds, the flower buds at the sepal development stage (Stage 3), the stamen and pistil initiation stage (Stage 4), the early corolla development stage (Stage 5), and the middle corolla development stage (Stage 6) were fixed, dehydrated through a graded ethanol series, and replaced with 2M2P as described in Chapter 2.2.5. The samples were freeze-dried in 2M2P, and analyzed by SEM (Keyence).

2.4. Quantitative real-time PCR analysis

The methods for total RNA isolation from the sepals, petals, stamens, and pistils of the flower buds at Stage 6 from transgenic and non-transgenic plants using an RNeasy Plant Mini Kit (Qiagen) and RNase-Free DNase Set (Qiagen), and cDNA synthesis using a CapFishing Full-length cDNA Premix Kit (Seegene) were the same as described in Chapter 2.2.4. Gene-specific primers for *AtIPT4* were designed for the 3′-terminal regions of the open reading frame and the 3′-untranslated regions of the gene. Primer sequences and the lengths of the PCR products used for qPCR reactions of *AtIPT4* were listed in Table 10. The primers for *TfRR1*, *TfCKX5*, and *TfACT3*, as an internal standard, were the same as described in Chapter 2.2.4. qPCR and data analysis was performed as the same procedure as described in Chapter 2.2.4. Fluorescence was measured at the end of the extension phase at 76°C for *TfRR1*, at 77°C for *TfACT3*, at 78°C for *TfCKX5*, and at 80°C for *AtIPT4*, to avoid calculating non-specific PCR products. The ratio of the expression of each gene to that of

TfACT3 was calculated. Expression analyses were conducted independently in triplicate.

2.5. Analysis of endogenous cytokinins

Endogenous cytokinins were extracted separately from the sepals, petals, stamens, and pistils at the late corolla development stage (Stage 7) from transgenic and non-transgenic plants. The methods used for cytokinin analysis were the same as those described by Dobrev and Kaminek (2002) and Nishijima et al. (2011a). Each floral organ (0.2–0.6 gFW) was homogenized in liquid nitrogen and extracted in ice-cold MeOH/water/formic acid (15/4/1, v/v/v), which includes 1 ng of each internal standard, [$^2H_6$] iP, [$^2H_5$] tZ, [$^2H_6$] iP riboside (iPR), and [$^2H_5$] tZ riboside (tZR) (OlChemim, Olomouc, Czech Republic). After overnight extraction at −20°C, solids were separated using centrifugation. The extract was passed through a Sep-Pak tC_{18} cartridge (Waters, Milford, MA, USA) and evaporated to near dryness. The residue was dissolved in 1 M formic acid and applied to an Oasis MCX column (Waters). The column was sequentially eluted with MeOH, 0.35 M NH_4OH, and 0.35 M NH_4OH in 60% (v/v) aqueous MeOH. The eluent with 0.35 M NH_4OH in 60% (v/v) aqueous MeOH comprising cytokinin nucleobases, cytokinin nucleosides, and cytokinin glucosides was evaporated to dryness. The dried sample was then dissolved in 10% aqueous MeOH containing 0.05% acetic acid and analyzed using a liquid chromatography–tandem mass spectrometry system (LC/MS/MS, model 2695/TSQ7000; Waters/Thermo Fisher Scientific, Waltham, MA, USA) coupled with positive ion electrospray ionization. Cytokinins were separated using an ODS column (MD, 5 μm, 2.5 mm × 250 mm; Shiseido Fine Chemicals, Tokyo, Japan) at a flow rate of 0.2 mL·min^{-1} with gradients of solvents A (MeOH containing 0.05% acetic acid) and B (water containing 0.05% acetic acid) as follows: 0 min, 10% A + 90% B; 45 min, 80% A + 20% B; and 55 min, 100% A. The column temperature was 35°C. Quantification was performed in selected ion recording mode. The ionization voltage was 4.7

kV, the capillary temperature was 200°C, and the collision energy was −22 to −34 V depending on the cytokinin species. Data were analyzed using Xcaliber software (Thermo Fisher Scientific). Endogenous cytokinins were quantified by the internal standard method using the corresponding deuterated cytokinins. Quantification of endogenous cytokinins was conducted independently and in triplicate.

3. Results

3.1. Changes of the flower morphology of transgenic torenia

Several morphological changes were induced in the flowers of both *AP1*::*AtIPT4* and *AP3*::*AtIPT4* plants, and these traits were inherited. The number of petals in *AP1*::*AtIPT4* plants was increased to 6–7 (Fig. 17b) from the characteristic 5 petals of the normal type (NT) plants (Fig. 17a). The number of sepals was increased to 5–7 in *AP1*::*AtIPT4* plants, whereas the NT plants had 5 sepals. In contrast, the number of stamens and pistils remained unchanged. In *AP3*::*AtIPT4* plants, the number of petals increased to 5–6 (Fig. 17c, d), although the increase was moderate compared with *AP1*::*AtIPT4* plants (Fig. 17b). In addition, remarkable petal expansion and serrated petal margins were observed in *AP3*::*AtIPT4* plants (Fig. 17c, d), but not in NT plants (Fig. 17a). Furthermore, extra floral organs resembling petals were observed on the corolla (Fig. 17d). *AP3*::*AtIPT4* plants had 4–5 stamens compared with the 4 stamens of NT plants, but the number of sepals and pistils was unchanged.

In Stage 3 of floral development, both NT and *AP3*::*AtIPT4* plants had 5 sepals (Fig. 18a, o); however, *AP1*::*AtIPT4* plants had more than 6 sepals (Fig. 18h). In the initiation stage of the stamen and pistil (Stage 4), the receptacle was larger in both *AP1*::*AtIPT4* and *AP3*::*AtIPT4* plants (Fig. 18i, p) compared with NT plants (Fig. 18b). Furthermore, the

receptacle of *AP3*::*AtIPT4* plants became markedly larger than those of NT and *AP1*::*AtIPT4* plants at Stage 5 (Fig. 18c, j, q). In Stage 5 and early Stage 6, increase in the number of petal primordia, was observed in *AP1*::*AtIPT4* plants (Fig. 18c, d, g, j, k, n). The staminoid of *AP3*::*AtIPT4* plants was also larger than that of the NT and *AP1*::*AtIPT4* plants (Fig. 18c, d, j, k, q, r). In late Stage 6, primordia of the extra floral organs were initiated and corolla expansion and serrated petal margins were observed in *AP3*::*AtIPT4* plants (Fig. 18s). These extra floral organs were formed on the abaxial and lateral sides of the basal part of the stamen, which corresponded to the middle part of the petal (Fig. 18t, u).

3.2. Cytokinin biosynthesis and signal transduction in transgenic torenia

To clarify the relationship between those morphological changes of flowers in the transgenic plants and distribution of cytokinin signals within flower buds, the expression pattern of introduced gene in floral organs of the transgenic plants were analyzed. As expected, the *AtIPT4* transgene was mainly expressed in the sepals and petals of *AP1*::*AtIPT4* plants and in the petals and stamens of *AP3*::*AtIPT4* plants (Fig. 19).

In NT plants, iP and iPR were not detected in the sepals and petals, while the stamens contained high concentrations of iP (Fig. 20A, B). The concentrations of iP in the pistils and iPR in the stamens and pistils were slight in NT plants (Fig. 20A, B). Both iP and iPR accumulated in the sepals and petals in *AP1*::*AtIPT4* plants; whereas changes in iP and iPR concentrations in the stamens and pistils compared with those of NT plants were obscure (Fig. 20A, B). On the other hand, both iP and iPR accumulated in the petals of *AP3*::*AtIPT4* plants, but were undetected in the sepals; whereas changes in iP and iPR concentrations in the stamens and pistils compared with those of NT plants were obscure (Fig. 20A, B). The other cytokinin species quantified, tZ and tZR, were accumulated mainly in the stamen in NT plants, although they were also detected in the other floral organs (Fig. 20C, D). The

accumulations of tZ and tZR among the floral organs in *AP1*::*AtIPT4* and *AP3*::*AtIPT4* plants showed mostly the same pattern as those of NT plants, except tZR was higher in the sepals of *AP1*::*AtIPT4* plants than those of NT plants (Fig. 20C, D).

Because the changes of cytokinin concentrations in the stamens of *AP3*::*AtIPT4* plants from those of NT plants were obscure, the expression of *TfRR1* and *TfCKX5,* which reflects the extent of cytokinin signals as described above was analyzed. The expression of *TfRR1* and *TfCKX5* was low or undetectable in all floral organs of NT plants (Fig. 21). In *AP1*::*AtIPT4* plants, the expression of *TfRR1* and *TfCKX5* in the sepals and petals was more than 10-fold that in NT plants (Fig. 21). On the other hand, the expression of *TfRR1* and *TfCKX5* was increased more than 10-fold in the petals and stamens of *AP3*::*AtIPT4* compared with NT plants (Fig. 21). These expression patterns among floral organs coincided with those of introduced *AtIPT4*.

4. Discussion

The results described above indicate that enhanced cytokinin signals through the accumulation of biologically active iP in the sepals and petals of *AP1*::*AtIPT4* plants and in the petals and stamens of *AP3*::*AtIPT4* plants induced change of flower morphologies (Figs. 19, 20A, B and 21). On the other hand, the other biologically active cytokinin species tZ, which showed same accumulation pattern with NT plants, does not apparently participate in the morphological change (Figs. 20C, D).

However, why was the endogenous cytokinin concentration in the stamens of *AP3*::*AtIPT4* plants not markedly different from that in NT plants (Fig. 20A, B)? The stamen would be the organ synthesizing cytokinins because cytokinin is necessary for pollen development (Huang et al., 2003; Sawhney and Shukla, 1994). The result that cytokinin concentration in the

stamen in NT plants was higher than that of the other floral organs coincides with the fact. At the same time, the development of the anther and pollen is inhibited by elevated cytokinin concentrations in transgenic tobacco plants overexpressing *IPT* in an anther-specific manner (Geng et al., 2002). Therefore, in the stamens of *AP3*::*AtIPT4* torenia plants, intensive expression of *AtIPT4* possibly had an inhibitory effect on stamen development, which may have raised a barrier in cytokinin biosynthesis.

In *AP3*::*AtIPT4* plants of torenia, extra floral organs were induced and the morphology resembled the narrow paracorollas induced by CPPU treatment (Niki et al., 2012; Nishijima and Shima, 2006; Figs. 17d and 18u). Furthermore, the site and the floral stage in which the extra floral organ initiation occurred coincided with those of the narrow paracorollas induced by CPPU treatment and those of *A. majus* paracorolla (Fig. 18s, t). Those paracorollas were probably originated from stipule of the stamen (Nishijima and Shima, 2006; Yamaguchi et al., 2010). Therefore, the extra floral organs formed in *AP3*::*AtIPT4* flowers may be paracorollas originating from the stipule of the stamen.

In *Arabidopsis*, the number of sepals, petals, and stamens increases when *AtIPT4* is expressed under the control of *AP1* promoter (Li et al., 2010). Some morphological changes, such as the development of a small petal on top of the filament, a lobed petal, and the formation of the filament and a small petal between the sepal and petal, are observed in transgenic *Arabidopsis* overexpressing *IPT* in anther-specific manner (Geng et al., 2002). Furthermore, *IPT* expression under the control of *AP3* promoter leads to an increase in the size of the corolla in petunia (Verdonk et al., 2008). However, there has been no research analyzing the relationship between spatial distributions of elevated cytokinin signals and flower morphologies using a same plant material in a same experimental condition. In this study, the increase in petal number, corolla expansion, and the development of paracorollas and serrated petal margins were induced by localized expression of *AtIPT4* in the petals and

stamens of torenia plants, whereas only the petal number increased when *AtIPT4* was expressed in the sepals and petals (Figs. 17 and 18). These results indicate that elevated cytokinin signals in the stamen may be critical for corolla expansion, development of paracorollas and serrated petal margins (Fig. 22).

In *Arabidopsis*, the increase in the number of floral organs in response to the application of cytokinin has been caused by an enlarged floral meristem, and consequently by an enlarged receptacle (Bartrina et al., 2011; Lindsay et al., 2006). In addition, an enlarged receptacle is observed in *Arabidopsis* with *AP1*::*AtIPT4* transgene (Li et al., 2010) and in CPPU-treated torenia (Nishijima et al., 2007) accompanied with an increase in the number of floral organs. Because the organ primordia tend to differentiate at constant intervals, the number of organs increases when the receptacle is enlarged. In this study, receptacle enlargement was observed at Stage 4 in both *AP1*::*AtIPT4* and *AP3*::*AtIPT4* torenia plants (Fig. 18i, p). This suggests that elevated cytokinin signals in whorl 2 causes receptacle enlargement, resulting in an increase in the number of petals (Fig. 22). However, only *AP3*::*AtIPT4* plants showed enhanced receptacle enlargement progressively in Stage 5 (Fig. 18q). The receptacle enlargement preferably occurred in whorl 3. When enhanced receptacle enlargement continues to Stage 5, the distance between each stamen is increased markedly (Fig. 22). Because the stipule of the stamen, which develops into paracorolla, is located at the lateral sides of the stamen and included in whorl 3, sufficient space allowing paracorolla primordia to be initiated may have been supplied. The same phenomenon is observed when the paracorollas are induced by CPPU treatment (Nishijima and Shima, 2006). That is, the paracorollas are generated synchronously with receptacle enlargement at Stage 5. In *Arabidopsis*, receptacle enlargement by cytokinin is caused through coordinated regulation of *WUSCHEL* (*WUS*) and *CLAVATA* (*CLV*) (Bartrina et al., 2011; Clark et al., 1993; Lindsay et al., 2006). *WUS*, which maintains meristematic activity of shoot apical meristem (SAM),

expresses at central zone in SAM. *WUS* expression is restricted in the central zone by *CLV1* that promotes organ differentiation (Schoof et al., 2000). Cytokinin expands *WUS* expression area and consequently meristem size through repression of *CLV1* expression (Bartrina et al., 2011; Lindsay et al., 2006). This regulation mechanism of SAM size is thought to function also in floral meristem, which regulates receptacle size (Bartrina et al., 2011; Lindsay et al., 2006). If, in the transgenic torenia, *CLV* expression was repressed on the site where cytokinin signals were elevated, it is presumable that elevation of cytokinin signals in whorl 3 was more effective for receptacle enlargement than that in whorl 2. This is because whorl 3 is located more closely to the central zone of floral meristem than whorl 2. Meanwhile, it can not be ruled out that the elevated cytokinin signals in whorl 3 of *AP3*::*AtIPT4* torenia induced the development of the stipule of the stamen independently of any receptacle enlargement. This is because cytokinin promotes organ differentiation and development by directly promoting meristematic activity of the organ (Dewitte et al., 1999; Mok and Mok, 2001; Pernisová et al., 2009).

The serrated petal margin is generated by changes in the arrangement of the vascular bundle in the petal limb (Niki et al., 2013; Nishijima and Shima, 2006). In contrast, it was demonstrated that elevated cytokinin signals in the stamen were critical for induction of a serrated petal margin, as described above. A serrated petal margin is also induced in a transgenic torenia in which the function of *AGAMOUS* (*AG*), a floral homeotic gene expressed in whorls 3 and 4, is inhibited by a plant-specific transcriptional repression domain (*AG-SRDX*, Narumi et al., 2008). This shows that a functional change in a gene expressed in whorls 3 and 4 may affect the arrangement of the vascular bundle in whorl 2. Thus, the elevated cytokinin signals in whorl 3, which inevitably alter gene expression profile, might remotely affect the vascular bundle arrangement in the petal (Fig. 22).

Another possibility is that excess cytokinin biosynthesis causes the translocation of

cytokinin into adjacent floral organs. In this experiment, developed flower buds (Stage 7), in which each floral organ is located relatively distant, were used in the analyses of cytokinin concentrations. Thus, the elevated cytokinin concentration caused by *AtIPT4* did not probably affect its concentration in adjacent floral organs, i.e., the stamens in *AP1*::*AtIPT4* plants and the sepal and pistils in *AP3*::*AtIPT4* plants, respectively (Fig. 20A, B). In younger and smaller flower buds, however, cytokinin accumulated in whorl 3 might have been translocated to closely adjacent whorl 2 and thereby affect the arrangement of the vascular bundle in the petal, resulting in a serrated petal margin.

Table 9. Primers used for transgene construction.

Target gene	Product length	Direction	Primer sequence
AtIPT4	970 bp	forward	5'-CTCAGAATTCGACATGAAGTGT-3'
		reverse	5'-CTAGTTAAGACTTAAAAATCT-3'
AP1	1729 bp	forward	5'-TGTATCGTTTCAAAACTCAGG-3'
		reverse	5'-TACTGAATTCGAACCAAACAAAAC-3'
AP3	1197 bp	forward	5'-GACCAGATCAAGAGTGCGTG-3'
		reverse	5'-GTTTGAATTCTTTGTTGAAG-3'
AP1::*AtIPT4*	2689 bp	forward	5'-CACCTGTATCGTTTCAAAACTC-3'
		reverse	5'-CTAGTTAAGACTTAAAAATCT-3'*
AP3::*AtIPT4*	2157 bp	forward	5'-CACCGACCAGATCAAGAGTGC-3'
		reverse	5'-CTAGTTAAGACTTAAAAATCT-3'*

Sequences of *Eco* RI site were underlined.

*Same primer used for isolation of *AtIPT4* gene.

Table 10. Primers used for qPCR analysis of *AtIPT4* gene.

Target gene	Product length	Direction	Primer sequence
AtIPT4	120 bp	forward	5'-ACAGCATCGTTTCGAGAGG-3'
		reverse	5'-GTGGCTCCTGACAATCTTCAC-3'

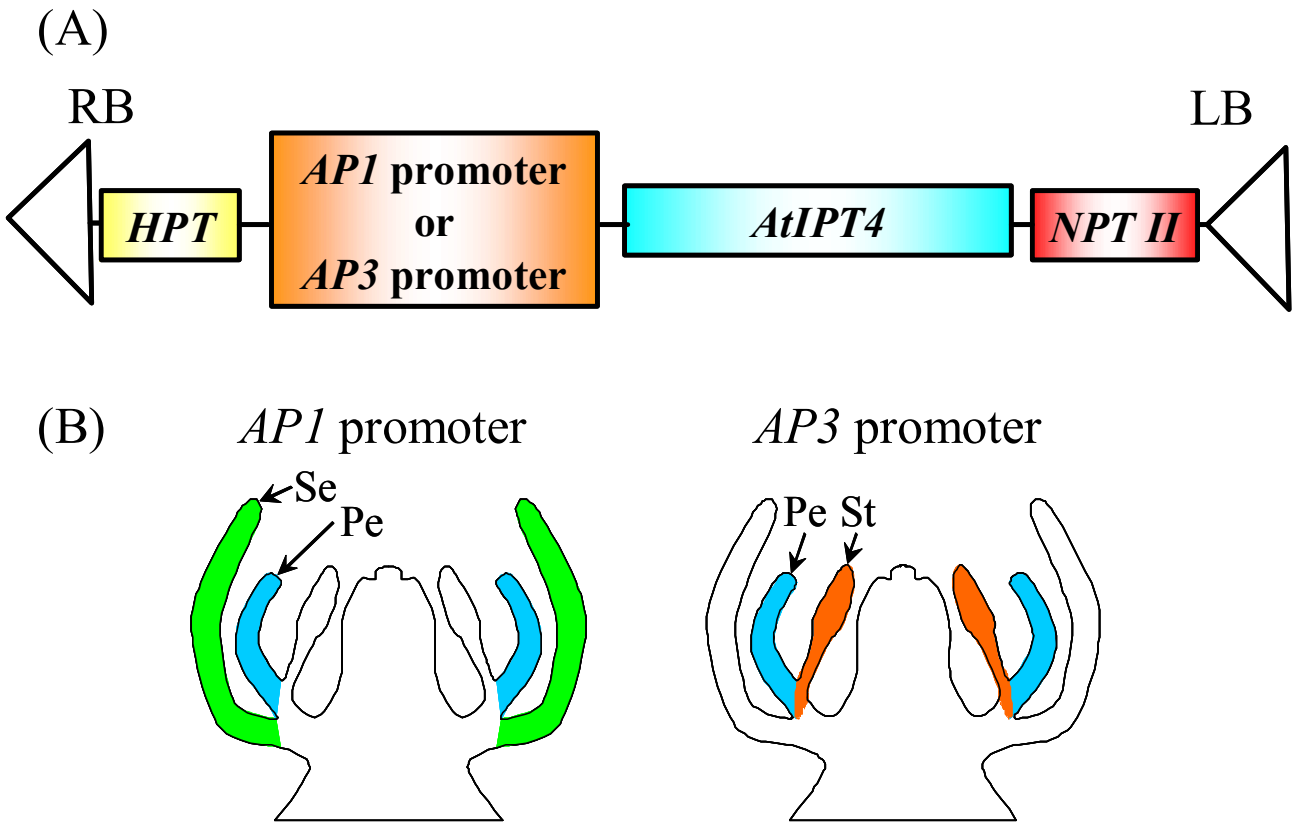

Fig. 16. Transgene construct for floral organ-specific expression of cytokinin biosynthesis gene. (A) T-DNA region of introduced vector (pGWB1). Hygromycin phosphotransferase (HPT) and neomycin phosphotransferase (NPT) II were used for transformant selection. (B) Predicted effect of the transgene. Floral organs expected to have elevated cytokinin production were colored with green in sepal, blue in petal, and orange in stamen. *AP1*, *APETALA1*; *AP3*, *APETALA3*; *AtIPT4*, *Arabidopsis thaliana* isopentenyltransferase4; LB, Left border; Pe, Petal; RB, Right border; Se, Sepal; St, Stamen.

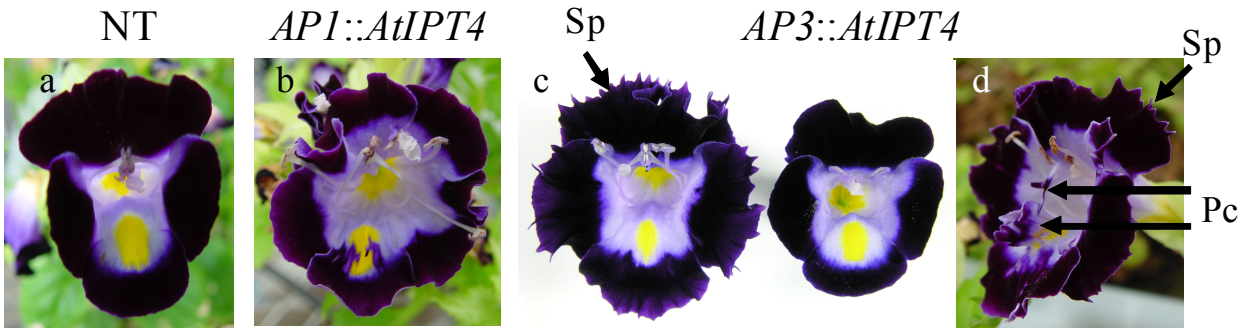

Fig. 17. Morphological changes in the flowers of torenia. a, Normal type (NT); b, *AP1*::*AtIPT4*; c and d, *AP3*::*AtIPT4*. Pc, Paracorolla; Sp, Serrated petal.

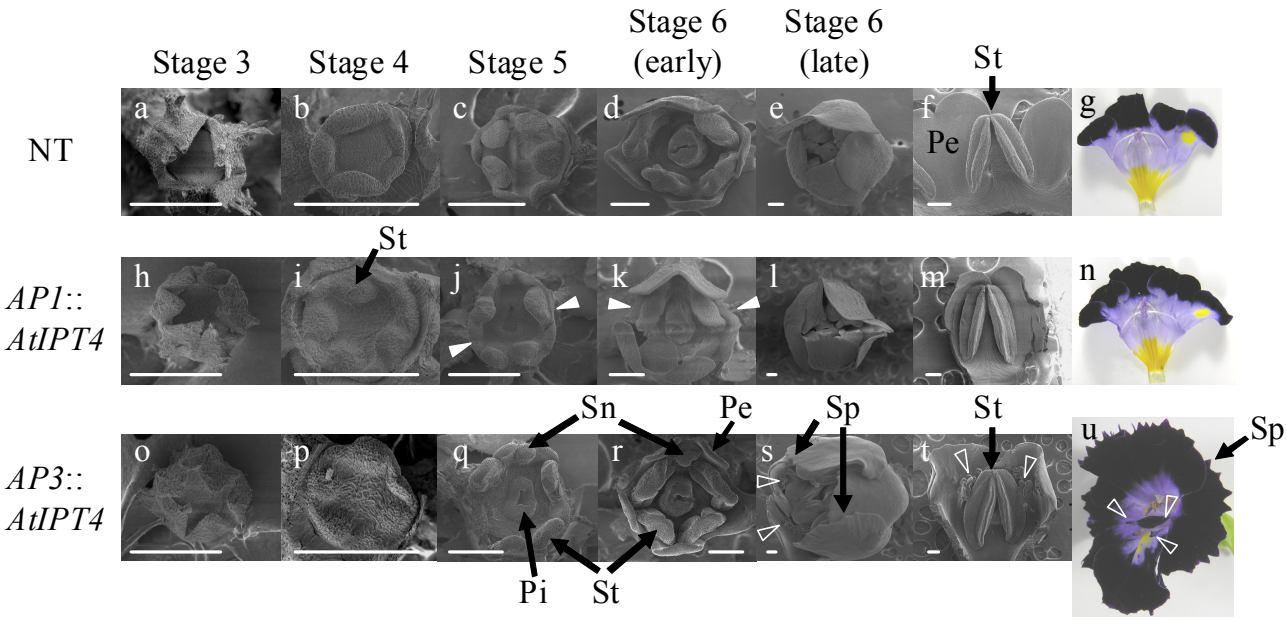

Fig. 18. Floral development of transgenic torenia. a–g, Normal type (NT); h–n, *AP1*::*AtIPT4*; o–u, *AP3*::*AtIPT4*. Floral stages were defined as described by Nishijima and Shima (2006). Closed and open triangles represent lobes from a petal primordium and the site of paracorolla initiation, respectively. Pe, Petal; Pi, Pistil; Sn, Staminoid; Sp, Serrated petal; St, Stamen. Scale bars = 100 μm.

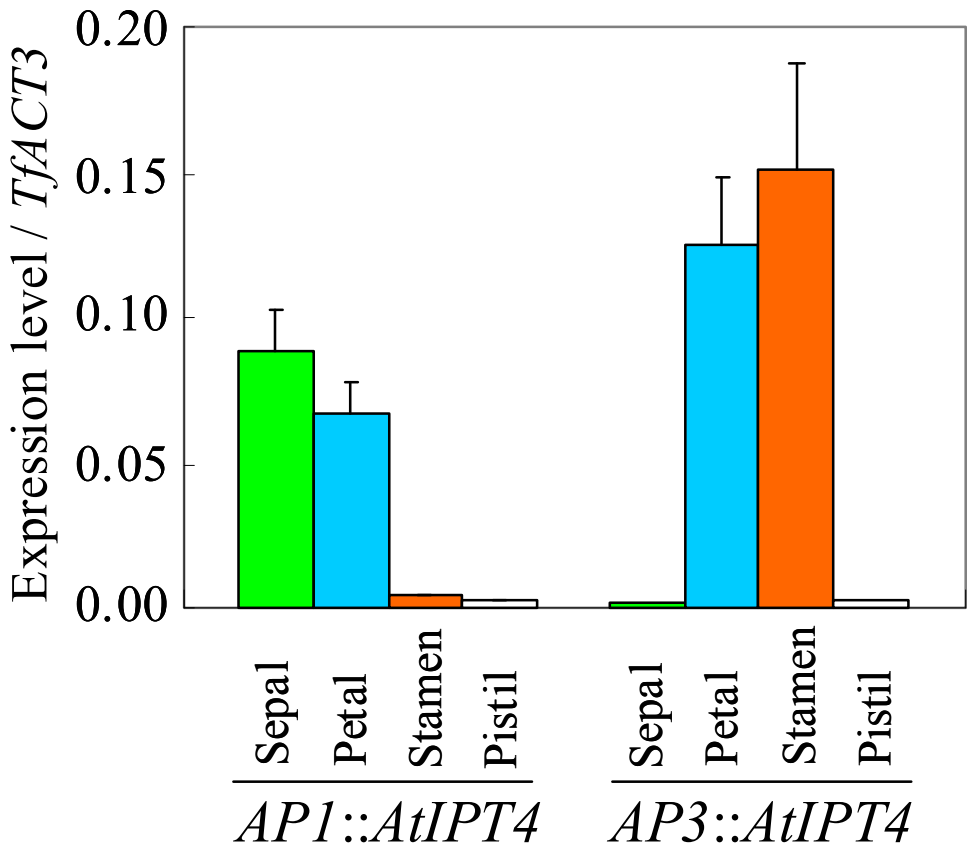

Fig. 19. *AtIPT4* expression in the floral organs of transgenic torenia. The expression levels are shown as a value relative to that of *TfACT3*, which was used as an internal standard. Vertical bars represent ± SE (n = 3).

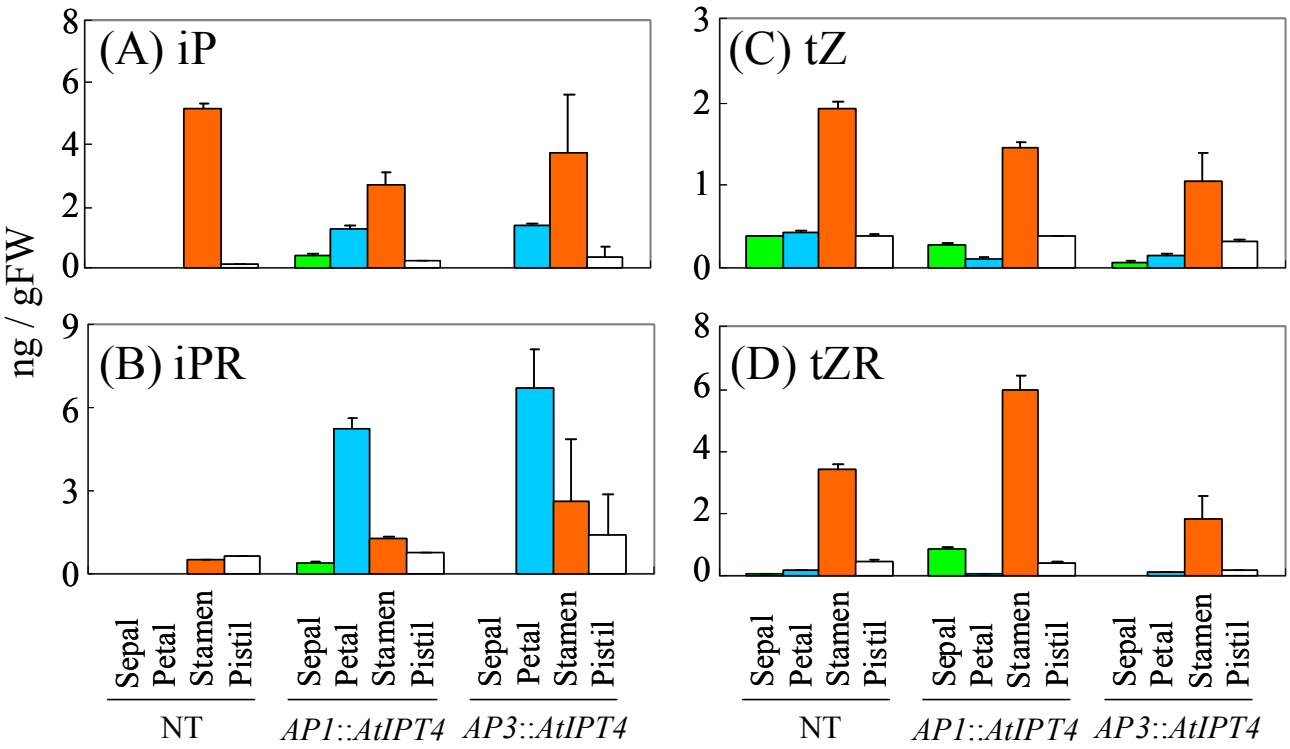

Fig. 20. Concentration of endogenous cytokinins in the floral organs of normal type (NT) and transgenic torenia. iP, isopentenyladenine; iPR, isopentenyladenine riboside; tZ, *trans*-zeatin; tZR, *trans*-zeatin riboside. Vertical bars represent ± SE (n = 3).

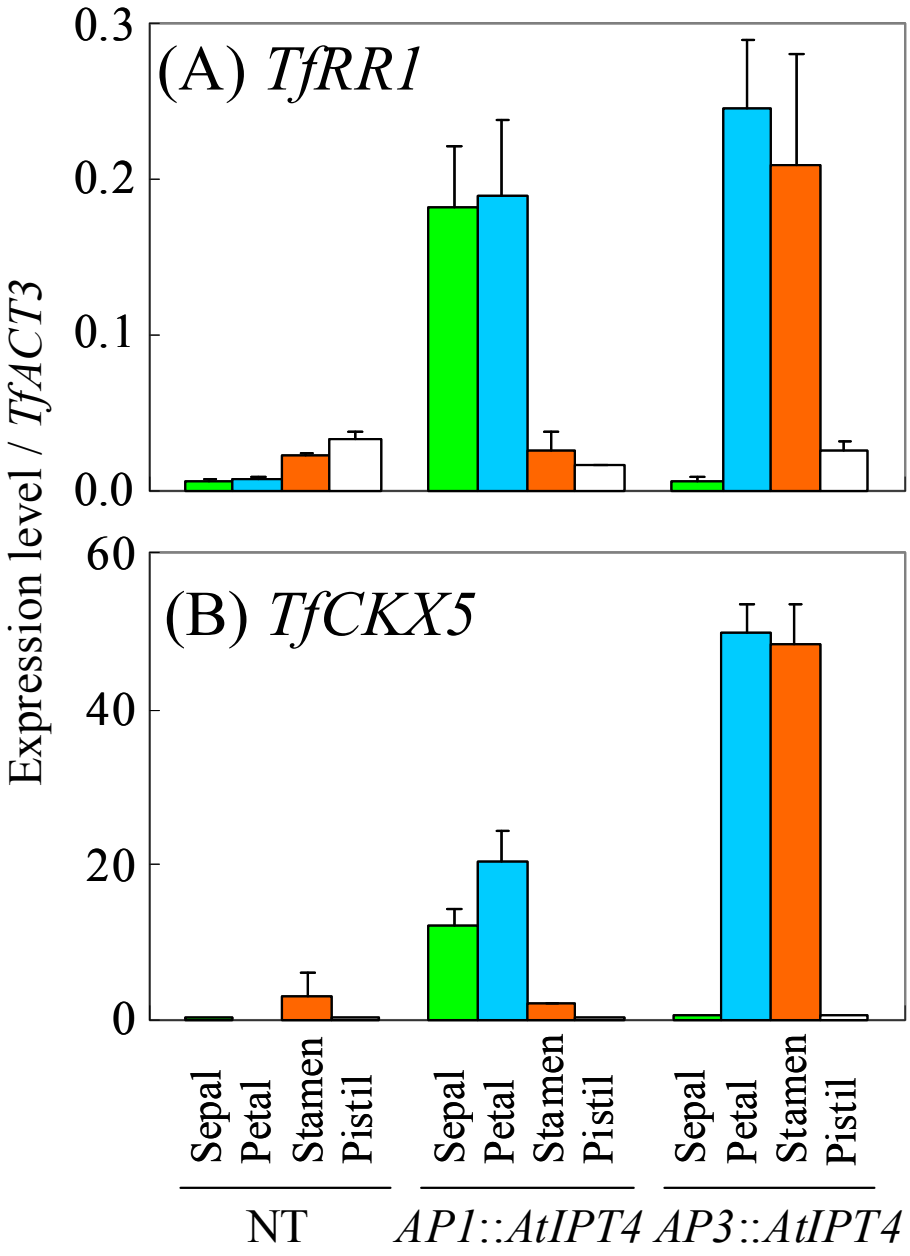

Fig. 21. Expression of *TfRR1* and *TfCKX5* in the floral organs of normal type (NT) and transgenic torenia. The expression levels of *TfRR1* (A) and *TfCKX5* (B) are shown as values relative to that of *TfACT3*, which was used as an internal standard. Vertical bars represent ± SE (n = 3).

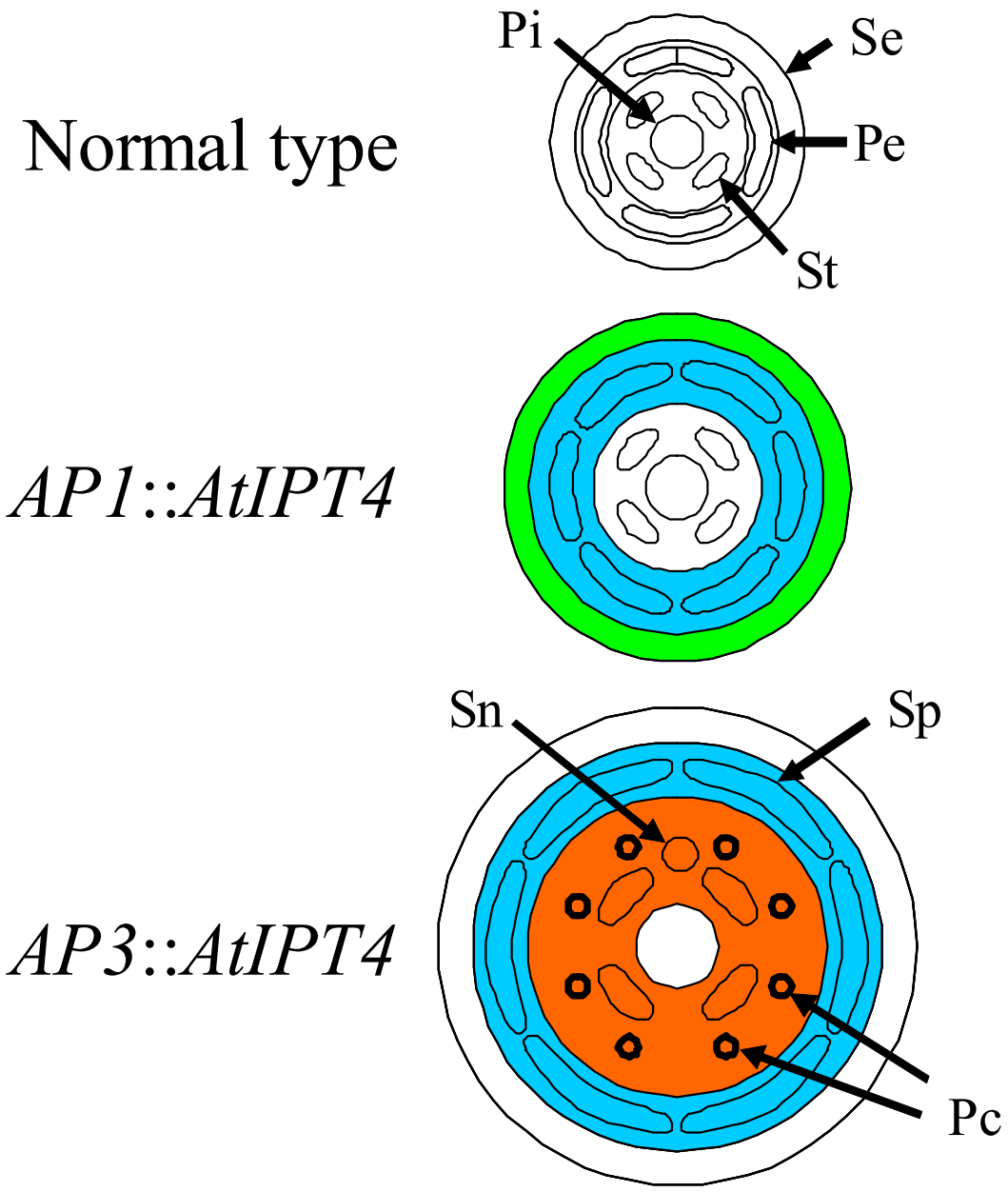

Fig. 22. Model accounting for the effect of localized elevation of cytokinin signal in flower buds on flower morphology. *AP1*::*AtIPT4* and *AP3*::*AtIPT4* indicate the transgenic plants promoted floral organ specific cytokinin biosynthesis described in Fig. 16. Whorls with elevated cytokinin levels are colored with green in whorl 1, blue in whorl 2, and orange in whorl 3. Pc, Paracorolla; Pe, Petal; Pi, Pistil; Se, Sepal; Sn, Staminoid; Sp, Serrated petal; St, Stamen.

Chapter 5

General discussion

In this study, it was shown that spatial and temporal distribution patterns of cytokinin signals in flower buds are important for inducing ornamental flower morphologies such as paracorolla and serrated petal margin in torenia. Thus far, the results of morphological changes by CPPU treatment (Chapters 2 and 3) and by genetic engineering (Chapter 4) have been discussed individually. In Chapter 5, we will try, by elaborating on the results described in Chapters 2 to 4, to identify more universal molecular mechanisms underlying these ornamental flower morphologies. Based on the molecular mechanisms uncovered in this study, we will also discuss future prospects for basic research and the development of transgenic technology.

Of the ornamental flower morphologies induced in CPPU-treated torenia, it was discussed in Chapter 2 that elevated cytokinin signals at the paracorolla initiation site, i.e., at the abaxial side of the basal part of the stamen for wide paracorolla and at the middle part of the petal for narrow paracorolla, is critical for paracorolla induction. In Chapter 4 it was suggested that the paracorolla was induced in *AP3*::*AtIPT4* torenia plants by marked receptacle enlargement after differentiation of the stamen primordia. This induction occurs because the receptacle enlargement remarkably increases the space between the stamens, promoting the initiation of paracorolla primordia. On the basis of the discussion in each chapter, it may be expected that receptacle enlargement is not induced by CPPU treatment and that a spatial elevation of cytokinin signals at the paracorolla initiation site does not occur in *AP3*::*AtIPT4* torenia plants. However, the receptacle is enlarged when the paracorollas are induced by CPPU treatment (Nishijima et al., 2007). In contrast, it is

unlikely that elevated cytokinin signals are spatially localized to the paracorolla initiation site in *AP3*::*AtIPT4* torenia plants. This is because *AP3*, like its ortholog *TfDEF*, is expressed in the whole petal and stamen (Krizek and Meyerowitz, 1996; Fig. 13B in Chapter 3).

It accordingly hypothesized that paracorolla induction is promoted by two factors: (1) receptacle enlargement after differentiation of the stamen primordia and (2) localization of elevated cytokinin signals to the paracorolla initiation site in flower buds. This hypothesis is supported by the finding that paracorolla induction by CPPU treatment is much more stable and stronger than that in *AP3*::*AtIPT4* torenia plants (Nishijima and Shima, 2006), given that both receptacle enlargement and the precise localization of cytokinin signals to the paracorolla initiation site occurred in CPPU-treated torenia, but only receptacle enlargement occurred in *AP3*::*AtIPT4* torenia plants (Fig. 23).

To test the above hypothesis, it is necessary to exploit an experimental system that specifically induces receptacle enlargement, spatially elevated cytokinin signals at the paracorolla initiation site, or both. As described in the discussion in Chapter 4, receptacle enlargement is probably caused by enlargement of the floral meristem via the expression of the genes (*WUS* and *CLV*) regulating meristematic activity (Bartrina et al., 2011; Lindsay et al., 2006). Thus, the production of a transgenic plant overexpressing *WUS* or suppressing *CLV* expression in floral meristem may serve to reveal the effect of receptacle enlargement on paracorolla induction, exclusive of the effect of the localization of cytokinin signals to the paracorolla initiation site. In contrast, promotion of *IPT* expression under the control of a specific promoter at the paracorolla initiation site may be useful for revealing the effect of localization of elevated cytokinin signals at the paracorolla initiation site in the absence of receptacle enlargement. However, to date, appropriate promoters have not been developed and further research is required.

To date, the molecular mechanism responsible for the genetically induced paracorollas seen in *Narcissus*, *Passiflora*, and other flowers has not been described. Based on the results of this study, two strategies may be considered as clues to the mechanism. One is to determine whether marked receptacle enlargement after differentiation of the stamen primordia occurs, and the other is to determine whether cytokinin signals are spatially elevated at the paracorolla initiation site in flower buds. If one or both events occur, the same mechanism as that in torenia may function in the induction of paracorolla differentiation and development. Only one study in *A. majus* has morphologically analyzed paracorolla differentiation and development in detail (Yamaguchi et al., 2010), but the extent of receptacle enlargement was not clearly different between cultivars with and without paracorolla. Accordingly, we recommend that studies based on the above two strategies will be performed in other plant species forming paracorollas.

As described in introduction in Chapter 3, morphologies of the genetically-induced paracorollas vary depending on the plant species. Whether the expression pattern of floral homeotic genes is involved in the regulation of the morphologies of genetically induced paracorollas remains to be determined. In Chapter 3, we showed that the expression pattern of floral homeotic genes determined by the site of paracorolla initiation is responsible for paracorolla morphologies. It may accordingly be hypothesized that the paracorolla initiation site, depending on the plant species, affects paracorolla morphology. In *A. majus*, the paracorolla initiation site is on the abaxial and lateral side of the basal part of the stamen, as is the case in the wide paracorolla of torenia; therefore, the expression of floral homeotic genes dictates petal identity (Yamaguchi et al., 2010). Detailed morphological observations of paracorolla initiation in other plants with genetically induced paracorollas have not yet been made.

The serrated petal margin induced by CPPU treatment is caused by the rearrangement of

vascular bundles in the limb of the petal (Nishijima and Shima, 2006). Given that CPPU treatment enhances cytokinin signals in the limb as shown in Fig. 7C, we discussed in Chapter 2 that serrated petal margins are induced by the elevation of cytokinin signals in the limb. However, in Chapter 4, we discussed that elevated cytokinin signals in the stamen induced serrated petal margins, given that the serrated petal margins were observed only in *AP3*::*AtIPT4* torenia plants and not in *AP3*::*AtIPT4* plants. These assertions seem to contradict each other; however, cytokinin signals were elevated not only in petals but also in stamens after CPPU treatment, as shown in Fig. 6 in Chapter 2. In addition, cytokinin signals were elevated both in petals and stamens in *AP3*::*AtIPT4* torenia plants (Fig. 21, Chapter 4). Therefore, it is assumed that elevated cytokinin signals in both the petals and stamens are necessary to induce serrated petal margins (Fig. 24). With respect to this hypothesis, it has already been shown in Chapter 4 that cytokinin signals elevated in petals, but not in stamens, are unable to induce serrated petal margins in *AP1*::*AtIPT4* torenia plants. Production of a transgenic plant with elevated cytokinin signals in stamens, but not in petals, may allow testing this hypothesis. Studies of *Arabidopsis* mutants have shown that cytokinin affects the arrangement of vascular bundles in the stem and root (Cui et al., 2011; Pineau et al., 2005). However, in floral organs, the molecular mechanism of cytokinin action on vascular bundle arrangement remains to be determined.

In this study, floral organ-specific promotion of cytokinin biosynthesis was achieved by the production of transgenic torenia with induced ornamental flower morphologies. Elevated cytokinin signals in sepals and petals increased petal number in *AP1*::*AtIPT4* plants, and elevated cytokinin signals in petals and stamens induced corolla expansion, paracorollas, and serrated petal margins in *AP3*::*AtIPT4* plants. Of these morphological changes, corolla expansion and serrated petal margins were stable phenotypes in *AP3*::*AtIPT4* torenia plants. Corolla enlargement is also promoted in petunia transformed with the *Agrobacterium IPT*

gene under the control of the *AP3* promoter (Verdonk et al., 2008). Thus, the induction of corolla enlargement by promotion of cytokinin biosynthesis with the *AP3* promoter may be a universal phenomenon among plant species so that this strategy may be applied to other horticultural plants. However, we do not yet know whether induction of serrated petal margins by this strategy is a universal phenomenon.

The *AP3*::*AtIPT4* torenia plant described in this study is the first example of paracorolla induced by genetic engineering. Introduction of *AP3*::*AtIPT4* into petunia also induced an extra floral organ on the lateral side of the basal part of the stamen, presumably a paracorolla based on the position of initiation (Nishijima, unpublished). These results suggest that induction of the paracorolla by an *AP3*::*AtIPT4* construct is a universal phenomenon among plant species. Thus, a paracorolla may be induced in other floricultural plants by elevation of cytokinin signals, particularly in petals and stamens. In *AP3*::*AtIPT4* plants, only narrow paracorollas were weakly induced. In contrast, CPPU treatment stably and strongly induces both narrow and wide paracorollas (Niki et al., 2012; Nishijima and Shima, 2006), suggesting that transgenic technology needs further development for practical application to paracorolla induction. As described above, both receptacle enlargement and localization of elevated cytokinin signals to the site of paracorolla initiation will be necessary for stable paracorolla induction. Although receptacle enlargement was observed in *AP3*::*AtIPT4* torenia plants, precise localization of cytokinin signals to the site of paracorolla initiation was impossible with the *AP3*::*AtIPT4* construct, given that the *AP3* promoter induces the transgene in the entire area of whorls 2 and 3 throughout flower bud development (Krizek and Meyerowitz, 1996). A promoter whose induction is more precisely localized to the site of paracorolla initiation will be necessary.

Taking the above results and discussions together, effect of localized cytokinin signal to the floral stage-dependent induction of ornamental flower is summarized in Fig. 25. When

enhanced receptacle enlargement up to Stage 5 is combined with localized cytokinin signal at the abaxial side of the basal part of the stamen at Stage 4, paracorolla primordia are initiated at this site in Stage 4 to 5. These primordia develop into wide paracorollas because class A and B floral homeotic genes are expressed at the site of paracorolla initiation. When enhanced receptacle enlargement up to Stage 5 is combined with localized cytokinin signal at middle part of the petal at Stage 5, paracorolla primordia are initiated at this site in Stage 6 to 7. These primordia develop into narrow paracorollas because class B floral homeotic genes are expressed at the site of paracorolla initiation without substantial expression of class A and C genes. Serrated petal margins are induced at Stage 6 to 7 by localized cytokinin signals in sepals and petals.

To date, many transgenic floricultural plants have been developed with the aim of producing carnations and roses with violet flowers (Chandler and Sanchez, 2012). However, with respect to improvement of flower morphology, increasing petal number in cyclamen is the only technology aimed at practical use (Terakawa et al., 2010), given that ornamental flower morphologies in the form of double and large flowers have already been bred into major floricultural plants by conventional breeding programs. Thus, application of the transgenic technology employed in this study is likely to be targeted to the plants showing little variation in flower morphology. For example, *Gentiana*, *Gloriosa*, *Platycodon grandiflorus* as cut flower, *Catharanthus roseus*, *Bougainvillea*, *Salvia*, *Mandevilla* as bedding and/or pot plant, and many other floricultural plants may be proper targets. However, for practical use of transgenic plants, much expense is entailed in paying royalties on genetic engineering tools and performing biosafety risk assessment. In minor floricultural plants, it is difficult to pay these costs for genetic engineering unless sales will surely and dramatically increase. Thus, future reduction of these costs is desirable. Biosafety risk assessment requires much expense to investigate the extent of transgene flow to the wild

relatives when these species can be crossed with the transgenic plants (Yoshikura, 2006). Therefore, induction of male sterility will reduce the risk of pollen-mediated transgene flow to the wild relatives, which may reduce the cost required for practical use of transgenic plants. For this purpose, the use of anther-specific promoters fused to cytotoxic genes is a useful method for inducing male sterility (Koltunow et al., 1990; Mariani et al., 1990; Xu et al., 1995). On the other hand, royalties of genetic engineering tools could be reduced when commercial production of transgenic plants increases. Basic patent of transgenic tools, e.g., *Agrobacterium*-mediated transformation, has been occupied by several major international companies. Together with the fact that some of these basic patents have been proceedingly expired, reduction of the royalties will be expected also by international competition of research and development.

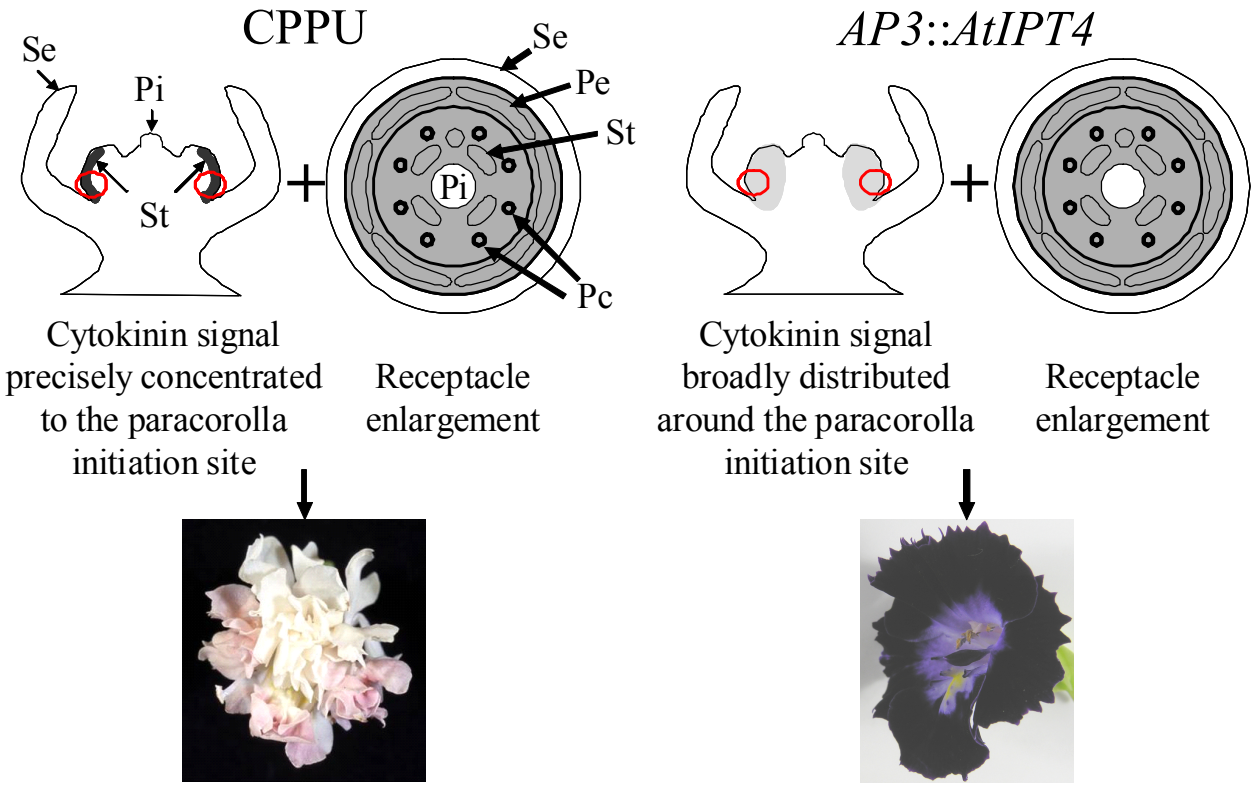

Fig. 23. Dual-factor hypothesis on paracorolla induction in torenia. In this hypothesis, both cytokinin signal precisely localized to the site of paracorolla initiation and receptacle enlargement are necessary for stable and strong paracorolla induction. The floral organs and whorls with high level of cytokinin signal are indicated by gray. The darkness of shade gray area represents extent of cytokinin signal. Paracorolla initiation sites are indicated by red circle. Pc, Paracorolla; Pe, Petal; Pi, Pistil; Se, Sepal; St, Stamen.

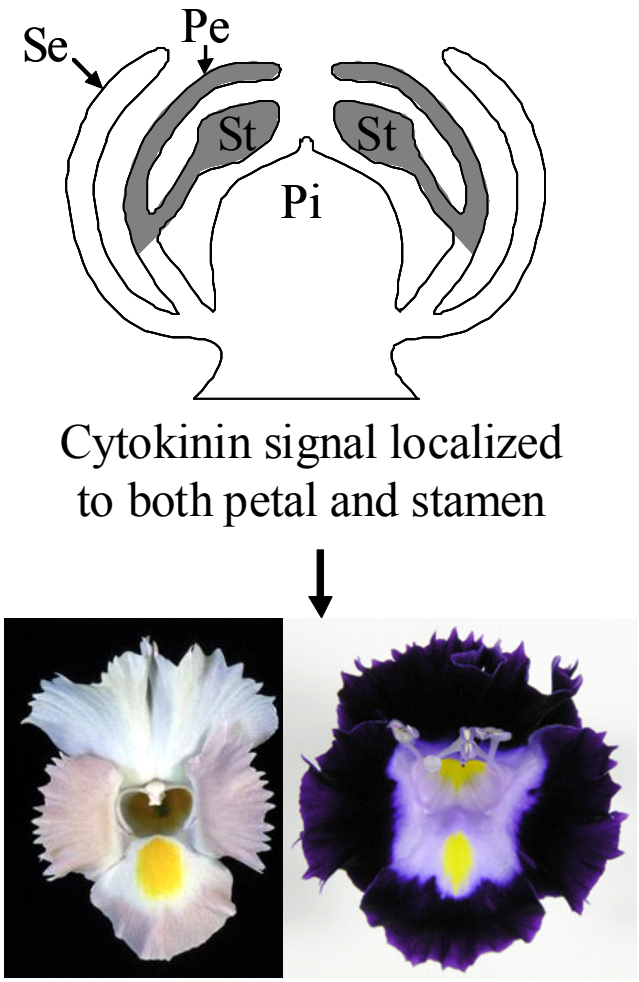

Fig. 24. Hypothesis on induction of serrated petal margin in torenia. In this hypothesis, cytokinin signal localized to both petal and stamen is necessary for the induction of serrated petal margin. The floral organs with high level of cytokinin signal are indicated by gray. Pe, Petal; Pi, Pistil; Se, Sepal; St, Stamen.

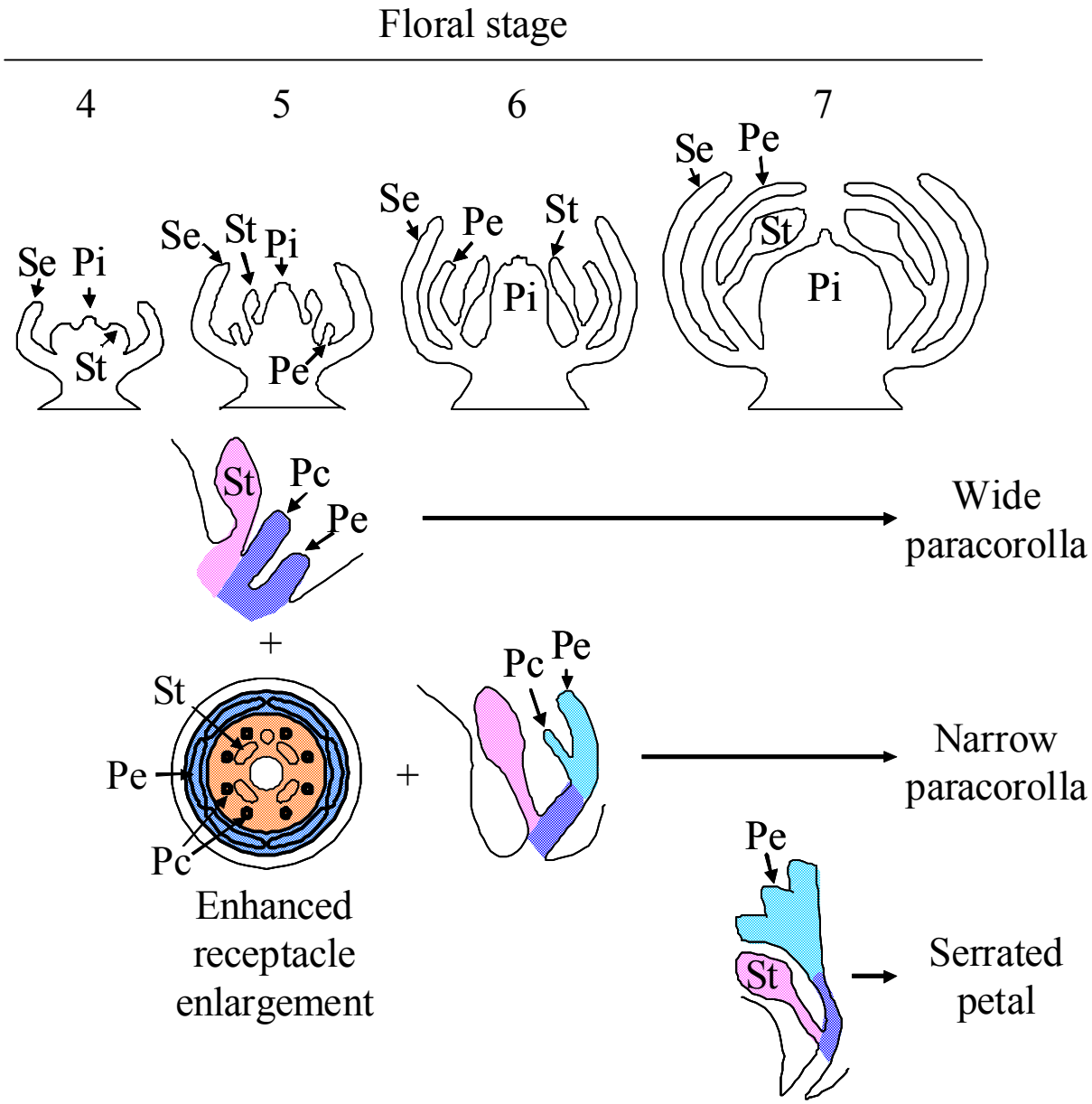

Fig. 25. Mechanism responsible for floral stage-dependent induction of paracorollas and serrated petal margins by elevated cytokinin signal. Illustrations shown in the top row indicate normal type flower buds at the corresponding floral stage. The floral organ with high level of cytokinin signal is indicated by dotted pattern. Expression pattern of floral homeotic genes is indicated by coloring; class A alone (green), class A and B (blue), class B alone (light blue), class B and C (pink), and class C alone (orange). Pc, Paracorolla; Pe, Petal; Pi, Pistil; Se, Sepal; St, Stamen.

Summary

For floricultural plants, flower morphology is one of the most important traits determining attractiveness and commercial value. Improvement of flower morphology toward more ornamental flowers is a major objective of breeding programs, but conventional breeding programs can be time-consuming, and the development of efficient breeding methods is desired. In recent studies, treatment with forchlorfenuron (CPPU), an inhibitor of the cytokinin degradation enzyme cytokinin oxidase/dehydrogenase (CKX), induces several ornamental flower morphologies in torenia (*Torenia fournieri* L.) depending on the floral stage of CPPU treatment.

In this study, we aimed to elucidate the molecular mechanism responsible for CPPU-induced ornamental flower morphologies in torenia. Furthermore, we employed floral organ-specific promotion of cytokinin biosynthesis using transgenic technologies to produce torenia with ornamental flower morphologies.

In the work described in Chapter 2, we investigated the temporal and spatial distributions of cytokinin signals in CPPU-treated flower buds as indicated by type-A response regulator (RR) and CKX gene expression. Quantitative real-time PCR analysis showed that the expression of both *TfRR1* and *TfCKX5* was induced from 1 day after CPPU treatment in sepals, petals, stamens, and pistils and maintained at a high level until 5 days after treatment when the earliest morphological changes due to CPPU treatment were observed. *In situ* hybridization analysis showed weak expression of both genes in stamens and pistils through all floral stages of untreated flower buds. However, when CPPU was applied at the sepal development stage, expression of both genes was strongly induced at the abaxial side of the stamen primordia, which are sites of initiation of the wide paracorolla. When CPPU was applied during the early stage of corolla development, high expression of these genes was

observed in the stamen and in the basal and middle parts of the petal, which are the sites of initiation of the narrow paracorolla. When CPPU was applied during the middle corolla development stage, strong expression of these genes was detected in the middle to apical parts of the petal, which is the site of changes in the distribution pattern of vascular bundles and the resulting serrated margins.

In the work described in Chapter 3, we investigated the morphological properties and the role of floral homeotic genes in the formation of two CPPU-induced types of paracorolla, wide and narrow paracorolla. The morphology of epidermal cells and distribution pattern of vascular bundles were the same in wide paracorolla as in petals; however, in the narrow paracorolla, the morphology of epidermal cells was either petal-like or stamen-like, and the distribution pattern of vascular bundles was stamen-like. *In situ* hybridization analysis of floral homeotic genes showed that a class A gene, *TfSQUA*, and the class B genes, *TfDEF* and *TfGLO*, were expressed in the broad region of the primordia of the wide paracorolla, as in petals. Class C genes, *TfPLE1* and *TfFAR*, were only expressed at margins of the paracorolla primordia. However, in primordia of the narrow paracorolla, *TfSQUA* was expressed only at the margin of the primordia, whereas the class B genes and one of the class C genes *(TfPLE1*) were expressed in a broad region of the primordia, similar to the case of the primordia of the wide paracorolla. Thus, this expression pattern in the narrow paracorolla was intermediate between that of petals and stamens. Furthermore, these expression patterns were similar to those at the paracorolla initiation sites.

In the work described in Chapter 4, we introduced *AtIPT4* into torenia under the control of the *AP1* or *AP3* promoter to characterize the relationship between organ-specific promotion of cytokinin biosynthesis within flower buds and flower morphology. *AP1*::*AtIPT4* plants had an increased number of petals, whereas *AP3*::*AtIPT4* plants had expanded corolla, paracorolla, and serrated petal margins along with an increased number of petals. In

AP3::*AtIPT4* plants, marked receptacle enlargement was observed when flower buds were in the early corolla development stage in which the paracorolla primordia differentiate. As expected, *AtIPT4* was expressed in the sepals and petals of *AP1*::*AtIPT4* plants and in the petals and stamens of *AP3*::*AtIPT4* plants. Cytokinin signals as revealed by *TfRR1* and *TfCKX5* expression were elevated in the floral organs in which the transgene was expressed.

The results described above suggest that the paracorolla and serrated petal margins are induced by high localized levels of cytokinin signals at the site of those morphological changes (Chapter 2). The expression patterns of floral homeotic genes at the early stage of paracorolla development determine paracorolla morphology, and the expression pattern is determined by the site within flower buds where the paracorolla is formed (Chapter 3). Localized cytokinin signals in sepals and petals increase in the petal number and in petals and stamens are necessary to induce corolla expansion and serrated petal margins (Chapters 4 and 5). Furthermore, both receptacle enlargement and localization of elevated cytokinin signals to the paracorolla initiation site are necessary for stable induction of the paracorollas (Chapter 5). These findings may aid in the development of efficient breeding methods for improvement of flower morphology.

Acknowledgments

I wish to express my deeply gratitude to Dr. Takaaki Nishijima, Professor of Graduate School of Life and Environmental Sciences of Tsukuba University, for his kind guidance and for giving me useful suggestion and invaluable discussion throughout this study as well as for critical reading of my manuscripts and this doctoral dissertation.

I would like to extend my sincerest appreciation to my advisory committee members, Dr. Akemi Ohmiya, Dr. Masayoshi Nakayama, Professors of Graduate School of Life and Environmental Sciences of Tsukuba University, and Dr. Naoya Fukuda, Associate Professor of Graduate School of Life and Environmental Sciences of Tsukuba University, for their valuable comments and critical review to further improve this doctoral dissertation.

I am heartily thankful to Dr. Akira Kanno, Professor of Graduate School of Life Sciences of Tohoku University, and Dr. Masayo Hirai for their kind guidance in the work for *in situ* hybridization experiment.

I am very grateful to Dr. Ryutaro Aida, National Agriculture and Food Research Organization Institute of Floricultural Science (NIFS), for his helpful support and guidance in production of transgenic torenia.

I acknowledge Dr. Tsuyoshi Nakagawa, Professor of Interdisciplinary Center for Science Research of Shimane University, for kindly supplying us with the pGWB1 vector.

Thanks are also due to Mr. Taximaimaiti Mahesumu (Yili Teachers' College, China) and Dr. Hiroyasu Yamaguchi (NIFS) for their experimental assistance and suggestion.

I thank Dr. Tomoko Niki (NIFS) for her technical assistance especially in molecular works and Mrs. Yoshiko Kashiwagi, Mrs. Satoko Ohtawa, and Mrs. Yasuko Taniji for their technical assistance especially in production and maintenance for transgenic plants. I also thank Mrs. Tomoko Kurobe for her supports in experimental works.

I sincerely thank the laboratory members, Dr. Tamotsu Hisamatsu, Dr. Norihiro Ohtsubo, Dr. Katsutomo Sasaki, Dr. Ichiro Kasajima, Mrs. Toshie Iida, and other all members of NIFS for their helpful comments, kindness and encouragement.

References

Aida, R. 2008. *Torenia fournieri* (torenia) as a model plant for transgenic studies. Plant Biotechnol. 25: 541–545.

Aida, R. and M. Shibata. 1995. *Agrobacterium*-mediated transformation of torenia (*Torenia fournieri*). Breed. Sci. 45: 71–74.

Aida, R. and M. Shibata. 2001. Transgenic *Torenia fournieri* Lind (torenia). p. 294–305. In: Y. P. S. Bajaj (ed.). Biotechnology in agriculture and forestry, vol 48 transgenic crops III. Springer, Berlin.

Aida, R., S. Kishimoto, Y. Tanaka and M. Shibata. 2000. Modification of flower color in torenia (*Torenia fournieri* Lind.) by genetic transformation. Plant Sci. 153: 33–42.

Aida, R., T. Yoshida, K. Ichimura, R. Goto and M. Shibata. 1998. Extension of flower longevity in transgenic torenia plants incorporating ACC oxidase transgene. Plant Sci. 138: 91–101.

Auer, C. A. 2002. Discoveries and dilemmas concerning cytokinin metabolism. J. Plant Growth Regul. 21: 24–31.

Bartrina, I., E. Otto, M. Strnad, T. Werner and T. Schmülling. 2011. Cytokinin regulates the activity of reproductive meristems, flower organ size, ovule formation, and, thus, seed yield in *Arabidopsis thaliana*. Plant Cell 23: 69–80.

Benková, E., M. Michniewicz, M. Sauer, T. Teichmann, D. Seifertová, G. Jürgens and J. Friml. 2003. Local, efflux-dependent auxin gradients as a common module for plant organ formation. Cell 15: 591–602.

Bennett, M. D., I. J. Leitch, H. J. Price and J. S. Johnston. 2003. Comparisons with *Caenorhabditis* (~100 Mb) and Drosophila (~175 Mb) using flow cytometry show

genome size in Arabidopsis to be ~157 Mb and thus ~25% larger than the Arabidopsis Genome Initiative of ~125 Mb. Ann. Bot. 91: 547–557.

Bilyeu, K. D., J. L. Cole, J. G. Laskey, W. R. Riekhof, T. J. Esparza, M. D. Kramer and R. O. Morris. 2001. Molecular and biochemical characterization of a cytokinin oxidase from maize. Plant Physiol. 125: 378–386.

Bowman, J. L., D. R. Smyth and E. M. Meyerowitz. 1991. Genetic interactions among floral homeotic genes of *Arabidopsis*. Development 112: 1–20.

Bradley, D., R. Carpenter, H. Sommer, N. Hartley and E. Coen. 1993. Complementary floral homeotic phenotypes result from opposite orientations of a transposon at the *plena* locus of *Antirrhinum*. Cell 72: 85–95.

Brandstatter, I. and J. J. Kieber. 1998. Two genes with similarity to bacterial response regulators are rapidly and specifically induced by cytokinin in *Arabidopsis*. Plant Cell 10: 1009–1019.

Brugière, N., S. Jiao, S. Hantke, C. Zinselmeier, J. A. Roessler, X. Niu, R. J. Jones and J. E. Habben. 2003. Cytokinin oxidase gene expression in maize is localized to the vasculature, and is induced by cytokinins, abscisic acid, and abiotic stress. Plant Physiol. 132: 1228–1240.

Chandler, S. F. and C. Sanchez. 2012. Genetic modification; the development of transgenic ornamental plant varieties. Plant Biotechnol. J. 10: 891–903.

Chen, C. M. and M. Kristopeit. 1981. Metabolism of cytokinin: dephosphorylation of cytokinin ribonucleotide by 5'-nucleotidases from wheat germ cytosol. Plant Physiol. 67: 494–498.

Clark, S. E., M. P. Running and E. M. Meyerowitz. 1993. *CLAVATA1*, a regulator of meristem and flower development in *Arabidopsis*. Development 119: 397–418.

Coen, E. S. and E. M. Meyerowitz. 1991. The war of the whorls: genetic interactions

controlling flower development. Nature 353: 31–37.

Cui, H., Y. Hao, M. Kovtun, V. Stolc, X-W. Deng, H. Sakakibara and M. Kojima. 2011. Genome- wide direct target analysis reveals a role for SHORT-ROOT in root vascular patterning through cytokinin homeostasis. Plant Physiol. 157: 1221–1231.

D′Agostino, I. B., J. Deruère and J. J. Kieber. 2000. Characterization of the response of the *Arabidopsis* response regulator gene family to cytokinin. Plant Physiol. 124: 1706–1717.

Davies, B., P. Motte, E. Keck, H. Saedler, H. Sommer and Z. Schwarz-Sommer. 1999. *PLENA* and *FARINELLI*: redundancy and regulatory interactions between two *Antirrhinum* MADS-box factors controlling flower development. EMBO J. 18: 4023–4034.

Dewitte, W., A. Chiappetta, A. Azmi, E. Witters, M. Strnad, J. Rembur, M. Noin, D. Chriqui and H. Van Onckelen. 1999. Dynamics of cytokinins in apical shoot meristems of a day-neutral tobacco during floral transition and flower formation. Plant Physiol. 119: 111–121.

Dobrev, P. I. and M. Kaminek. 2002. Fast and efficient separation of cytokinins from auxin and abscisic acid and their purification using mixed-mode solid phase extraction. J. Chromatogr. A 950: 21–29.

Drews, G. N., J. L. Bowman and E. M. Meyerowitz. 1991. Negative regulation of the Arabidopsis homeotic gene *AGAMOUS* by the *APETALA2* product. Cell 65: 991–1002.

Estruch, J. J., A. Granell, G. Hansen, E. Prinsen, P. Redig, H. van Onckelen, Z. Schwarz-Sommer, H. Sommer and A. Spena. 1993. Floral development and expression of floral homeotic genes are influenced by cytokinins. Plant J. 4: 379–384.

Ewart, L. 1984. Plant breeding. p. 180–253. In: K. C. Sink (ed.). Petunia. Springer-Verlag, Berlin.

Ferrario, S., I. J. Leitch, R. G. H. Immink and G. C. Angenent. 2004. Conservation and diversity in flower land. Curr. Opin. Plant Biol. 7: 84–91.

Frébort, I., M. Kowalska, T. Hluska, J. Frébortová and P. Galuszka. 2011. Evolution of cytokinin biosynthesis and degradation. J. Exp. Bot. 62: 2431–2452.

Geng, S., M. Ma, H-C. Ye and G-F. Li. 2002. Anther-specific expression of *ipt* gene in transgenic tobacco and its effect on plant development. Transgenic Res. 11: 269–278.

Gustafson-Brown, C., B. Savidge and M. F. Yanofsky. 1994. Regulation of the arabidopsis floral homeotic gene *APETALA1*. Cell 76: 131–143.

Hayata, Y., Y. Niimi, N. Iwasaki and S. Aoki. 1991. Studies on inducing of parthenocarpie fruit set and fruit setting of water melon 1. The effect of Fulmet treatment. J. Japan. Soc. Hort. Sci. (Japan) 60 (Suppl. 2): 304–305 (In Japanese).

Hayata, Y., Y. Niimi, K. Makita and R. Isoda. 1990. Effect of cytokinin on the fruit set and sugar accumulation of melon fruit. J. Japan. Soc. Hort. Sci. (Japan) 59 (Suppl. 1): 370–371 (In Japanese).

Hirai, M., T. Kamimura and A. Kanno. 2007. The expression patterns of three class B genes in two distinctive whorls of petaloid petals in *Alstromeria ligtu*. Plant Cell Physiol. 48: 310–321.

Hou, B., E. K. Lim, G. S. Higgins and D. J. Bowles. 2004. N-Glucosylation of cytokinins by glycosyltransferases of *Arabidopsis thaliana*. J. Biol. Chem. 279: 47822–47832.

Huang, S,. R. E. Cerny, Y. Qi, D. Bhat, C. M. Aydt, D. D. Hanson, K. P. Malloy and L. A. Ness. 2003. Transgenic studies on the involvement of cytokinin and gibberellin in male development. Plant Physiol. 131: 1270–1282.

Huxley, A. J., M. Griffiths and M. Levy. 1992. The New Royal Horticultural Society Dictionary of Gardening, The Macmillan Press Limited, London and Basingstoke, pp. 728–731.

Ikeda, T., K. Tanabe, K. Banno, F. Tamura and Y. Kimura. 1990. Promotion of fruit set and growth by 4PU in Melon (*Cucumis melo* L. cv. Bohnas). J. Japan. Soc. Hort. Sci. (Japan) 59 (Suppl. 2): 434–435 (In Japanese).

Jack, T., L. L. Brockman and E. M. Meyerowitz. 1992. The homeotic gene *APETALA3* of *Arabidopsis thaliana* encodes a MADS box and is expressed in petals and stamens. Cell 68: 683–687.

Kakimoto, T. 2001. Identification of plant cytokinin biosynthetic enzymes as dimethylallyl diphosphate: ATP/ADP isopentenyltransferases. Plant Cell Physiol. 42: 677–685.

Kataoka, K., S. Date, T. Goto and T. Asahira. 1994. Reducing of tomato puffiness in auxin-induced parthenocarpic fruits by forchlorfenuron (1-(2-chloro-4-pyridyl)-3-phenylurea). J. Japan. Soc. Hort. Sci. (Japan) 63: 61–66 (In Japanese).

Kiba, T., T. Naitou, N. Koizumi, T. Yamashino, H. Sakakibara and T. Mizuno. 2005. Combinatorial microarray analysis revealing *Arabidopsis* genes implicates in cytokinin responses through the His→Asp phosphorelay circuitry. Plant Cell Physiol. 46: 339–355.

Kikuchi, S., H. Tanaka, T. Shiba, M. Mii and H. Tsujimoto. 2006. Genome size, karyotype, meiosis and a novel extra chromosome in *Torenia fournieri*, *T. baillonii* and their hybrid. Chromosome Res. 14: 665–672.

Koiwai, M., F. Okuyama, K. Tanaka, A. Yamazaki, H. Honma, K. Ikeda and S. Taira. 2012. Induction of parthenocarpy by GA and CPPU treatments aimed for seedless berry production in female vines of Japanese wild grape, *Vitis coignetiae* Pulliat. Hort. Res. (Japan) 11: 87–95 (In Japanese).

Koltunow, A. M., J. Truettner, K. H. Cox, M. Wallroth and R. B. Goldberg. 1990. Different temporal and spatial gene expression patterns occur during anther development. Plant

Cell 2: 1201–1224.

Kramer, E. M., M. A. Jaramillo and V. S. Di Stilio. 2004. Patterns of gene duplication and functional evolution during the diversification of the *AGAMOUS* subfamily of MADS Box Genes in Angiosperms. Genetics 166: 1011-1023.

Krizek, B. A. and E. M. Meyerowitz. 1996. The *Arabidopsis* homeotic genes *APETALA3* and *PISTILLATA* are sufficient to provide the B class organ identity function. Development 122: 11–22.

Kurakawa, T., N. Ueda, M. Maekawa, K. Kobayashi, M. Kojima, Y. Nagato, H. Sakakibara and J. Kyozuka. 2007. Direct control of shoot meristem activity by a cytokinin-activating enzyme. Nature 445: 652–655.

Leibfried, A., J. P. C. To, W. Busch, S. Stehling, A. Kehle, M. Demar, J. J. Kieber and J. U. Lohmann. 2005. *WUSCHEL* controls meristem function by direct regulation of cytokinin-inducible response regulators. Nature 438: 1172–1175.

Letham, D. S. 1963. Zeatin, a factor inducing cell division isolated from *Zea mays*. Life Sci. 8: 569–573.

Li, Q. Z., X. G. Li, S. N. Bai, W. L. Lu and X. S. Zhang. 2002. Isolation of *HAG1* and its regulation by plant hormones during in vitro floral organogenesis in *Hyacinthus orientalis* L. Planta 215: 533–540.

Li, X. G., Y. H. Su, X. Y. Zhao, W. Li, X. Q. Gao and X. S. Zhang. 2010. Cytokinin overproduction-caused alteration of flower development is partially mediated by *CUC2* and *CUC3* in Arabidopsis. Gene 450: 109–120.

Lindsay, D. L., V. K. Sawhney and P. C. Bonham-Smith. 2006. Cytokinin-induced changes in *CLAVATA1* and *WUSCHEL* expression temporary coincide with altered floral development in *Arabidopsis*. Plant Sci. 170: 1111–1117.

Litt, A. and V. F. Irish. 2003. Duplication and diversification in the *APETALA1/FRUITFULL*

floral homeotic gene lineage: Implications for the evolution of floral development. Genetics 165: 821-833.

Mandel, M. A., C. Gustafson-Brown, B. Savidge and M. F. Yanofsky. 1992. Molecular characterization of the *Arabidopsis* floral homeotic gene *APETALA1*. Nature 360: 273–277.

Mariani, C., M. De Beuckeleer, J. Truettner, J. Leemans and R. B. Goldberg. 1990. Induction of male sterility in plants by a ribonuclease gene. Nature 347: 737–741.

Miller, C. O., F. Skoog, M. H. von Saltza and M. Strong. 1955. Kinetin, a cell division factor from deoxyribonucleic acid. J. Am. Chem. Soc. 77: 1329–1334.

Miyawaki, K., M. Matsumoto-Kitano and T. Kakimoto. 2004. Expression of cytokinin biosynthetic isopentenyltransferase genes in *Arabidopsis*: tissue specificity and regulation by auxin, cytokinin, and nitrate. Plant J. 37: 128–138.

Mizuno, T. 2005. Two-component phosphorelay signal transduction systems in plants: From hormone responses to circadian rhythms. Biosci. Biotechnol. Biochem. 69: 2263–2276.

Mok, D. W. and M. C. Mok. 2001. Cytokinin metabolism and action. Annu. Rev. Plant Physiol. Plant Mol. Biol. 52: 89–118.

Mok, D. W. S. and M. C. Mok. 1994. Cytokinins: Chemistry, Activity, and Function. CRC Press. Boca Raton, Florida.

Müller, B. 2011. Generic signal-specific responses: cytokinin and context-dependent cellular responses. J. Exp. Bot. 62: 3273–3288.

Nakagawa, T, T. Kurose, T. Hino, K. Tanaka, M. Kawamukai, Y. Niwa, K. Toyooka, K. Matsuoka, T. Jinbo and T. Kimura. 2007. Development of series of gateway binary vectors, pGWBs, for realizing efficient construction of fusion genes for plant transformation. J. Biosci. Bioeng. 104: 34–41.

Narumi, T., R. Aida, T. Niki, T. Nishijima, N. Mitsuda, K. Hiratsu, M. Ohme-Takagi and N.

Ohtsubo. 2008. Chimeric *AGAMOUS* repressor induces serrated petal phenotype in *Torenia fournieri* similar to that induced by cytokinin application. Plant Biotechnol. 25: 45–53.

Niki, T. and T. Nishijima. 2008. Relationship between homeotic gene expression and floral morphology in CPPU-treated torenia. Hort. Res. (Japan) 7 (Suppl. 2): 347 (In Japanese).

Niki, T., M. Hirai, T. Niki, A. Kanno and T. Nishijima. 2012. Role of floral homeotic genes in the morphology of forchlorfenuron-induced paracorollas in *Torenia fournieri* Lind. J. Japan. Soc. Hort. Sci. 81: 204–212.

Niki, T., T. Hisamatsu, R. Aida, M. Koshioka and T. Nishijima. 2006a. Production of dwarf plant by genetic engineering in transgenic torenia introduced GA 2-oxidase gene from torenia. 27th International Horticultural Congress & Exibition. Abstract: 338.

Niki, T., T. Mahesumu, T. Niki and T. Nishijima. 2013. Localized high expression of type-A response regulator and cytokinin oxidase/dehydrogenase genes in relation to forchlorfenuron-induced changes in flower morphology in *Torenia fournieri* Lind. J. Japan. Soc. Hort. Sci. 82: 69–77.

Niki, T., H. Yamaguchi and T. Nishijima. 2006b. Cloning and expression profiles of MADS-box genes in CPPU-treated flower buds of torenia. J. Japan. Soc. Hort. Sci. (Japan) 75 (Suppl. 2): 326 (In Japanese).

Nishijima, T. 2007. Hanagata. p. 37–43. In Nosangyosonbunkakyokai (ed.). Nogyogijututaikei Kakihen 5 (Tsuiroku) 9 (In Japanese). Nosangyosonbunkakyokai, Tokyo.

Nishijima, T. 2012. Large flower size: Molecular basis and role of cytokinin. J. Japan. Soc. Hort. Sci. 81: 129–139.

Nishijima, T. and K. Shima. 2006. Change in flower morphology of *Torenia fournieri* Lind. induced by forchlorfenuron application. Sci. Hortic. 109: 254–261.

Nishijima, T., H. Miyaki, K. Sasaki and T. Okazawa. 2006. Cultivar and anatomical analysis of corolla enlargement of petunia (*Petunia hybrida* Vilm.) by cytokinin application. Sci. Hortic. 111: 49–55.

Nishijima, T., T. Niki and T. Niki. 2011a. Corolla of the large-flowered petunia (*Petunia hybrida* Vilm.) cultivars exhibit low endogenous cytokinin concentration through enhanced expression of the genes encoding cytokinin oxidases. J. Japan. Soc. Hort. Sci. 80: 334–342.

Nishijima, T., T. Niki and T. Niki. 2011b. The large-flowered petunia (*Petunia hybrida* Vilm.) genotype promotes expressions of type-A response regulator and cytokinin receptor genes like cytokinin response. J. Japan. Soc. Hort. Sci. 80: 343–350.

Nishijima, T., H. Yamaguchi and T. Niki. 2007. Enlargement of floral bud and change in flower morphology induced by cytokinin biosynthesis inhibitor. Hort. Res. (Japan) 6 (Suppl. 1): 250 (In Japanese).

Ono, E., M. Fukuchi-Mizutani, N. Nakamura, Y. Fukui, K. Yonekura-Sakakibara, M. Yamaguchi, T. Nakayama, T. Tanaka, T. Kusumi and Y. Tanaka. 2006. Yellow flowers generated by expression of the aurone biosynthetic pathway. Proc. Natl. Acad. Sci. USA 103: 11075–11080.

Pernisová, M., P. Klíma, J. Horák, M. Válková, J. Malbeck, P. Soucek, P. Reichman, K. Hoyerová, J. Dubová, J. Friml, E. Zažímalová and J. Hejátko. 2009. Cytokinins modulate auxin-induced organogenesis in plants via regulation of the auxin efflux. Proc. Natl. Acad. Sci. USA 106: 3609–3614.

Pineau, C., A. Freydier, P. Ranocha, A. Jauneau, S. Turner, G. Lemonnier, J-P. Renou, P. Tarkowski, G. Sandberg, L. Jouanin, B. Sundberg, A-M. Boudet, D. Goffner and M. Pichon. 2005. *hca*: an Arabidopsis mutant exhibiting unusual cambial activity and altered vascular patterning. Plant J. 44: 271–289.

Potenza, C., L. Aleman and C. Sengupta-Gopalan. 2004. Targeting transgene expression in research, agricultural, and environmental applications: promoters used in plant transformation. In Vitro Cell. Dev. Biol. Plant 40: 1–22.

Rahmanzadeh, R., K. Müller, E. Fischer, D. Bartels and T. Borsch. 2005. The Linderniaceae and Gratiolaceae are further lineages distinct from the Scrophulariaceae (Lamiales). Plant Biol. 7: 1–12.

Rashotte, A. M., S. D. B. Carson, J. P. C. To and J. J. Kieber. 2003. Expression profiling of cytokinin action in Arabidopsis. Plant Physiol. 132: 1998–2011.

Reinhardt, D., T. Mandel and C. Kuhlemeier. 2000. Auxin regulates the initiation and radial position of plant lateral organs. Plant Cell 12: 507–518.

Rijpkema, A. S., T. Gerats and M. Vandenbussche. 2007. Evolutionary complexity of MADS complexes. Curr. Opin. Plant Biol. 10: 32–38.

Rupp, H. M., M. Frank, T. Werner, M. Strnad and T. Schmülling. 1999. Increased steady state mRNA levels of the *STM* and *KNATI* homeobox genes in cytokinin overproducing *Arabidopsis thaliana* indicate a role for cytokinins in the shoot apical meristem. Plant J. 18: 557–563.

Sakakibara, H., H. Kasahara, N. Ueda, M. Kojima, K. Takei, S. Hishiyama, T. Asami, K. Okada, Y. Kamiya, T. Yamaya and S. Yamaguchi. 2005. *Agrobacterium tumefaciens* increases cytokinin production in plastids by modifying the biosynthetic pathway in the host plant. Proc. Natl. Acad. Sci. USA 102: 9972–9977.

Sasaki, K., R. Aida, H. Yamaguchi, M. Shikata, T. Niki, T. Nishijima and N. Ohtsubo. 2010. Functional divergence within class B MADS-box genes *TfGLO* and *TfDEF* in *Torenia fournieri* Lind. Mol. Genet. Genomics 284: 399–414.

Sawhney, V. K. and A. Shukla. 1994. Male sterility in flowering plants: Are plant growth substances involved? Am. J. Bot. 81: 1640–1647.

Schmülling, T., T. Werner, M. Riefler, E. Krupková and I. B. Manus. 2003. Structure and function of cytokinin oxidase/dehydrogenase genes of maize, rice, *Arabidopsis* and other species. J. Plant Res. 116: 241–252.

Schoof, H., M. Lenhard, A. Haecker, K. F. X. Mayer, G. Jürgens and T. Laux. 2000. The stem cell population of *Arabidopsis* shoot meristems is maintained by a regulatory loop between the *CLAVATA* and *WUSCHEL* genes. Cell 100: 635–644.

Shibata, M. 2008. Importance of genetic transformation in ornamental plant breeding. Plant Biotechnol. 25: 3–8.

Takahashi, S., K. Shudo, T. Okamoto, K. Yamada and Y. Isogai. 1978. Cytokinin activity of *N*-phenyl-*N′*-(4-pyridyl)urea derivatives. Phytochemistry 17: 1201–1207.

Takeda, Y. 1996. Saibai-Ikushu-no-Rekisi. p. 7–11. In Nosangyosonbunkakyokai (ed.). Nogyogijututaikei Kakihen 7 (In Japanese). Nosangyosonbunkakyokai, Tokyo.

Takei, K., H. Sakakibara and T. Sugiyama. 2001. Identification of genes encoding adenylate isopentenyltransferase, a cytokinin biosynthesis enzyme, in *Arabidopsis thaliana*. J. Biol. Chem. 276: 26405–26410.

Tanase, K., R. Aida, H. Yamaguchi, N. Tanikawa, M. Nagata, T. Onozaki and K. Ichimura. 2011. Heterologous expression of a mutated carnation ethylene receptor gene, *Dc-ETR1nr*, suppresses petal abscission and autocatalytic ethylene production in transgenic *Torenia fournieri* Lind. J. Japan. Soc. Hort. Sci. 80: 113–120.

Tanase, K., C. Nishitani, H. Hirakawa, S. Isobe, S. Tabata, A. Ohmiya and T. Onozaki. 2012. Transcriptome analysis of carnation (*Dianthus caryophyllus* L.) based on next-generation sequencing technology. BMC Genomics 13: 292.

Taniguchi, M., T. Kiba, H. Sakakibara, C. Ueguchi, T. Mizuno and T. Sugiyama. 1998. Expression of *Arabidopsis* response regulator homologs is induced by cytokinins and nitrate. FEBS Lett. 429: 259–262.

Terakawa, T., T. Yamamura, Y. Tanaka, M. Sugiyama, N. Mitsuda and M. Takagi-Ohme. 2010. The modification of flower traits in cyclamen using the CRES-T. Abst. Annu. Meet. JSPP 2010: P0384.

Troll, W. 1957. Praktische Einführung in die Pflanzenmorphologie 2. Fischer, Jena. (Troll, W. 2004. Zusetu-shokubutukeitaigaku-handobukku 2 (In Japanese). Translated by S. Nakamura and H. Tobe. Asakurashoten, Tokyo.)

Venglat, S. P. and V. K. Sawhney. 1996. Benzylaminopurine induces phenocopies of floral meristem and organ identity mutants in wild-type *Arabidopsis* plants. Planta 198: 480–487.

Verdonk, J. C., K. Shibuya, H. M. Loucas, T. A. Colquhoun, B. A. Underwood and D. G. Clark. 2008. Flower-specific expression of the *Agrobacterium tumefaciens isopentenyltransferase* gene results in radial expansion of floral organs in *Petunia hybrida*. Plant Biotechnol. J. 6: 694–701.

Wang, H., J. Jiang, S. Chen, X. Qi, H. Peng, P. Li, A. Song, Z. Guan, W. Fang, Y. Liao and F. Chen. 2013. Next-generation sequencing of the *Chrysanthemum nankingense* (Asteraceae) transcriptome permits large-scale unigene assembly and SSR marker discovery. PLoS One 8: e62293.

Werner, T. and T. Schmülling. 2009. Cytokinin action in plant development. Curr. Opin. Plant Biol. 12: 527–538.

Xu, H., R. B. Knox, P. E. Taylor and M. B. Singh. 1995. *Bcp1*, a gene required for male fertility in *Arabidopsis*. Proc. Natl. Acad. Sci. USA 92: 2106–2110.

Yamaguchi, H., T. Niki, T. Niki and T. Nishijima. 2010. Morphological property and role of homeotic genes in paracorolla development of *Antirrhinum majus*. J. Japan. Soc. Hort. Sci. 79: 192–199.

Yanofsky, M. F., H. Ma, J. L. Bowman, G. N. Drews, K. A. Feldman and E. M. Meyerowitz.

1990. The protein encoded by the *Arabidopsis* homeotic gene *agamous* resembles transcription factors. Nature 346: 35–39.

Yashiro, Y. 1994. Gensan-to-Raireki. p. 387–390. In Nosangyosonbunkakyokai (ed.). Nogyogijututaikei Kakihen 8 (In Japanese). Nosangyosonbunkakyokai, Tokyo.

Yoshikura, H. 2006. In Gyousei (ed.). Kenkyusya-no-tameno-Carutahenahou Kaisetsu (In Japanese). Idenshikumikaejikkenanzentaisakukenkyukai, Tokyo.